HEAT TRANSFER IN BEDS OF CITRUS FRUITS DURING FORCED CONVECTION COOLING

By

Carl Direlle Baird

A DISSERTATION PRESENTED TO THE GRADUATE
COUNCIL OF THE UNIVERSITY OF FLORIDA IN PARTIAL
FULFILLMENT OF THE REQUIREMENTS FOR THE DEGREE OF
DOCTOR OF PHILOSOPHY

UNIVERSITY OF FLORIDA
1973

ACKNOWLEDGMENTS

The author wishes to express his sincere appreciation to Dr. E. A. Farber who served as chairman of his supervisory committee. He has been a source of real assistance, inspiration, and encouragement.

Appreciation is extended to the other members of his supervisory committee: Professor J. M. Myers, Agricultural Engineering, Dr. Z. R. Pop Stojanovic, Mathematics, and Dr. F. L. Schwartz, Mechanical Engineering, for their leadership, interest, and assistance throughout his program. Appreciation is expressed to Dr. R. B. Gaither, Chairman of the Mechanical Engineering Department, and to each of the faculty members who contributed to his graduate program.

He is indebted to the Department of Agricultural Engineering for financial support of his research and to Dr. E. T. Smerdon, Chairman, for his leadership, encouragement and untiring willingness to cope with the administrative problems involved. Thanks are also due to each of the many staff and faculty members who assisted in numerous ways; especially to Dr. D. T. Kinard and Mr. J. J. Gaffney who actively supported his research as project leaders. Mr. Gaffney also provided indispensable help with the computer programming.

For their cheerful sacrifices and loving patience, the author dedicates this dissertation to his wife Judy and daughters Sally Ann and Julia.

TABLE OF CONTENTS

Page

ACKNOWLEDGMENTS ii

LIST OF TABLES. vii

LIST OF FIGURES viii

ABSTRACT. xi

INTRODUCTION. 1

REVIEW OF LITERATURE. 4

  Studies on the Thermal Properties of Fruits and Vegetables 4

  Studies on Fruit and Vegetable Precooling. 7

CONDUCTION HEAT TRANSFER IN SINGLE CITRUS FRUITS. 14

  Theory and Assumptions 14

    Homogeneous Sphere. 15

    Heat of Respiration 17

  Analytical Solution. 17

  Numerical Solution for Heat Conduction in a Sphere with Time-Dependent Boundary Conditions. 21

TEMPERATURE DISTRIBUTION WITHIN A BED OF CITRUS DURING COOLING 29

  Laplace Transform Solution of Simplified Model 29

  Numerical Solution of Realistic Model. 42

  Determination of Convective Heat Transfer Coefficient and Thermal Diffusivity. 46

    Theory. 46

Page

Development of Method 59

Experimental Evaluation of Thermal Diffusivity. . . 62

Design and Description of Experimental Facilities. . . 63

Basic Construction of Precooler 64

Refrigeration Components and Controls 64

Example illustrating capacity of system. 67

Components used for control. 67

Evaporator coils 68

Air Temperature and Humidity. 69

Air Flow. 70

Reheat Section. 72

Experimental Test Procedures 72

Data and Results 77

Numerical Solution of Deep Bed Cooling. 77

Convective Heat Transfer Coefficient (h). 82

Thermal Diffusivity (α) 82

Experimental Deep Bed Cooling Tests 82

Discussion 86

Comparison of Laplace Transform Solution for the Simplified Model and Numerical Solution for the Realistic Model 86

Convective Heat Transfer Coefficient. 95

Comparison of Experimental Data With Numerical Solution 98

Experimental data. 99

Analyses of the differences between experimental and theoretical data 99

Evaporative cooling 99

Page

Radiation heat transfer. 103

Conduction along the thermocouple wire . . . 104

Insulating effect of rind. 104

Suggestions for Further Study. 108

Optimum design and operating conditions 108

Modification of numerical model 109

CONCLUSIONS. 110

REFERENCES 112

APPENDICES 117

Appendix A - Computer Program and Sample Output for Conduction in a Sphere with Specified Surrounding Temperature. . . . 117

Appendix B - Computer Program and Sample Output for Cooling a Deep Bed of Citrus Fruit. 121

Appendix C - Graphical Results Showing Comparison of Experimental Data with Numerical Solution 134

BIOGRAPHICAL SKETCH. 165

LIST OF TABLES

Table Page

1. Comparison of Rind and Juice Vesicle Components of Marsh Grapefruit. 7

2. Approximate Heat of Respiration of Oranges and Grapefruit at Various Temperatures 9

3. Particle Shape Factors for Packed-Bed Correlation . 52

4. Coefficients and Exponents for Emperical Heat Transfer Correlations. 59

5. Coefficients, Exponents and Linear Correlation Coefficients for Equation [84] Determined for Forced-Air Cooling in Bulk Containers. 62

6. Thermal and Physical Properties of Valencia Oranges and Marsh Grapefruit Used in Cooling Tests. 91

7. The Effect of Increment Size on the Accuracy of the Numerical Solution. 96

LIST OF FIGURES

Figure Page

1. Internal temperature distribution in Marsh grapefruit plotted from raw experimental data recorded during transient cooling test runs. 16

2. Diagram indicating a heat balance on the three types of nodes used in a sphere. . . . 23

3. Flow diagram for digital computer program of heat conduction in a sphere with arbitrarily varying air temperature. 27

4. Comparison of analytical solution with numerical solution for heat conduction in a sphere 28

5. Control volume for heat balance on bed 31

6. Schumann's curves for temperature history of solid for values of Y from 0 to 10 43

7. Schumann's curves for temperature history of gas for values of Y from 1 to 10 43

8. Flow diagram for the digital computer program to solve deep bed heat transfer equations. . 47

9. Magnitude and location of mass-average temperature of Marsh grapefruit cooled in agitated ice water 48

10. Unaccomplished temperature change and location of mass-average temperature during forced-air cooling 48

11. Nomograph for evaluating elements of the equation: $M_1^2 = f_3(G,Bi)$ 57

12. Elevation view of forced-air cooler. 65

13. Precooler refrigeration components and controls 66

LIST OF FIGURES (Continued)

Figure Page

14. Bulk load of fruit showing the four levels at which product temperature was measured. Dimensions A, B, C, and D are indicated for each test. 74

15. Method used for placing thermocouples in product. 75

16. Theoretical mass-average temperature response of oranges to forced-air cooling as predicted by numerical model. 78

17.-18. Theoretical mass-average and surface temperature response of oranges to forced-air cooling as predicted by numerical model. 79

19. Theoretical mass-average and surface temperature response of grapefruit to forced-air cooling as predicted by numerical model. 81

20. Linear regression relating Nusselt number and Reynolds number for forced-air cooling of oranges in bulk loads 83

21. Linear regression relating Nusselt number and Reynolds number for forced-air cooling of grapefruit in bulk loads. 84

22. Linear regression relating Nusselt number and Reynolds number for forced-air cooling of oranges and grapefruit in bulk loads. . . 85

23. Experimental mass-average and surface temperature response of oranges to forced-air cooling. 87

24. Experimental mass-average temperature response of oranges to forced-air cooling. . 88

25. Experimental mass-average and surface temperature response of oranges to forced-air cooling. 89

26. Experimental mass-average temperature response of grapefruit to forced-air cooling. 90

LIST OF FIGURES (Continued)

Figure Page

27. Comparison of Laplace transform solution of simplified model with numerical solution of realistic model for a slow cooling rate (25 fpm) 92

28. Comparison of Laplace transform solution of simplified model with numerical solution of realistic model for a fast cooling rate (400 fpm). 94

29.-31. Comparison of experimental and theoretical temperature response of oranges to forced-air cooling 100

32. Comparison of the temperature profile in a homogeneous sphere with average properties of a grapefruit and the temperature profile in a composite sphere with properties corresponding to the rind and juice vesicles. 107

33.-52. Theoretical and experimental temperature response of oranges to forced-air cooling 135

53.-62. Theoretical and experimental temperature response of grapefruit to forced-air cooling 155

Abstract of Dissertation Presented to the Graduate
Council of the University of Florida in Partial Fulfillment
of the Requirements for the Degree of Doctor of Philosophy

HEAT TRANSFER IN BEDS OF CITRUS FRUITS DURING FORCED CONVECTION COOLING

By

Carl Direlle Baird

June, 1973

Chairman: Dr. E. A. Farber
Major Department: Mechanical Engineering

The removal of heat from fruits and vegetables as soon after harvest as practical has long been recognized as effective in retarding the ripening process and controlling microbial processes. Presently, very little citrus is being precooled. Hydrocooling of citrus has been attempted, but was not satisfactory due to the detrimental effect of the chemically treated water on the surface appearance of the fruit. It is believed that forced-air precooling of citrus would receive favorable attention if additional basic information were available on heat transfer characteristics of citrus in bulk.

Equations describing the heat transfer in a bed of citrus fruit were derived. A numerical solution of these equations was obtained and evaluated utilizing a digital computer. Temperature was determined as a function of 1) position within the individual fruit, 2) distance from inlet of bed, and 3) time. Variable input data for the computer program include: diameter of fruit, thermal diffusivity of fruit, specific heat of fruit, density of fruit, initial fruit temperature, air temperature, air flow rate, total weight of fruit, depth of bed, and convective heat transfer coefficient. An equation was developed for determining the average convective heat transfer coefficient for a bed of citrus in the form of a Nusselt number-Reynolds number relationship. The constants in this equation were experimentally evaluated for oranges and grapefruit utilizing a method which made use of the computer solution.

Fifteen experimental cooling tests were conducted on oranges and grapefruit in bulk containers. Mass-average and surface temperatures were measured at four levels within the bed of citrus with air velocity ranging from 15 to 400 fpm.

A comparison between the experimental and theoretical results indicated good agreement except for surface temperatures of grapefruit. The experimental surface temperatures of grapefruit were consistently lower than those predicted by the numerical solution. This was shown to be caused primarily by the low thermal conductivity of the thick rind. A solution was obtained for the temperature gradient in a composite sphere which indicated a much steeper temperature gradient through the rind than through the juice vesicles.

INTRODUCTION

The removal of field heat from fruits and vegetables prior to processing, transportation and storage has long been recognized as effective in retarding the ripening process and controlling microbial processes (21, 40, 41)[1]. The term "precooling" is commonly used to describe this rapid cooling process (1, 2, 42). Maxie _et al_. (34) have described the biological basis for prompt cooling, listing a series of physiological, biochemical, pathological and physical changes that are temperature-dependent in fruits. Precooling is likely the most important of all the operations used in establishing and maintaining desirable, fresh, and salable produce.

According to Guillou (22), the rate of various changes such as moisture loss and the action of enzymes and microorganisms, are commonly doubled or tripled with each 10 F rise in temperature. He estimated that some fresh fruits and vegetables deteriorate as much in an hour at 90 F as in a day at 50 F or in a week at 32 F.

According to the 1972 Citrus Summary (17), approximately 20% of Florida's citrus crop is consumed in the fresh form.

---

[1] Numbers in parentheses refer to numbered references.

The total value of this fruit is approximately $110 million annually. This amounts to over 7% of the total value of Florida's annual agricultural production.

At present most of the citrus fruits are not cooled until they are placed in the refrigerated vehicle that will carry them to market. The refrigeration systems on these vehicles are not designed to remove great quantities of heat rapidly; therefore, the temperature of the fruit is not decreased to the desired level for a considerable period after harvesting.

It has been conservatively estimated that 10% of all fresh citrus fruits shipped are never consumed because of waste and spoilage (48). The value of these fruits is over $10 million.

A small quantity of citrus fruit is presently being precooled by hydrocooling and air cooling. Hydrocooling of citrus has been tried by some producers, primarily due to the successful hydrocooling of peaches and vegetables. However, it soon became apparent that fungicide in the cooling water was essential to hold decay to tolerable levels. Unfortunately, the chemically treated water had a detrimental effect on the surface appearance of the fruit. Also, fruit cooled with water seemed more susceptible to decay upon warming than fruit which had received no cooling. Certain types of citrus, notably grapefruit, exhibited subsequent chilling injury (28).

It is believed that forced-air precooling of citrus would receive more favorable attention if additional basic information were available on heat transfer characteristics in beds of citrus fruit. Much of the research on precooling has been done in production operations or in experimental facilities which were not designed for obtaining basic heat transfer data. Thus the objective of this investigation is to obtain and test a mathematical model that can predict the temperature distribution within a bed of citrus during forced-air cooling. Other objectives incident to this investigation are to devise methods for obtaining thermal and physical properties for beds of citrus fruit.

REVIEW OF LITERATURE

Studies on the Thermal Properties of Fruits and Vegetables

The response in temperature of a body to a given input or removal of energy in the form of heat is dependent upon certain properties of the body. These properties govern the storage and transfer of heat energy through the body. Two of these properties are specific heat capacity (c), BTU/lb-°F, and thermal conductivity (k), BTU/hr-°F-ft. Another property, which is convenient to use since it consists of a combination of three properties as they appear in the heat conduction equation, is thermal diffusivity $(k/\rho c)$, ft^2/hr.

Since most fruits and vegetables contain a high percentage of water it can be expected that their properties will have values near that of water. Formulas for the specific heat and thermal conductivities of fruits and vegetables based on their percent water have been developed (15).

$$c = p/100 + 0.2\ (100-p)/100 \text{ BTU/lb-°F} \qquad [1]$$

$$k = 0.32\ /100 + 0.15\ (100-p)/100 \text{ BTU/hr-ft-°F} \qquad [2]$$

where

c = specific heat

p = percent water

k = thermal conductivity

Gane (20) investigated the thermal diffusivity of fruits and vegetables by using the graphical method of Gurney and Lurie (23) for solutions to the conduction heat transfer equation for various shaped bodies. The temperature history of of the center of fruits and vegetables was monitored with thermocouple junctions during cooling and was used in conjunction with these graphical solutions to estimate the thermal diffusivity. He found the following average diffusivity values (ft^2/hr): apples -- 0.0049, oranges -- 0.0049, grapefruit -- 0.0049, and squash -- 0.0044. He also found the thermal conductivity of oranges and grapefruit to be 0.24 and 0.25 BTU/hr-ft-°F respectively.

Kethley *et al*. (30) conducted a series of cooling experiments with eight different fruits and vegetables. They used the same graphical methods of Gurnie and Lurie. In the temperature range 80 to 32 F their values of diffusivity ranged from 0.00535 to 0.00615 ft^2/hr.

Turrell and Perry (50) found the specific heat by using a calorimeter. They obtained values of 0.885 for Marsh grapefruit, 0.892 for Eureka lemons, 0.840 for Valencia oranges and 0.875 for Washington Navel oranges.

Several investigators have determined the thermal conductivity (k) of citrus by assuming it to be homogeneous. Turrell and Perry (50) found the thermal conductivity averaged 0.23 BTU/hr-ft-°F for Marsh grapefruit, Eureka lemons, Valencia oranges and Washington Navel oranges when all varieties were considered. Perry et al. (37) determined the following mean values for thermal diffusivity: Valencia oranges -- 0.00368, Washington Navel oranges -- 0.00415, Marsh grapefruit -- 0.00355, and Eureka lemons -- 0.00417 ft^2/hr.

Smith et al. (47) developed a technique of evaluating thermal diffusivity which corrects for deviation from the conventional shapes. The technique incorporates a geometry index (G) into the basic Fourier heat conduction equation for a sphere. The geometry index was obtained from a measure of two orthogonal areas of the shape. Using this technique they determined an average thermal diffusivity of 0.00363 ft^2/hr from 15 tests run on Marsh grapefruit. Bennett et al. (7) used the same procedure and obtained an average thermal diffusivity of 0.00355 ft^2/hr for five maturity groups of Marsh grapefruit. This value was obtained from temperature response at the approximate mass average point. Values calculated from temperature response at the center and one-half radius point were slightly lower, probably due to the nonhomogeneity of the product.

Bennett et al. (7) also made separate determinations for the thermal properties of the rind and juice vesicle components of Marsh grapefruit. Table 1 indicates average values for each component. The thermal diffusivity determined here

Table 1. Comparison of Rind and Juice Vesicle Components of Marsh Grapefruit.

	Specific Heat BTU/lb-°F	Density lb/ft^3	Thermal Conductivity BTU/hr-ft-°F	Thermal Diffusivity x10^{-3} ft^2/hr
Juice Vesicle	0.907	63.2	0.2716	4.56
Rind	0.829	36.1	0.1397	4.67

is considerably higher than that determined by assuming the fruit to be homogeneous. It is interesting to note that the thermal diffusivity of the rind and juice vesicle components has values very near the same while the thermal conductivity and density variation is much greater. This has been explained by Perry _et al_. (37) that in a given material where density changes because of changes in porosity, the thermal conductivity is approximately proportional to density, so that the diffusivity remains about constant.

Bennett _et al_. (7) conducted similar tests on Valencia oranges and found the combined thermal conductivity to be 0.248 BTU/hr-ft-°F.

Studies on Fruit and Vegetable Precooling

Presently, most citrus fruit is not cooled until it is placed in the refrigerated vehicle that will carry it to market. The refrigeration systems of these vehicles are not designed to remove great quantities of heat rapidly; thus the temperature of the fruit is not decreased to the desired level for several days after harvesting. During this time respiration reduces the quality, nutrient value and shelf life of the fruit, thus indicating the importance of precooling.

During the respiration process oxygen from the air is combined with carbon from the plant tissues to form various decomposition products and eventually carbon dioxide and water. In addition to this, the enzymes present act on various substances in the plant tissues and gradually cause changes in color, texture, and chemical composition which mature fruit and may eventually cause serious deterioration.

During the respiration process heat is released varying in amount with the commodity and its temperature. Table 2 illustrates the large difference between the heats of respiration at high and low temperatures.

The respiration process is generally believed to cause consumption of a simple hexose sugar glucose. With the aid of an enzyme system and oxygen, glucose sugar is reduced to carbon dioxide and water in accordance with the following reaction:

$$C_6H_{12}O_6 + 6O_2 = 6CO_2 + 6H_2O + \text{Heat} \qquad [3]$$

Table 2. Approximate Heat of Respiration of Oranges and Grapefruit at Various Temperatures (26)

	(BTU per 24 hours per ton of fruit)			
	Temp.(°F)	Sensible Heat	Latent Heat	Total Heat
Oranges	32	900	63	963
	40	1400	97	1497
	60	5000	348	5348
	80	8000	557	8557
Grapefruit	32	460	32	492
	40	1070	74	1144
	60	2770	193	2963
	80	4180	291	4471

The enzyme acts as a catalyst but is not consumed during the reaction. The effectiveness of the enzyme as a catalyst is greatly reduced at low temperatures which causes a reduction in the heat of respiration when the temperature is reduced.

Precooling usually refers to the rapid removal of heat from a fruit or vegetable. In regards to what "pre" means, Thevenot (49) stated: a) in a restrictive sense: previous to transporation; b) in a wide sense: previous to transportation or to storing; c) in a very wide sense: previous to transportation, storing, or processing. Redit and Hamer (42) referred to precooling as the rapid cooling of a commodity to a suitable transit or storage temperature soon after harvest, before it is stored or moved in transit.

A small quantity of citrus fruit is now precooled by several methods. Of these hydrocooling and air cooling are probably the only two that can be combined with the mechanized methods of packing that are now used. However, some investigations on hydrocooling of oranges have indicated that an increase in respiration rate, over that of uncooled oranges, occurred when they were allowed to return to room temperature. Thus, hydrocooling can actually be detrimental to oranges(14).

On the other hand, Hopkins and Loucks (28) found that air precooled oranges were outstanding in their keeping quality and resistance to decay.

Sainsbury (43) investigated high velocity air as a means of rapidly precooling fruits. In cooling experiments involving such fruits as cherries, apples, and apricots, predictability of the cooling behavior was established by identifying the cooling rate (CR) for a given experiment.

$$CR = \frac{\underline{\text{Fruit temperature reduction}} \atop TD_i - TD_f}{\log_e (TD_i/TD_f)} \text{ Time} \qquad [4]$$

where

TD_i = initial temperature difference between fruit and air.

TD_f = final temperature difference between fruit and air.

This equation for cooling rate (CR) reduces to

$$CR = \frac{\log_e \cdot \frac{TD_i}{TD_f}}{\text{Time}} \qquad [5]$$

when the air temperature is maintained constant. The slope of the line established by plotting $\log_e$ (TD_i/TD_f) as a function of time identifies the cooling rate (CR).

Guillou (22) reports that Newton's law of cooling will predict quite well the average temperature progression of fruits and vegetables during cooling. Newton's law is applicable for an object placed in surroundings at a constant lower temperature provided the resistance to heat transfer is constant. The equation expressing this law using the notation of Guillou is

$$\frac{dT}{dt} = C\ (T-T_o) \qquad [6]$$

where

t = time of exposure to surroundings

T = temperature of the object at time "t"

T_o = temperature of the surroundings

C = "cooling coefficient"

The integration of the equation by separation of variables shows that

$$C = \frac{1}{t} \log_e \frac{T-T_o}{T_1-T_o} \qquad [7]$$

where T_1 equals the initial temperature of the object. This equation for the "cooling coefficient" corresponds to the equation of Sainsbury (43) for cooling rate (CR).

Bennett et al. (9) conducted tests on forced-air precooling of Florida citrus. These tests were conducted on citrus in bulk containers through which they forced high velocity air. They developed an equation to predict the cooling rate. Since the inlet air temperature was not held constant, the air temperature at the end of the run was used as the reference temperature. They did not investigate the temperature distribution within the bed.

Leggett and Sutton (33) also conducted precooling tests on citrus fruits. They developed cooling curves and obtained cooling coefficients for oranges and grapefruit in crates. Both hydrocooling and air cooling tests were made for different crate spacings and arrangements.

Several investigators (5, 27, 36, 53, 29) have conducted tests involving transport phenomena of heat and moisture in beds of biological materials. Most of these investigations involved analysis similar to that of Schumann (45) and Furnas (19) who were evidently the first to solve the differential equations governing heat transfer in a deep bed of particles. For a system in which a fluid passes through a prism of crushed material, Schumann developed a series of temperature history curves subject to the following assumptions:

a) that the particles are small and no temperature gradient exists within any particle at any time.
b) that no heat is produced by particles.
c) that no heat is transferred from particle to particle by conduction.

d) that the fluid is incompressible.

e) and that the thermal properties of the particles are uniform throughout and do not vary with time.

Furnas found that Schumann's theoretical curves would predict the temperature behavior of beds of coke and iron through which air was moving.

CONDUCTION HEAT TRANSFER IN SINGLE CITRUS FRUITS

Theory and Assumptions

Foundation for the theory of heat conduction is universally attributed to Fourier (18). It is apparent that Fourier entertained a hope that practical use might be made of his work. He stated, "It is easy to judge how much these researches concern the physical sciences and civil economy, and what may be their influence on the progress of the arts which require the employment and distribution of heat." Fourier's work was awarded a generous prize by the French Royal Academy of Science in 1812. Fourier's work was treated like a work of art for more than 100 years with no practical use being made of it, mainly due to the difficulty encountered in obtaining practical solutions. However, in 1923 engineers Furney and Lurie (23) presented their solutions based on theory but with an experimental character. Answers to many practical problems of interest to engineers were made readily accessible by means of the time-temperature charts of Gurney and Lurie. Other such charts have been developed by means of the experimental technique of the electric analog (25). A large collection of time-temperature charts for conduction in various shapes with several different boundary conditions is given in a book by Schneider (44).

A considerable amount of effort has been given by researchers (24, 27, 38, 39, 46, 52) to correlate the theoretical solutions for regular-shaped objects with experimental data for biological materials that can be approximated by these regular-shapes.

Homogeneous Sphere

Most citrus fruits have the general shape of a sphere and therefore could be expected to exhibit heat transfer characteristics similar to that of a sphere. As noted in the preceding section, citrus fruits are not composed of homogeneous materials but consist of two main sections, the rind and the juice vesicles. It was also noted that although the thermal conductivity (k) and density (ρ) were quite different for the two portions, their thermal diffusivities ($\frac{k}{\rho c}$) were surprisingly close to one another.

Bennett et al. (8) investigated the temperature distribution in Marsh grapefruit, which has a rind that constitutes 30 to 40 percent of its total volume, and found that the presence of the rind has very little effect on the temperature profile. This is indicated in Figure 1 which shows the internal temperature distribution in Marsh grapefruit plotted from raw experimental data recorded during transient cooling.

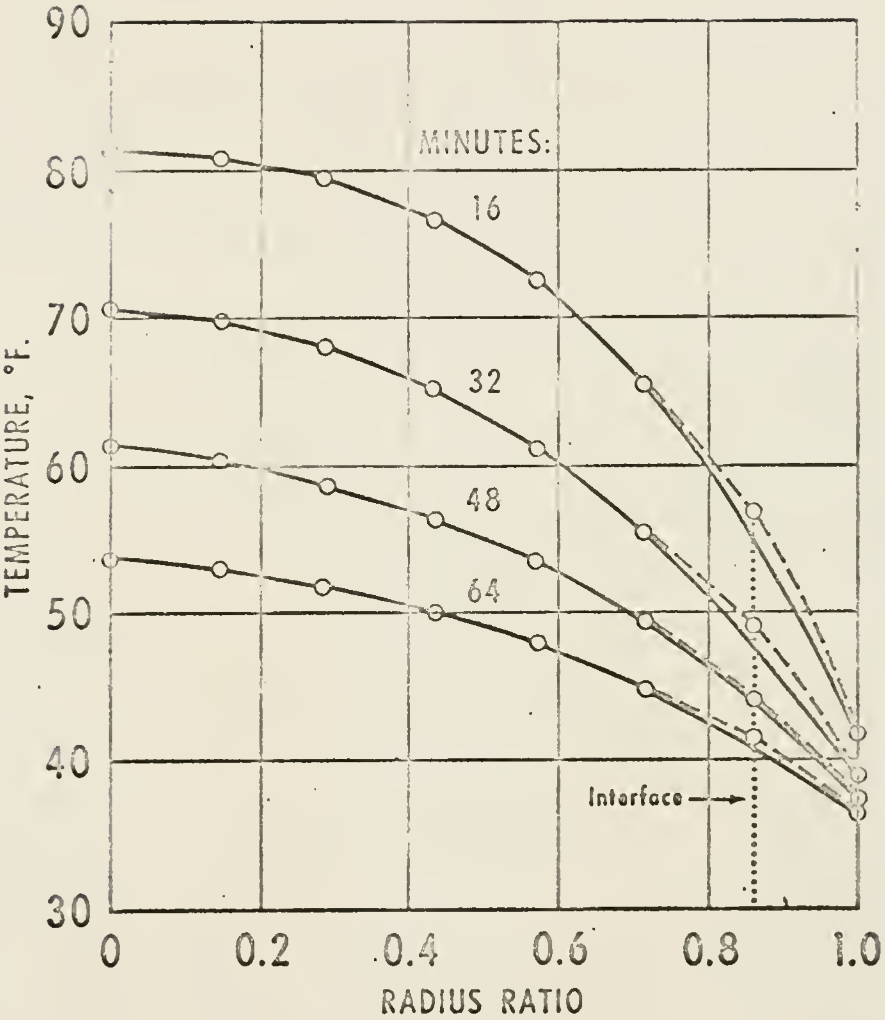

Figure 1. Internal temperature distribution in Marsh grapefruit plotted from raw experimental data recorded during transient cooling test runs. Dotted lines show discontinuity in temperature gradient at interface.

The dotted lines show a discontinuity in the temperature gradient at the interface between the juice vesicles and rind.

On the basis of these findings, it will be assumed that citrus fruits may be treated as homogeneous without significant error in the temperature profile.

Heat of Respiration

The justification for not including the heat of respiration as a heat source in the conduction equation is based on the findings of Awberry (4) and Hood (27). Awberry calculated the temperature excess at the center of an apple due to its heat of respiration, after two hours of cooling and found it to be 0.0232 C, while Hood calculated a value of 0.011 F at the center of the cucumber after 30 minutes of cooling. Both of these products have heats of respiration higher than citrus, thus the effect of heat of respiration on citrus during cooling is believed to be negligible. It should be pointed out that the effect of heat of respiration should not be neglected in some other cases such as storage at elevated temperatures.

Analytical Solution

The governing equations for conduction heat transfer from a homogeneous sphere without heat sources, initially at a uniform temperature (T_1) and surrounded by a fluid of constant temperature (T_∞) are

$$\frac{\partial T}{\partial t} = \alpha\left(\frac{\partial^2 T}{\partial r^2} + \frac{2}{r}\frac{\partial T}{\partial r}\right) \qquad [8]$$

$$T(r,o) = T_1 \qquad [9]$$

$$\left(k\,\frac{\partial T}{\partial t}\right)_{r=a} = h(T_s - T_\infty) \qquad [10]$$

where

t = time, hr

r = radial distance from center, ft

a = radius of sphere, ft

T = temperature at r and t, °F

α = thermal diffusivity, ft^2/hr

k = thermal conductivity, BTU/hr-ft-°F

The theory for the following solution of equations [8], [9], and [10] was taken from Arpaci (3) and equation [21] agrees with his solution.

Equation [8] can be written as:

$$\frac{\partial T}{\partial t} = \frac{\alpha}{r^2}\,\frac{\partial}{\partial r}\left(r^2\,\frac{\partial T}{\partial r}\right) \qquad [11]$$

and substituting $\theta = T - T_\infty$ into equations [9], [10], and [11] gives:

$$\frac{\partial \theta}{\partial t} = \frac{\alpha}{r^2}\,\frac{\partial}{\partial r}\left(r^2\,\frac{\partial \theta}{\partial r}\right) \qquad [12]$$

$$\theta(r,0) = \theta_1 \tag{13}$$

$$-k \left[\frac{\partial\theta(a,t)}{\partial r}\right] = h\theta(a,t) \tag{14}$$

One more boundary condition is:

$$\theta(0,t) = \text{finite or } \frac{\partial\theta(0,t)}{\partial r} = 0 \tag{15}$$

Using the transformation:

$$\theta(r,t) = \Psi(r,t)/r \tag{16}$$

reduces the spherical Laplacian to the cartesian Laplacian whose solution is expressible in terms of circular functions.

We may now express equations [12] through [15] in terms of Ψ by using equation [16]. The result is:

$$\frac{\partial\Psi}{\partial t} = \alpha \frac{\partial^2\Psi}{\partial r^2}, \qquad \Psi(r,0) = r$$

$$\tag{17}$$

$$\Psi(0,t) = 0, \qquad -k \frac{\partial\Psi(a,t)}{\partial r} = (h - \frac{k}{a})\ \Psi(a,t)$$

Hence the problem is reduced to a problem of cartesian geometry.

The product solution $\Psi(r,t) = R(r)\ \tau(t)$ yields:

$$\frac{d^2R}{dr^2} + \lambda^2 R = 0$$

$$R(0) = 0, \qquad \frac{dR(a)}{dr} + (\frac{h}{k} - \frac{1}{a})\ R(a) = 0 \tag{18}$$

in r and equation [19] in time.

$$\frac{d\tau}{dt} + \alpha\lambda^2 = 0 \qquad [19]$$

The solution of equation [18] is:

$$R_n(r) = A_n\phi_n(r), \qquad \phi_n(r) = \sin\lambda_n r$$

and the zeros of

$$(\lambda_n a)\cos\lambda_n a = (1-Bi)\sin\lambda_n a$$

are the characteristic values, where $Bi = ha/k$.

The solution of equation [19] is:

$$\tau_n(t) = C_n e^{-\alpha\lambda_n^2 t}$$

Thus the product solution becomes:

$$\Psi(r,t) = \sum_{n=1}^{\infty} b_n e^{-\alpha\lambda_n^2 t} \sin\lambda_n r \qquad [20]$$

The initial value of equation [20] is:

$$r\theta_1 = \sum_{n=1}^{\infty} b_n \sin\lambda_n r$$

The coefficient b_n is obtained by the expansion of $r\theta$, into a Fourier sine series evaluated from zero to a.

$$b_n = \frac{2\theta_1 \; (\sin\lambda_n a - \lambda_n a \cos\lambda_n a}{\lambda_n \; (\lambda_n a - \sin\lambda_n a \cos\lambda_n a)}$$

Thus the unsteady temperature of the sphere is:

$$\frac{T(r,t) - T_\infty}{T_1 - T_\infty} = 2 \sum_{n=1}^{\infty} \left(\frac{\sin\lambda_n a - \lambda_n a \cos\lambda_n a}{\lambda_n a - \sin\lambda_n a \cos\lambda_n a}\right) e^{-\alpha\lambda_n^2 t} \frac{\sin\lambda_n r}{\lambda_n r} \qquad [21]$$

Numerical Solution for Heat Conduction in a Sphere with Time-Dependent Boundary Conditions

The analytical solutions for the heat conduction equation presented in the preceding section are based upon assumed initial and boundary conditions which can seldom be satisfied in practical applications. Especially in dealing with many biological products, there is a need for information when initial and boundary conditions may exist such as: with time-varying environmental conditions or surface conductances, with change-of-phase or mass transfer at the boundary, or with initial object temperature distributions.

The only practical method for solving this type problem is by numerical methods, such as those presented by Arpaci (3). Since cooling in a deep bed involves time-dependent boundary conditions, a numerical solution of the heat conduction equation for a sphere surrounded by a fluid with arbitrarily varying temperature will be derived.

The difference equations which approximate the governing differential equations can be obtained by approximating each term of the differential equation with its equivalent finite difference expression or by performing a heat balance method on each type of node in the solid. The heat balance method will be used in this formulation. For a sphere there are three types of nodes as indicated in Figure 2, surface nodes, interior nodes, and center nodes.

The first law of thermodynamics applied to the interior node gives:

$$q_{i-1}[4\pi(r-\frac{\Delta r}{2})^2]+q_{i+1}[4\pi(r+\frac{\Delta r}{2})^2]=$$

$$\rho C\ \frac{4}{3}\pi[(r+\frac{\Delta r}{2})^3-(r-\frac{\Delta r}{2})^3]\ \frac{T_i^{n+1}-T_i^n}{\Delta t} \qquad [22]$$

where

T_i^{n+1} denotes the temperature at the ith node at time n+1. Now stating Fourier's law of conduction, we have:

$$q_{i+1} = K\ \frac{T_{i-1}^n-T_i^n}{\Delta r}\ , \qquad q_{i+1} = k\ \frac{T_{i+1}^n-T_i^n}{\Delta r}$$

Substituting into equation [22] results in:

$$\frac{4\pi k}{\Delta r}\ (r-\frac{\Delta r}{2})^2\ \frac{T_{i-1}^n-T_i^n}{\Delta r} + \frac{4\pi k}{\Delta r}\ (r+\frac{\Delta r}{2})^2\ \frac{T_{i+1}^n-\ T_i^n}{\Delta r} =$$

$$\rho c\ \frac{4}{3}\ \pi[(r+\frac{\Delta r}{2})^3\ -\ (r-\frac{\Delta r}{2})^3]\ \frac{T_i^{n+1}-T_i^n}{\Delta t}$$

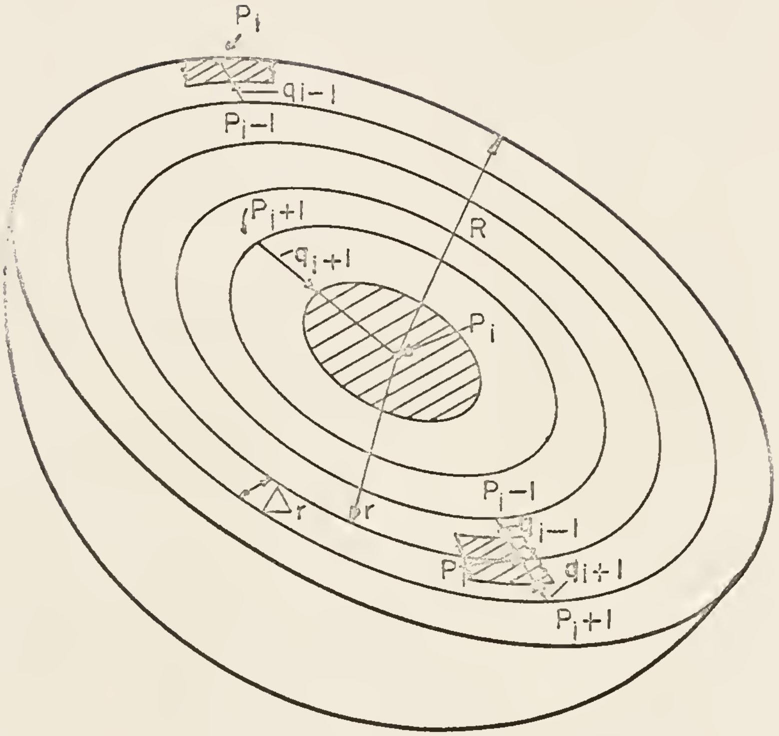

Figure 2. Diagram indicating a heat balance on the three types of nodes used in a sphere

rearranging:

$$T_i^{n+1} = \{1 - \frac{\alpha\Delta\ t}{(\Delta r)^2}\ [(1-\frac{\Delta r}{2r})^2 + (1+\frac{\Delta r}{2r})^2]\}\ T_i^n$$

$$+ \frac{\alpha\Delta\ t}{(\Delta r)^2}\ [(1-\frac{\Delta r}{2r})^2\ T_{i-1}^n + (1+\frac{\Delta r}{2r})^2\ T_{i+1}] \qquad [23]$$

where $\{\quad\} \geqq 0$ to insure convergence.

Now consider the surface node. The first law of thermodynamics applied to the surface node gives:

$$q_{i-1}[4\pi(R-\frac{\Delta r}{2})^2] + q_{conv}[4\pi R^2] =$$

$$\rho c\ \frac{4}{3}\pi[R^3-(R-\frac{r}{2})^3]\ \frac{T_i^{n+1}-T_i^n}{\Delta t}$$

Substitution for:

$$q_{i-1} = k\ \frac{T_{i-1}^n-T_i^n}{\Delta r}\ , \qquad q_{conv} = h(T_\infty^n-T_i^n)$$

gives:

$$k\ \frac{T_{i-1}^n-T_i^n}{\Delta r}\ [4\pi(R-\frac{\Delta r}{2})^2] + h(T_\infty^n-T_i^n)[\frac{4\pi R^2 h}{k}] =$$

$$\rho c\ \frac{4}{3}\ \pi[R^3-(R-\frac{\Delta r}{2})^3]\ \frac{T_i^{n+1}-T_i^n}{\Delta t}$$

rearranging:

$$T_i^{n+1} = \frac{3\alpha\Delta t}{\Delta r} \frac{(R-\frac{\Delta r}{2})^2}{[R^3-(R-\frac{\Delta r}{2})^3]} T_{i-1}^n +$$

$$\frac{3R^2h\alpha\Delta t}{k[R^3-(R-\frac{\Delta r}{2})^3]} T_\infty^n +$$

$$\{1 - \frac{3\alpha\Delta t}{[R^3-(R-\frac{\Delta r}{2})^3]} \frac{(R-\frac{r}{2})^2}{\Delta r} + \frac{R^2h}{k}\} T_i^n \qquad [24]$$

where $\{ \; \} \geqq 0$ to insure convergence.

Applying the first law to the center node results in:

$$q_{i-1}[4\pi(\frac{\Delta r}{2})^2] = \rho c \frac{4}{3}\pi(\frac{\Delta r}{2})^3 \frac{T_i^{n+1}-T_i^n}{\Delta t}$$

substituting for:

$$q_{i+1} = k\frac{T_{i+1}-T_i}{\Delta r}$$

gives:

$$k\frac{T_{i+1}-T_i}{\Delta r}[4\pi(\frac{\Delta r}{2})^2] = \rho c \frac{4}{3}\pi(\frac{\Delta r}{2})^3 \frac{T_i^{n+1}-T_i^n}{\Delta t}$$

Simplifying and rearranging:

$$T_i^{n+1} = \frac{6\alpha\Delta t}{(\Delta r)^2} T_{i+1}^n + \{1 - \frac{6\alpha\Delta t}{(\Delta r)^2}\} T_i^n \qquad [25]$$

where $\{ \; \} \geqq 0$ to insure convergence.

No similar solution was found in the literature for comparison.

A computer program was developed to evaluate equations [23], [24], and [25] for temperature, T, as a function of "r" and "t." The arbitrarily varying fluid temperature, T^n, is entered as input data. A flow diagram for the computer program is given in Figure 3 and the computer program is shown in Appendix A.

In order to test the accuracy of the numerical solution, the air temperature, T , was entered as a constant so that the results could be compared with the exact solution obtained in the preceding section. This comparison is shown in Figure 4. The data used to generate these curves are the following: radius = 0.113 ft, k = 0.256 BTU/hr-ft-°F, h = 11.7 BTU/hr-ft^2-°F, α = 0.0051 ft^2/hr, c = 0.9 BTU/lb-°F.

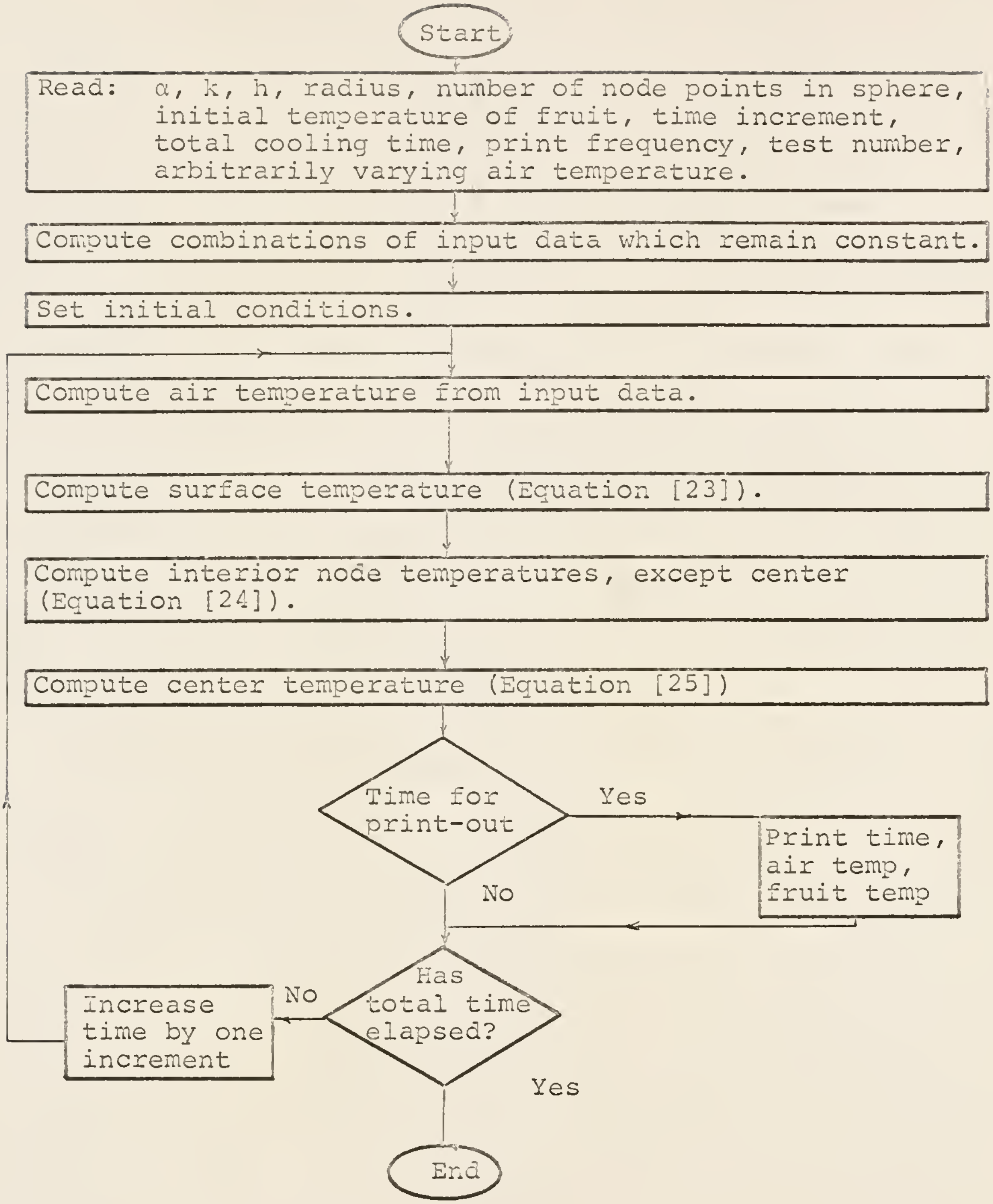
Start
Read: α, k, h, radius, number of node points in sphere, initial temperature of fruit, time increment, total cooling time, print frequency, test number, arbitrarily varying air temperature.
Compute combinations of input data which remain constant.
Set initial conditions.
Compute air temperature from input data.
Compute surface temperature (Equation [23]).
Compute interior node temperatures, except center (Equation [24]).
Compute center temperature (Equation [25])
Time for print-out
Yes
Print time, air temp, fruit temp
No
Has total time elapsed?
No
Increase time by one increment
Yes
End

Figure 3. Flow diagram for digital computer program of heat conduction in a sphere with arbitrarily varying air temperature.

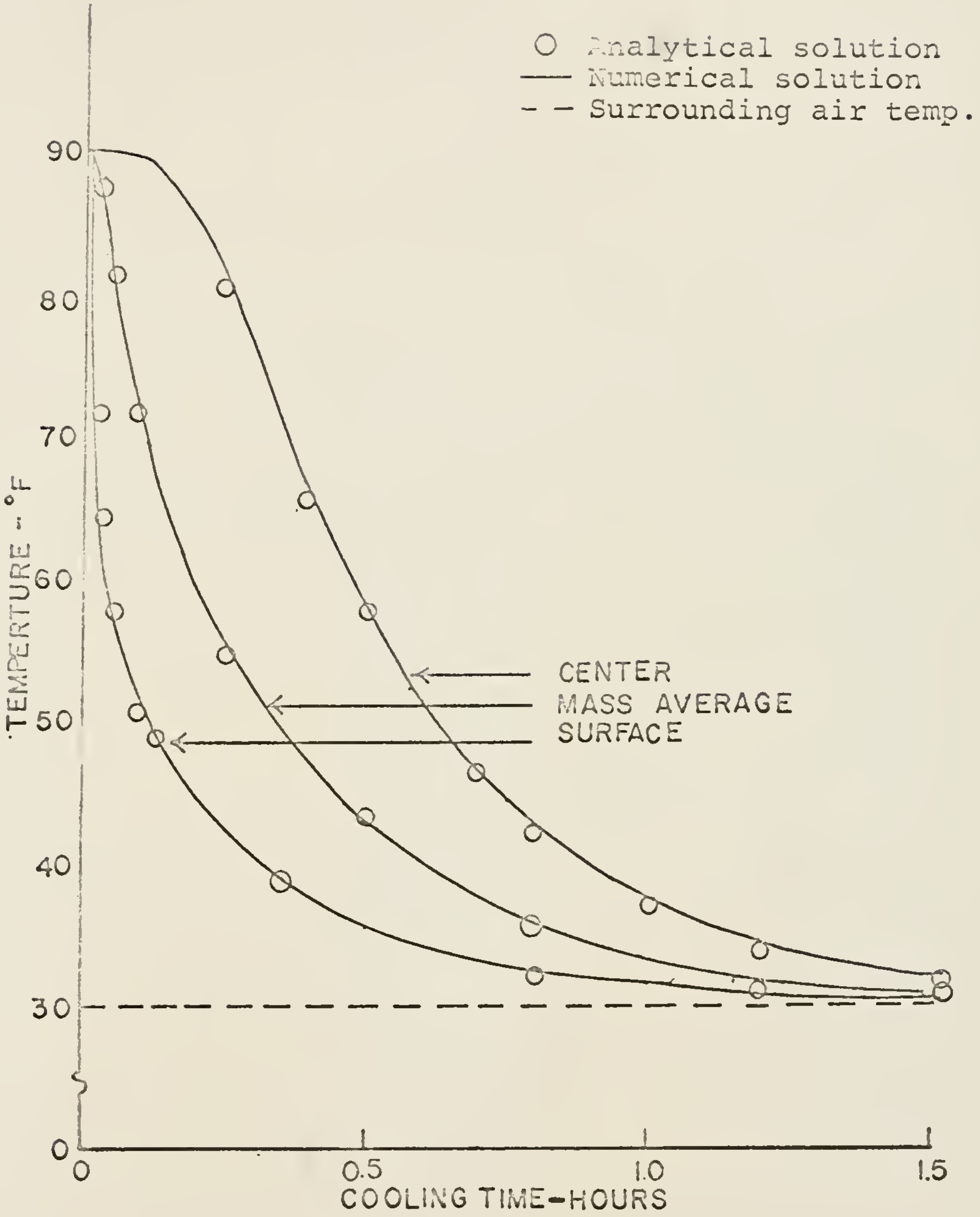

Figure 4. Comparison of analytical solution with numerical solution for heat conduction in a sphere

TEMPERATURE DISTRIBUTION WITHIN A BED OF CITRUS DURING COOLING

Laplace Transform Solution of Simplified Model

In the preceding section, solutions for temperature distribution within a single fruit were obtained. Now the analysis will be extended to include temperature distribution within a bed of citrus fruit. In this section a simplified model will be assumed in order that an exact mathematical solution can be obtained. This simplified model was developed by making the following assumptions:

a) No mass transfer occurs between the citrus fruit and the cooling medium.

b) There is no temperature gradient within the individual fruit.

c) The air velocity in all interstices of the bed will be constant.

d) No conduction heat transfer between the fruit.

e) Thermal properties of air and fruit are considered constant.

These assumptions are similar to those made by Schumann (45). The first assumption is believed to be reasonable due to the small amount of moisture loss from citrus during cooling (less than 1% for normal conditions).

This assumption has apparently introduced a considerable error for studies involving fruits and vegetables which do not have a waxy surface.

The second assumption is believed to be the weakest and probably causes a considerable error for the faster cooling rates. However, this error is believed to be minimized by using the mass-average temperature for the product. Although the last three assumptions are not precise, their effect is believed to be small.

In the next section the second assumption will be investigated by obtaining a numerical solution which accounts for temperature distribution within the fruits. The numerical solution will be compared with the exact mathematical solution obtained in this section, for a slow cooling rate which corresponds to a negligible temperature gradient in the individual fruit.

In order to obtain the differential equations describing the product temperture in a bed of citrus fruit and the temperature of the air flowing through it, a heat balance will be written for a volume A dx as shown in Figure 5. "A" is the cross-sectional area of the bed and dx is the height of the control volume. The following symbols will be used in this derivation:

T_a, temperature of air, °F

T_p, temperature of product, °F

h, convective heat transfer coefficient, BTU/hr ft^2°F

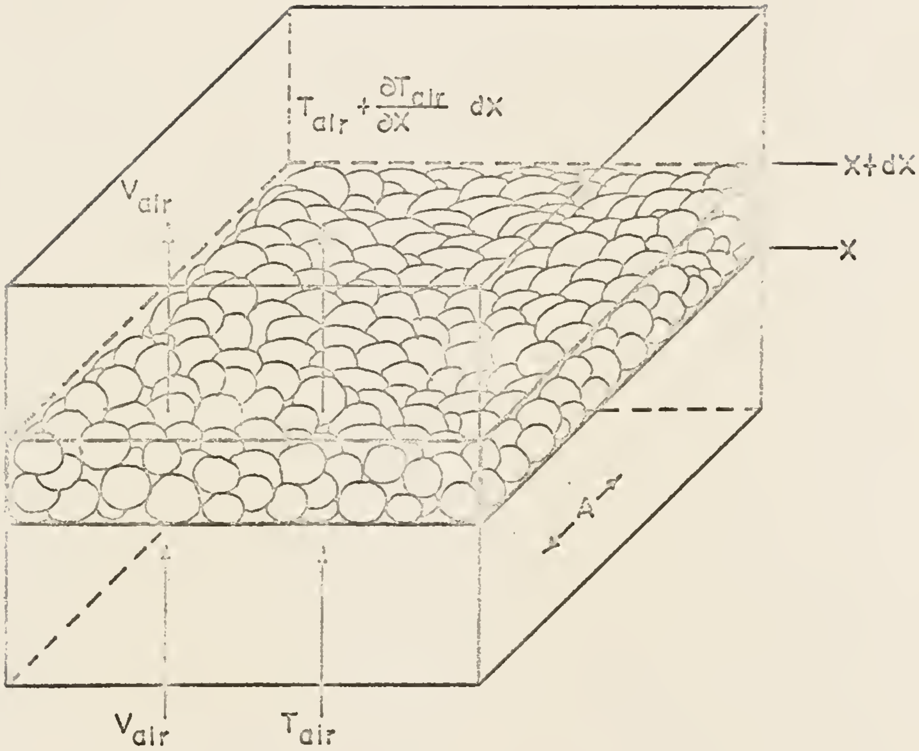

Figure 5. Control volume for heat balance on bed

A^*, product surface area per cubic foot, ft^{-1}

A, cross-sectional area of the packed bed, ft^2

V_a, superficial velocity of air, ft/hr

ρ_p, product bulk density, lb/ft^3

ρ_a, air density, lb/ft^3

c_a, specific heat air, BTU/lb °F

c_p, specific product, BTU/lb °F

θ_a, dimensionless temperature ratio of the air

θ_p, dimensionless temperature ratio of the product

Y, dimensionless height of packed bed

Z, dimensionless time

t, time, hr

μ, absolute viscosity, lb/ft-hr

x, distance from air inlet, ft

The amount of air flowing past a point "x" in the amount of time dt can be expressed as:

$$V_a A\rho_a \, dt \text{ (lb)} \qquad [26]$$

The heat content of the air entering A dx in dt is:

$$V_a A\rho_a c_a T_a \, dt \text{ (BTU)} \qquad [27]$$

The heat content of the air leaving A dx in dt is:

$$V_a A\rho_a c_a \left(T_a + \frac{\partial T_a}{\partial x} dx\right) dt \text{ (BTU)} \qquad [28]$$

The change in enthalpy of the air with respect to dx is the difference between equations [27] and [28] or

$$V_a A \rho_a c_a (\frac{\partial T_a}{\partial x} dx) dt \text{ (BTU)} \qquad [29]$$

The change in enthalpy of the air in the control volume with respect to time is equal to:

$$A dx \rho_a c_a \frac{\partial T_a}{\partial t} dt \qquad [30]$$

The total change in enthalpy of the air is:

$$A dx \rho_a c_a dt (V_a \frac{\partial T_a}{\partial x} + \frac{\partial T_a}{\partial t}) \qquad [31]$$

As air moves through the bed, convective heat transfer occurs. The enthalpy change of the air in time dt that results from this heat transfer is:

$$q_{conv} = h A^* (T_p - T_a) A dx dt \qquad [32]$$

where A* is the surface area of product per unit volume of the bed.

Setting equation [31] equal to [32], the enthalpy change in the air with respect to time and position, gives:

$$A \rho_a c_a (\frac{\partial T_a}{\partial t} + V_a \frac{\partial T_a}{\partial x}) dx dt =$$

$$h A^* (T_p - T_a) A dx dt \qquad [33]$$

or

$$\frac{1}{V_a} \quad \frac{T_a}{\partial t} \quad \frac{\partial T_a}{\partial x} + \frac{h\ A^*}{V_a\ \rho_a\ c_a} \quad (T_a - T_p) = 0 \qquad [34]$$

Equation [34] is the result of writing a heat balance on the air in the control volume A dx.

Now a heat balance will be written for the citrus fruit. At any time t the enthalpy of the volume A dx of the bed is:

$$\rho_p\ A\ dx\ c_p\ T_p \qquad [35]$$

At time t + dt the enthalpy is:

$$\rho_p\ A\ dx\ c_p\ (T_p + \frac{\partial T_p}{\partial t}\ dt) \qquad [36]$$

The change in enthalpy of the product in time dt is obtained by substracting equation [36] from [35]:

$$-\rho_p\ A\ dx\ c_p\ \frac{\partial T_p}{\partial t}\ dt \qquad [37]$$

This change in enthalpy of the product in the time dt is the result of heat transferred from the product (equation [37]).

Equating equations [37] and [33] gives:

$$-\rho_p\ \ c_p\ \frac{\partial T_p}{\partial t} = h\ A^*\ (T_p - T_a) \qquad [38]$$

Schumann (45) was the first person to obtain a solution of equations [34] and [38]. Businger (10), Bakker - Arkema and

and Bickert (5), and Huong et al. (29) observed that the $\frac{\partial T_a}{\partial t}$ in equation [34] is very small compared to V_a, the velocity of the cooling air, thus $\frac{\partial T_a}{\partial t}$ may be omitted from equation [34], making it possible to obtain a solution by Laplace transform. Then the two equations which must be solved are:

$$\frac{\partial T_a}{\partial x} + \frac{h\ A^*}{V_a\ \rho_a\ c_a} (T_a - T_p) = 0 \qquad [39]$$

and

$$\frac{\partial T_p}{\partial t} + \frac{h\ A^*}{\rho_p\ c_p} (T_p - T_a) = 0 \qquad [40]$$

The theory for this solution and the Laplace transforms were taken from Churchill (12).

It is advantageous to make the variables of temperature, time, and position dimensionless as follows:

Temperatures:

$$\frac{T_a - (T_p)_{t=0}}{(T_a)_{x=0} - (T_p)_{t=0}} = \Theta_a \qquad [41]$$

$$\frac{T_p - (T_p)_{t=0}}{(T_a)_{x=0} - (T_p)_{t=0}} = \Theta_p \qquad [42]$$

Distance:

$$\frac{h\ A^*}{\rho_a\ c_a\ V_a}\ x = Y \qquad [43]$$

Time:

$$\frac{h\ A^*}{\rho_p\ c_p}\ t = Z \qquad [44]$$

Substituting equations [41], [42], [43], and [44] into equations [39] and [40] gives:

$$\frac{\partial \Theta_a}{\partial Y} + \Theta_a - \Theta_p = 0 \qquad [45]$$

$$\frac{\partial \Theta_p}{\partial Z} + \Theta_p - \Theta_a = 0 \qquad [46]$$

In this study the initial fruit temperatures were uniform and the cooling air temperature was constant. This is expressed in terms of boundary and initial conditions as:

$$T_p\ (x,\ 0) = (T_p)_{t=o} \qquad [47]$$

and

$$T_a\ (O,\ t) = (T_a)_{x=o} \qquad [48]$$

In dimensionless form equations [47] and [48] becomes:

$$\Theta_p\ (Y,\ 0) = \frac{(T_p)_{t=o} - (T_p)_{t=o}}{(T_a)_{x=o} - (T_p)_{t=o}} = 0 \qquad [49]$$

and

$$\Theta_a\ (0,\ Z) = \frac{(T_a)_{x=0} - (T_p)_{t=o}}{(T_a)_{x=o} - (T_p)_{t=o}} \qquad [50]$$

Equations [45], [46], [49], and [50] can be solved by Laplace transforms. Let Laplace transforms

$$L_Y\ [\Theta_a\ (Y,\ Z)] = F\ (s,\ Z)$$

$$L_Y\ [\Theta_p\ (Y,\ Z)] = G\ (s,\ Z)$$

and

$$L_Y\ [\Theta_a'\ (Y,\ Z)] = SF\ (s,\ Z) - \Theta_a\ (0,\ Z)$$

Taking the Laplace transforms of equations [45] and [46] w. r. t. Y (Y → s) gives:

$$s\ F\ (s,\ Z) - \Theta_a\ (0,\ Z) + F\ (s,\ Z) - G\ (s,\ Z) = 0 \qquad [51]$$

and

$$\frac{dG\ (s,Z)}{d\ Z} + G\ (s,\ Z) - F\ (s,\ Z) = 0 \qquad [52]$$

at

$$Y = 0,\ \Theta_a\ (0,\ Z) = 1$$

substituting in equation [51] gives:

$$F\ (s,\ Z) = \frac{1 + G\ (s,\ Z)}{s + 1} \qquad [53]$$

substitute equation [53] into equation [52], then

$$\frac{d\ G\ (s,\ Z)}{d\ Z} = \frac{1}{s + 1} + \frac{G\ (s,\ Z)}{s + 1} - G\ (s,\ Z) =$$

$$\frac{1}{s + 1} - \frac{s}{s + 1}\ G\ (s,\ Z)$$

or

$$\frac{d\ G\ (s,Z)}{d\ Z} + \frac{s}{s + 1}\ G\ (s,\ Z) = \frac{1}{s + 1} \qquad [54]$$

Equation [54] is an ordinary differential equation of first order; the general solution is:

$$G\ (s,\ Z) = \frac{1}{s} + C_1 e^{-\frac{s}{s + 1}\ Z} \qquad [55]$$

Using I.C. at Z = 0

$$\Theta_a\ (Y,\ o) = 0$$

Thus,

$$G\ (s,\ 0) = 0$$

substitution into equation [55], yields

$$C_1 = -\ \frac{1}{s}$$

$$G\ (z,\ Z) = \frac{1}{s} - \frac{1}{s}\ e - \frac{s}{s + 1}\ Z \qquad [56]$$

Taking the inverse transform w. r. t. s. (s → Y), gives:

$$\theta_p\ (Y,\ Z) = L_s^{-1}\ [G\ (s,\ Z)] =$$

$$L_s^{-1}\ [\frac{1}{s} - \frac{1}{s}\ e - \frac{s}{s + 1}\ Z] \qquad [57]$$

where L_s^{-1} is the symbol for the inverse Laplace transform w. r. t. s.

Now rearrange $[\frac{1}{s} - \frac{1}{s}\ e - \frac{s}{s + 1}\ Z]$ so that available transform pairs can be used; since

$$\frac{1}{s}\ e - \frac{s}{s + 1}\ Z$$

$$= \frac{1}{s} + \frac{1}{s}\ e - \frac{1}{s + 1}\ Z - \frac{1}{s}$$

$$= \frac{1}{s} + \frac{1}{s + 1}\ (\frac{s + 1}{s})\ [e - \frac{s}{s + 1}\ Z - 1]$$

$$= \frac{1}{s} - \frac{1}{s+1} \int_0^Z e^{-\frac{s}{s+1} Z} dZ$$

$$= \frac{1}{s} - \int_0^Z \frac{1}{s+1} e^{-(1-\frac{1}{s+1}) Z} dZ$$

$$= \frac{1}{s} - \int_0^Z e^{-Z} \frac{1}{s+1} e^{\frac{1}{s+1} Z} dZ$$

Thus,

$$\frac{1}{s} - \frac{1}{s} e^{-\frac{s}{s+1} Z} = \int_0^Z e^{-Z} \frac{1}{s+1} e^{\frac{1}{s+1} Z} dZ$$

and we have:

$$\Theta_p(Y,Z) = L_s^{-1} \left[\int_0^Z e^{-Z} \frac{1}{s+1} e^{\frac{1}{s+1} Z} dZ \right] \qquad [58]$$

Utilizing the substitution theorem and tables of Laplace transform pairs given by Churchill (12):

$$f(s-a) = L\,[e^{at} F(t)] \qquad [59]$$

$$\frac{1}{s^{\nu}} e^{k/s} = L\,[(t/k)^{(\nu-1)/2} I_{\nu-1} (2\sqrt{kt})] \qquad [60]$$

where $\nu>0$

For this application, $a = 1$, $t = Y$, $\nu = 1$, $k = Z$. Applying equation [59] to equation [58] gives:

$$\Theta_p (Y, Z)\, e^{Y} = L_s^{-1}\left[\left(\int_0^Z e^{-Z}\, dZ\right)\left(\int_0^Z \frac{1}{s}\, e^{Z/s}\, dZ\right)\right]$$

Now applying equation [60] gives:

$$\Theta_p (Y, Z) = e^{-Y} \int_0^Z e^{-Z}\, I_o (2 \sqrt{YZ})\, dZ \qquad [61]$$

which is the solution for the product temperature as a function of position in the bed and time.

Differentiating equation [61] w.r.t. Z gives:

$$\frac{\partial \Theta \rho (Y,Z)}{\partial Z} = \frac{\partial}{\partial Z} \int_0^Z e^{-(Y + Z)}\, I_o (2 \sqrt{YX})\, dz$$

$$= e^{-(Y + Z)}\, I_o (2 \sqrt{YX})\, dZ$$

substituting into equation [46] yields:

$$\Theta_a (Y, Z) = \frac{\partial \Theta_p (Y, Z)}{\partial Z} + \Theta_a (Y, Z)$$

$$= e^{-(Y + Z)}\, I_o (2 \sqrt{YZ}) + e^{-Y} \int_0^Z e^{-Z}\, I_o (2 \sqrt{YZ})\, dZ$$

[62]

which is the solution for the air temperature as a function of position in the bed and time.

In equation [61] and [62], $I_o(2\sqrt{YZ})$ is known as the modified Bessel function of the first kind, of order zero, with argument $2\sqrt{YZ}$; in general,

$$I_\nu(x) = \sum_{K=o}^{\infty} \frac{(x/2)^{2K+\nu}}{K!\,(K+\nu)!}$$

Equations [61] and [62] have been evaluated numerically (19) and are shown in Figures 6 and 7.

Numerical Solution of Realistic Model

The notations and assumptions used in the preceding section will apply here, except that temperature gradients within the individual fruit may exist, but are a function of radius only. Thus, an additional equation is required to describe the conduction heat transfer within the fruit. This equation, with its initial and boundary conditions, was discussed in a previous section (equation [8], [9], [10]).

Consider an energy balance written on the air flowing through a differential volume a dx, as depicted in Figure 5.

Energy out = energy in + change in internal energy of the product:

$$V_a\ \rho_a\ c_a\ A\ t_a\ dt + V_a\ \rho_a\ c_a\ A\ \frac{\partial T_a}{\partial x}\ dx\ dt =$$

$$V_a\ \rho_a\ c_a\ A\ t_a\ dt - \rho_p\ c_p\ \frac{\partial T_p}{\partial t}\ dt\ A\ dx$$

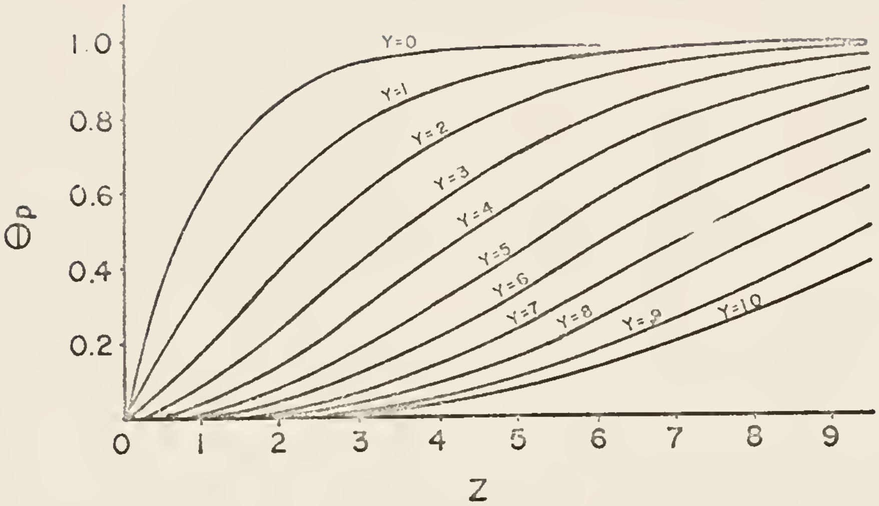

Figure 6. Schumann's curves for temperature history of solid for values of Y from 0 to 10

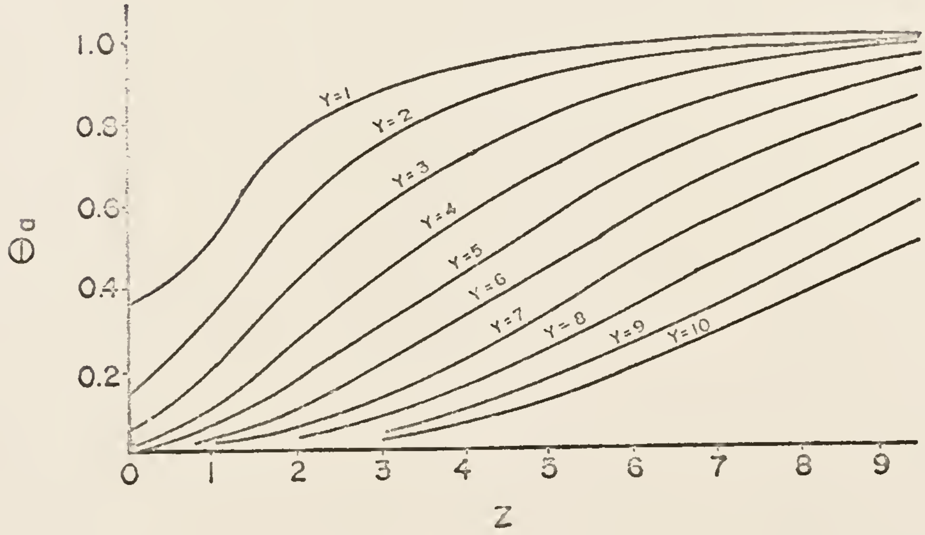

Figure 7. Schumann's curves for temperature history of gas for values of Y from 1 to 10

or

$$\frac{\partial T}{\partial x} = \frac{\rho_p\ c_p}{V_a\ \rho_a\ c_a}\ \frac{\partial T_p}{\partial t} \qquad [63]$$

Thus, equations [8], [9], [10], [63] describe the heat transfer within a bed of fruit in which temperature gradients exist within the individual fruit. A numerical solution for this set of equations will be developed utilizing the numerical solution that was previously obtained for the conduction equation.

Considering the differential layer of the bed to be a finite layer, equation [63] becomes:

$$\frac{\Delta T_a}{\Delta x} = \frac{\rho_p\ c_p\ \Delta T_p}{V_a\ \rho_a\ c_a\ \Delta t} \qquad [64]$$

Equation [64] along with equations [23], [24], [25], which were derived in a previous section, were used to develop a computer program which results in a printout of fruit temperature as a function of 1) position in bed, 2) point in the individual fruit and 3) time. In order to solve this set of equations it is necessary to compute the mass-average temperature of the fruit after each time period. This is accomplished by assuming a linear temperature profile within each segment of the fruit. This causes the mass-average temperature to be located at the mass-average point, which is located at r/radius equal to 0.7937 for a sphere. Mass-average temperature denotes a single value from the temperature profile of a product that would become the uniform product temperature upon reaching equilibrium under adiabatic conditions.

Since the temperature profile in a sphere is not linear, the mass-average temperature will not be located exactly at the mass-average point and will shift according to the shape of the temperature profile. For this solution the mass-average temperature of the fruit was determined by computing the mass-average temperature of each spherical shell and then computing a weighted average temperature based on the mass of each spherical shell.

In order to account for the shift in the location of the mass-average temperature due to the low heat capacity of the rind (pC), the outer and inner shells of the spherical model were given values for heat capacity corresponding to that of the rind and juice vesicles as determined separately. The heat capacities for the rind and juice vesicles of oranges and grapefruit were obtained from the findings of Bennett et al. (7) as 23.7, 57.6, 30.0, and 57.2 BTU/ft^3-°F respectively.

The average thickness of the rind for Valencia oranges and Marsh grapefruit was also taken from this reference and roughly corresponds to the outer segment of a ten-segment sphere for oranges and the outer two segments for a ten-segment sphere for grapefruit.

Soule *et al*. (48) experimentally located the points of mass-average temperature during forced-air cooling for oranges, grapefruit and tangelos. The values of r/radius were 0.7856, 0.7722, and 0.7953, respectively. Evidently the lower densities of the rind shift the location of the mass average temperature towards the center of the fruit. Soule *et al*. also presented their results in terms of locus of mass average temperature versus cooling time for a specific cooling rate (Figure 10). Bennett *et al*. (8) conducted the same type of tests for grapefruit cooled in agitated ice water (Figure 9) and got a much larger shift in the location of the mass-average temperature.

Each step of the numerical solution presented in this section is indicated by a flow diagram for the computer program (Figure 8). The computer program and sample output data for cooling a deep bed of citrus fruit are shown in Appendix B. This output is shown in graphical form in the Data and Results section of this chapter.

Determination of Convective Heat Transfer Coefficient and Thermal Diffusivity

Theory

Transfer of heat by transport of fluid material is known as convection. The transport may be natural convection, caused by buoyancy forces; or forced convection, accomplished

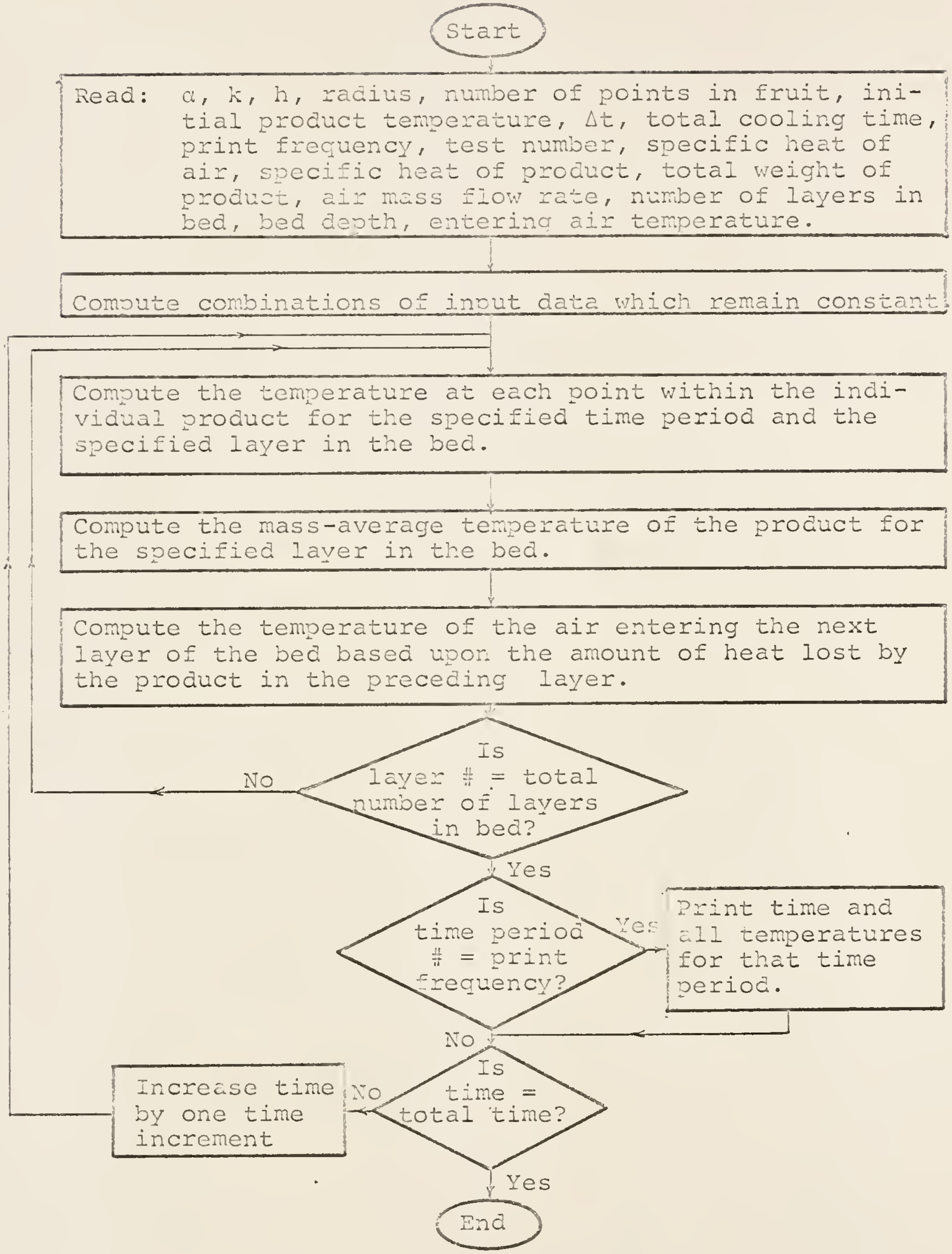
Start
Read: α, k, h, radius, number of points in fruit, initial product temperature, Δt, total cooling time, print frequency, test number, specific heat of air, specific heat of product, total weight of product, air mass flow rate, number of layers in bed, bed depth, entering air temperature.
Compute combinations of input data which remain constant
Compute the temperature at each point within the individual product for the specified time period and the specified layer in the bed.
Compute the mass-average temperature of the product for the specified layer in the bed.
Compute the temperature of the air entering the next layer of the bed based upon the amount of heat lost by the product in the preceding layer.
Is layer # = total number of layers in bed?
No
Yes
Is time period # = print frequency?
Yes
Print time and all temperatures for that time period.
No
Is time = total time?
No
Increase time by one time increment
Yes
End

Figure 8. Flow diagram for the digital computer program to solve deep bed heat transfer equations

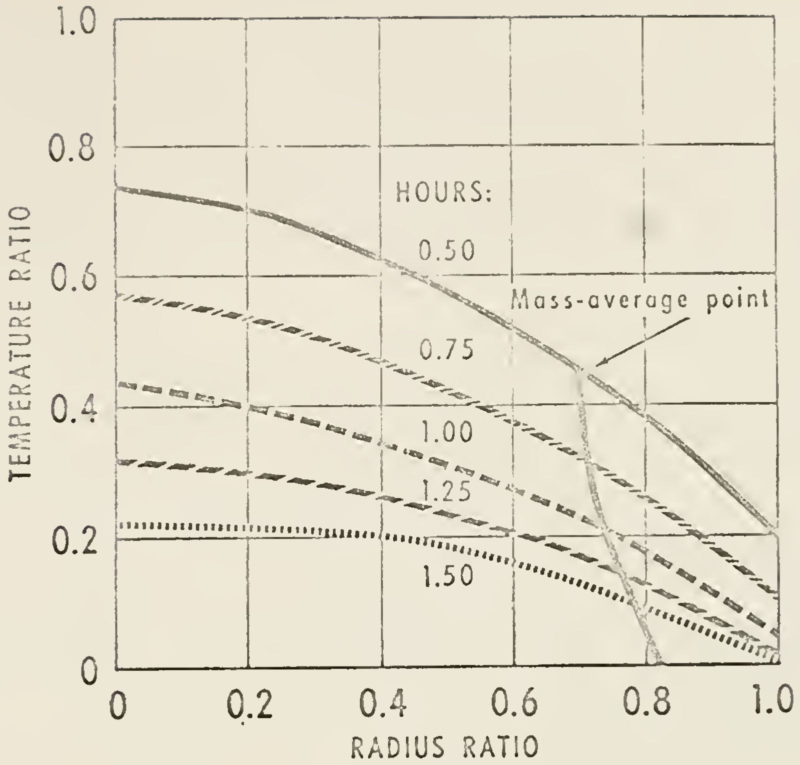

Figure 9. Magnitude and location of mass-average temperature of Marsh grapefruit cooled in agitated ice water

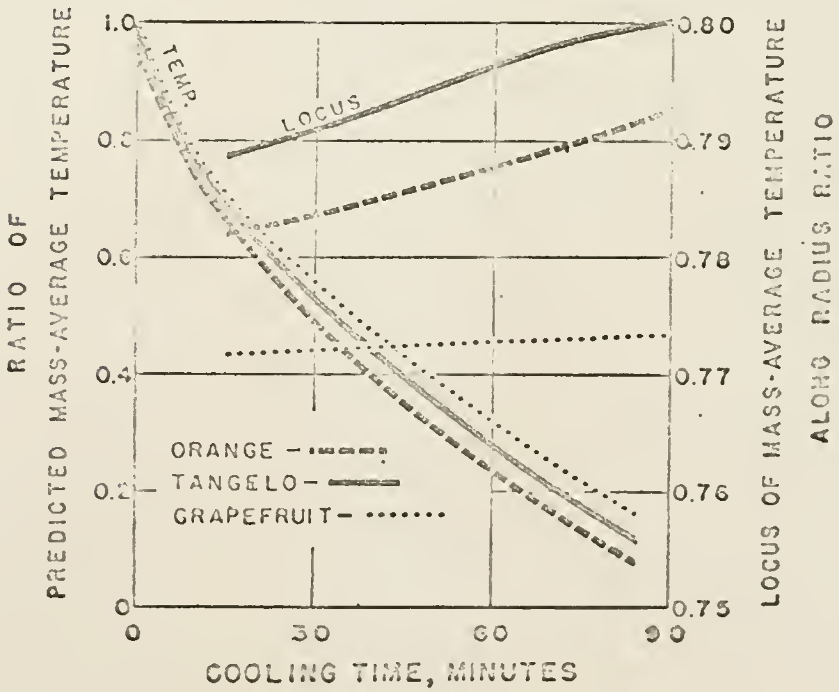

Figure 10. Unaccomplished temperature change and location of mass-average temperature during forced-air cooling

by some external means such as a pump or fan. The principal resistance to heat transfer is found in a relatively stagnant laminar layer adjacent to the solid surface. In laminar flow, fluid particles move only in a direction parallel to the solid surface, meaning that heat transfer through this layer must be accomplished by conduction only. Adjacent to this laminar layer is usually found a turbulent layer of slow moving particles which also gives resistance to heat transfer between the main bulk fluid and the solid surface. These two regions constitute the boundary layer and present a very complex problem when analyzed mathematically. Thus, the study of convection heat transfer, in general, has been empirical and semi-empirical.

The rate of convection heat transfer is proportional to the difference in temperature between the surface and the main bulk of fluid and to the surface area, thus:

$$q_c = h\ A\ (T_s - T_\infty) \qquad [65]$$

The proportionality constant (h) is called the convective heat transfer coefficient and is determined by the properties of the fluid, the nature of the surface, and the manner and velocity of fluid flow past the surface.

One method which has been used successfully to establish a relationship for h as a function of the important properties of the system is dimensional analysis. This method of analysis identifies the necessary dimensionless groupings as the Nusselt number (hD/k), the Reynolds number ($\rho DV/\mu$), the Prandtl number ($c\mu/k$), and sometimes a shape factor (l/D).

Numerous experimental and semi-empirical studies have been made for flow over various shaped objects, utilizing these dimensionless parameters. McAdams (35) recommended equation [66] for calculating the average convective heat transfer coefficient, h, for spheres heated or cooled by a gas for the Reynolds number range 25 to 100,000.

$$\frac{h\ D_p}{k} = 0.37\ \left(\frac{V\ \rho\ D}{\mu}\right)^{0.6} \qquad [66]$$

where:

D = diameter of sphere

k = thermal conductivity of the gas

V = velocity of fluid stream

ρ = density of fluid

μ = viscosity of fluid

Several equations for calculating h in a packed bed have been recommended, however, they give quite varied results. Eckert (16) proposed a general equation for h for a packed bed of solid particles:

$$\frac{hd}{k} = 0.8\ (Re_i)^{0.7}\ \left(\frac{c\mu}{k}\right)^{1/3} \qquad [67]$$

where

d = equivalent spherical diameter

Re_i = Reynolds number $(\frac{\rho V d}{\mu})$ where V is the interstitial velocity through the bed

c = specific heat of gas

Daizo and Motoyuki (13) gave the heat transfer correlation as:

$$\frac{hD}{k} = 1.2 \left[\frac{1-(1-\varepsilon)^{5/3}}{w}\right]^{1/3} \left[\frac{DcG}{k}\right]^{1/3} \qquad [68]$$

where

$w = 2-3r + 5r^5-2r^6$

$r = (1-\varepsilon)^{1/3}$

ε = void fraction of packed bed

G = superficial mass velocity of gas, lb/hr-ft^2

Lebedev and Petror-Denison (32) presented a correlation based on hydrodynamics:

$$\frac{hD}{k} = 0.124 \, R_e^{0.8} \, Pr^{0.33} \qquad [69]$$

where

$Pr = \frac{\mu c}{k}$

A large amount of experimental information on heat transfer in packed beds has been analyzed by chemical engineers (51) to arrive at the following empirical correlations:

$$\frac{h}{cG} Pr^{2/3} = 0.91\ Re_m^{-0.51}\ \psi,\quad Re_m < 50 \qquad [70]$$

$$\frac{h}{cG} Pr^{2/3} = 0.61\ Re_m^{-0.41}\ \psi,\quad Re_m > 50 \qquad [71]$$

where

$Re_m = \frac{G}{A^*\mu\psi}$ = modified Reynolds number

A^* = solid particle surface area per unit bed volume

The quantity ψ is an empirical coefficient that depends on the particle shape. A few sample values of ψ are given in Table 3(51).

Table 3. Particle Shape Factors for Packed-Bed Correlation.

Particle shape	ψ
Spheres	1.00
Cylinders	0.91
Flakes	0.86
Raschig rings	0.79
Partition rings	0.67
Berl saddles	0.80

Barker (6) has made an extensive review of literature on heat transfer in packed and fluidized beds and has compiled a bibliography of nearly 500 publications.

Smith *et al*. (47) describes a method of experimentally determining the convective heat transfer coefficient (h) and the thermal diffusivity (α) for regular shaped objects as well as for anomalous shapes. His method is based on the solution of the Fourier conduction equation for each specified geometry. The general form of the prediction equation, for boundary conditions of finite internal and surface thermal resistance is:

$$\theta = f_1\ (Fo,\ Bi,\ L_d,\ A,\ B) \qquad [72]$$

where

θ = dimensionless temperature ratio

$Fo = \frac{\alpha\tau}{\ell^2}$, Fourier number

$Bi = \frac{h\ell}{k}$, Biot number

L_d = Distance ratio indicating fractional distance from the center

$A = a/\ell$, distance ratio used to define the geometry of the ellipsoidal model for the shape

$B = b/\ell$

ℓ = characteristic length or minimum distance within the object with maximum temperature difference during transient period

a = semimajor axis of smaller model ellipse

b = semimajor axis of larger model ellipse

The solution of the heat conduction equation for a sphere was presented in the previous chapter as:

$$\Theta = 2 \sum_{n=1}^{\infty} \left(\frac{\sin M_n a - M_n a \cos M_n a}{M_n a - \sin M_n a \cos M_n a} \right) e^{-\alpha M_n^2 t} \frac{\sin M_n r}{M_n r} \qquad [21]$$

M_n is the separation constant arising from the solution of the differential equation and denotes the roots of the transcendental equation.

$$M_n a \cos M_n a = (1-Bi) \sin M_n a \qquad [73]$$

Smith et al. (47) suggested that equations [21] and [73] for various geometrics could be represented by

$$\Theta = f_2(A,B,Bi,L_d) e^{-Fo[f_3(A,B,Bi)]^2} \qquad [74]$$

with the following restrictions.

Temperatures in the solid are restricted to those along the characteristic length; the geometry may be described by the parameters A and B; only the first term of the infinite series is used; and M_n is used as a parameter for any specified geometry. For a specified geometry, equation [74] could be written as:

$$\Theta = Ce^{-M_1^2 Fo} \qquad [75]$$

Then a geometry index G is defined as the number that, when multiplied by π^2, gives the appropriate value for the coefficient M_1^2 in equation [75], for the geometry concerned and the conditions of negligible surface thermal resistance.

Experimental values for G ranged from 0.25 to 1.00 for the infinite slab and the sphere, respectively. The index for anamalons shapes is described by equation [76].

$$G = 1/4 + 3/8A^2 + 3/8B^2 \qquad [76]$$

For conditions of negligible surface thermal resistance (large h) and considering successive values of θ and Fo, Smith et al. arrived at the following equation for determining thermal diffusivity (α):

$$\alpha = \frac{\ell^2}{M_1^2} \left[\frac{\ln\theta_1 - \ln\theta_2}{t_1 - t_2}\right] \qquad [77]$$

For negligible surface thermal resistance:

$$M_1^2 = G\pi^2 \qquad [78]$$

For conditions other than negligible surface thermal resistance (finite h) the functional relationship between M_1^2 and G may be expressed in the form:

$$M_1^2 = f_3\ (G, Bi) \qquad [79]$$

A nomograph for evaluating elements of this equation is given in Figure 11.

After α has been determined from time-temperature data taken from a test where h is large, such as an agitated water bath, the convection heat transfer coefficient (h) can be determined from the following equation and Figure 11.

$$M_1^2 = \frac{\ell^2}{\alpha} \left[\frac{\ln\theta_1 - \ln\theta_2}{t_1 - t_2}\right] \qquad [80]$$

This equation is analogous to equation [77], but for conditions where h is finite and M_1^2 is no longer described by $M_1^2 = G\pi^2$.

One must be cautious when using equations [77] and [80] to insure that the boundary and initial conditions of the original conduction equation are satisfied, i.e. uniform initial temperature distribution and constant fluid temperature surrounding the object.

Minh et al. (36) evidently disregarded the boundary condition of constant fluid temperature when he used equation [80] to determine h at three depths within a bed of potatoes. It is obvious that this boundary condition is satisfied only for the layer of product at the entrance of the bed. Their values for h decreased as distance into bed increased, with the entrance value being approximately three times the exit value. They developed the following equation for white potatoes at the entrance to the bed:

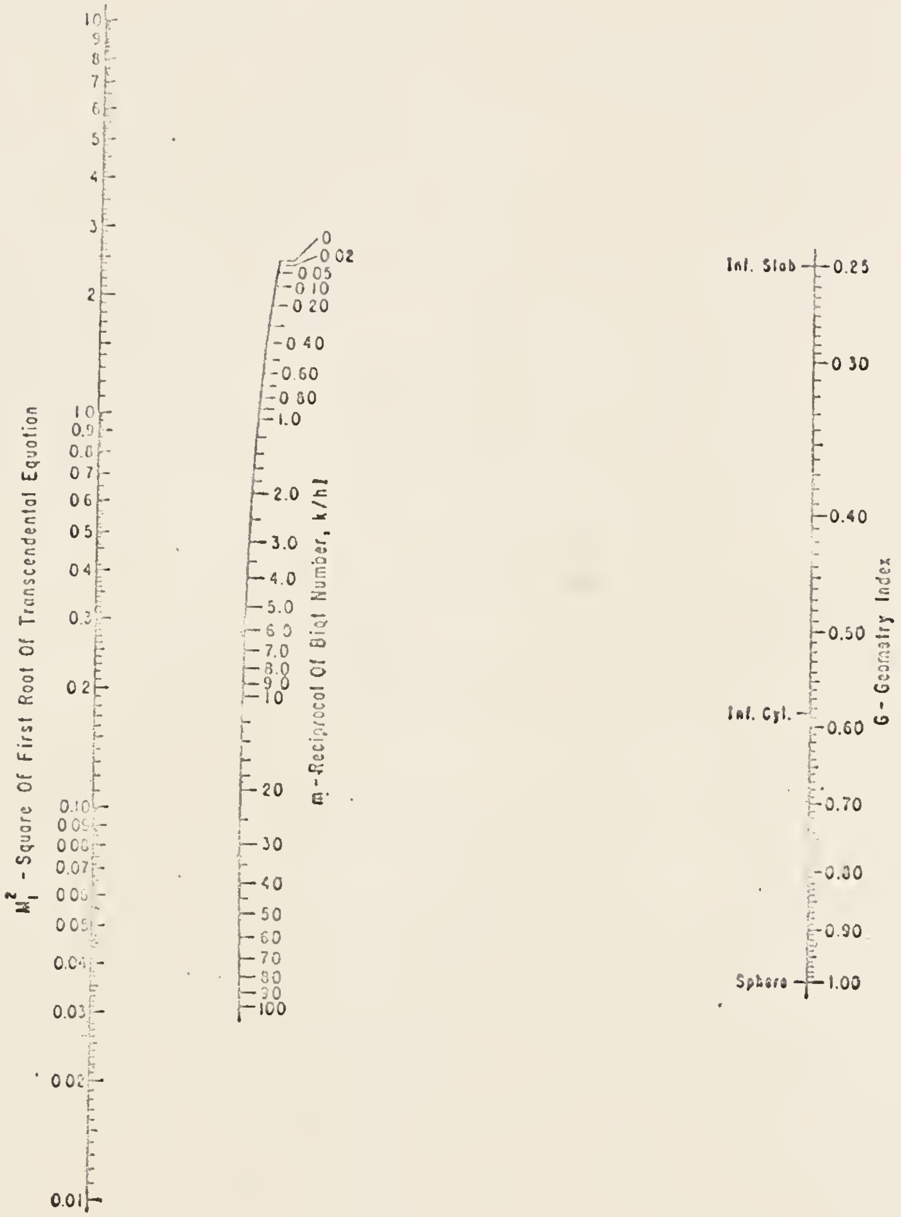

Figure 11. Nomograph for evaluating elements of the equation: $M_1^2 = f_3(G,Bi)$

$$\frac{h\ell}{K} = 0.564\ (Re)^{0.538}\ (Pr)^{1/3} \qquad [81]$$

Bennett et al. (9) conducted tests on the cooling of citrus fruits in bulk and developed a prediction equation for what they called an effective h (h_{eff}) as indicated in Newton's equation:

$$h_{eff} = Q/(A\Delta t) \qquad [82]$$

where for this equation, Q is the total heat removed from the mass of fruit per hour, A is the total surface area of all the fruit based on average diameter, and Δt is the average difference between temperature on the surface of the fruit and that of the air. They did not attempt to account for any variation of h as a function of position within the bed. By averaging all the values obtained at various points in the bed, they obtained the following heat transfer correlations:

$$\frac{hD}{k} = C(Re_i)^n \qquad [83]$$

where C and n are constants that were experimentally evaluated as indicated in Table 4. The correlation coefficient is denoted by r. Their reported correlation coefficients are indicative of the difficulty encountered in obtaining reliable data. In the tests from which these data were obtained the air entering the bed was not held constant, thus making it difficult to analyze the results and prevents the determination of h by the method described by Smith *et al*. (46).

Table 4. Coefficients and Exponents for Emperical Heat Transfer Correlations

	C	N	r
Orange	6.95	0.297	0.610
Grapefruit	40.9	0.153	0.204
Tangelo	6.30	0.314	0.464
Combined	5.05	0.333	0.586

Development of Method

A method similar to that described by Bennett *et al*. (9) utilizing Newton's equation was used in an attempt to investigate the variation of h with respect to depth in a bed of oranges. However, preliminary results indicated the precision of the measurements was not sufficient to detect any variation in h using this method. It is very difficult to obtain high level precision using this method since the placement of the thermocouples is very critical in addition to the normal variation which occurs in a bed of irregularly shaped particles. The effect of this irregularity on the determination of h is greater for this method than it is for the method described by Smith et al. Bennett et al. utilized surface temperatures which are more sensitive to local variations in the surrounding fluid and are in general more difficult to measure than internal temperatures. One notable advantage of the method described by Smith et al. is that, theoretically, it is independent of the location of the thermocouple and thus eliminates that source of error. The method for determining h, described by Smith et al. and previously outlined in this section, was used to evaluate h for the entrance layer of the bed. The values for h were determined for beds of oranges and grapefruit as a function of superficial air velocity (V) entering the bed. The results are presented in Figures 20 and 21 (Data and Results section) in terms of a Nusselt number versus Reynolds number plot. Since these h values were determined only for the bottom layer of fruit, it is expected that they do not represent the best average value for the entire bed.

To overcome this deficiency, another method for evaluating h was investigated. Using the h values determined for the bottom layer, the computer model for deep bed cooling, as described by Figure 8, was run for each air flow rate. Mass average temperatures from the model were compared with those from the experimental data for each test.

From these comparisons, h values were estimated so that at least one value would be lower and one value would be higher than the value which gave the best fit for the experimental data. Then these values were used to generate more data from the computer model. A comparison of the experimental and theoretical mass average temperature of the entire bed, determined at approximately "one half cooling time," was used as the criterion for determining the h value which resulted in the best fit to the experimental data. A one half cooling time is the time required to reduce the fruit temperature by one half of the difference between the initial product temperature and the temperature of the cooling air. These results are also shown in Figures 20, 21, and 22 (Data and Results section).

A linear regression, by least squares, of the log N versus log Re was used to evaluate the constants c and n in equation [84].

$$Nu = c(Re)^n \qquad [84]$$

where:

$Nu = \frac{hD}{K}$, Nusselt number

$Re = \frac{VD}{\mu}$, Reynolds number

A separate regression was made for each group of data as indicated in Figures 20, 21, and 22 and Table 5. Theoretically, oranges and grapefruit should be governed by the same equation. However, some variation would be expected since a homogeneous sphere is only an approximation of a grapefruit and an orange.

Table 5. Coefficients, Exponents and Linear Correlation Coefficients for Equation [84] Determined for Forced-Air Cooling in Bulk Containers.

	c	n	r
Orange (Bottom layer)	0.859	0.521	0.964
Orange (Average for bed)	0.374	0.620	0.991
Grapefruit (Bottom layer)	7.17	0.272	0.832
Grapefruit (Average for bed)	1.04	0.482	0.987
Oranges and Grapefruit Combined (Average for bed)	0.607	0.555	0.977

Experimental Evaluation of Thermal Diffusivity

The thermal diffusivity (α) was determined experimentally for oranges and grapefruit by the method described by Smith *et al*. (47). The fruit were cooled in an agitated water bath with a thermocouple placed at the approximate mass average point. Theoretically, the results are independent of the thermocouple position. The temperatures were recorded by a six-point potentiometer with a print frequency of three seconds. Equation [77] was used to calculate α, with the term $\frac{\log_e\theta_1 - \log_e\theta_2}{t_1 - t_2}$ determined from a semi-log plot of the experimental data. M_1^2 was calculated using equation [76] and [78]. Oranges were considered perfect spheres, while G for grapefruit was calculated from equation [77], based on the equatorial and polar diameters of each fruit tested. The thermal diffusivity (α) for oranges was found to be 0.00437 ft^2/hr with a standard deviation of 0.00010 based on five tests, while α for grapefruit was found to be 0.00362 ft^2/hr with a standard deviation of 0.00015 based on five tests.

Design and Description of Experimental Facilities

A number of investigators have conducted research on precooling using forced-air cooling equipment. Most of these investigators emphasized the response of the product to cooling. A lesser number were concerned with the variable factors which influence the design and operation of cooling equipment.

A forced-air cooler designed specifically for research, with a capability of controlling all of the important variables relating to cooling biological materials, was constructed for this study. Air velocity, air temperature, relative humidity, and product arrangement were the variables that could be controlled. Temperature distribution within the individual product and within the bulk load, static pressure loss through the product, and product moisture loss were among the parameters that could be measured during a test.

Basic Construction of Precooler

Figure 12 shows the general location of the components and the air circulation diagram for the cooling facility. The overall length of the cooler is 25 feet and the outside dimensions of the product chamber section are 8x8x12 feet. The product chamber was designed to accommodate a product load which could have dimensions of up to 4x4 feet in cross-section and 8 feet high. This would allow experimental units of pallet boxes or pallet loads. The basic wall construction is 2x4-inch studding with 1/2-inch plywood on each side. Insulation material consisted of rigid polyurethane foamed in place between the plywood sheets. The outside of the cooler was sealed with caulking and epoxy paint. The complete structure is built on skids and can be moved when necessary.

Refrigeration Components and Controls

Figure 13 shows each component of the refrigeration system. The condensing unit is water cooled and is preferred over an air-cooled unit when precise control is necessary, since changes in ambient conditions have little effect on its performance. The two-cylinder compressor is belt driven

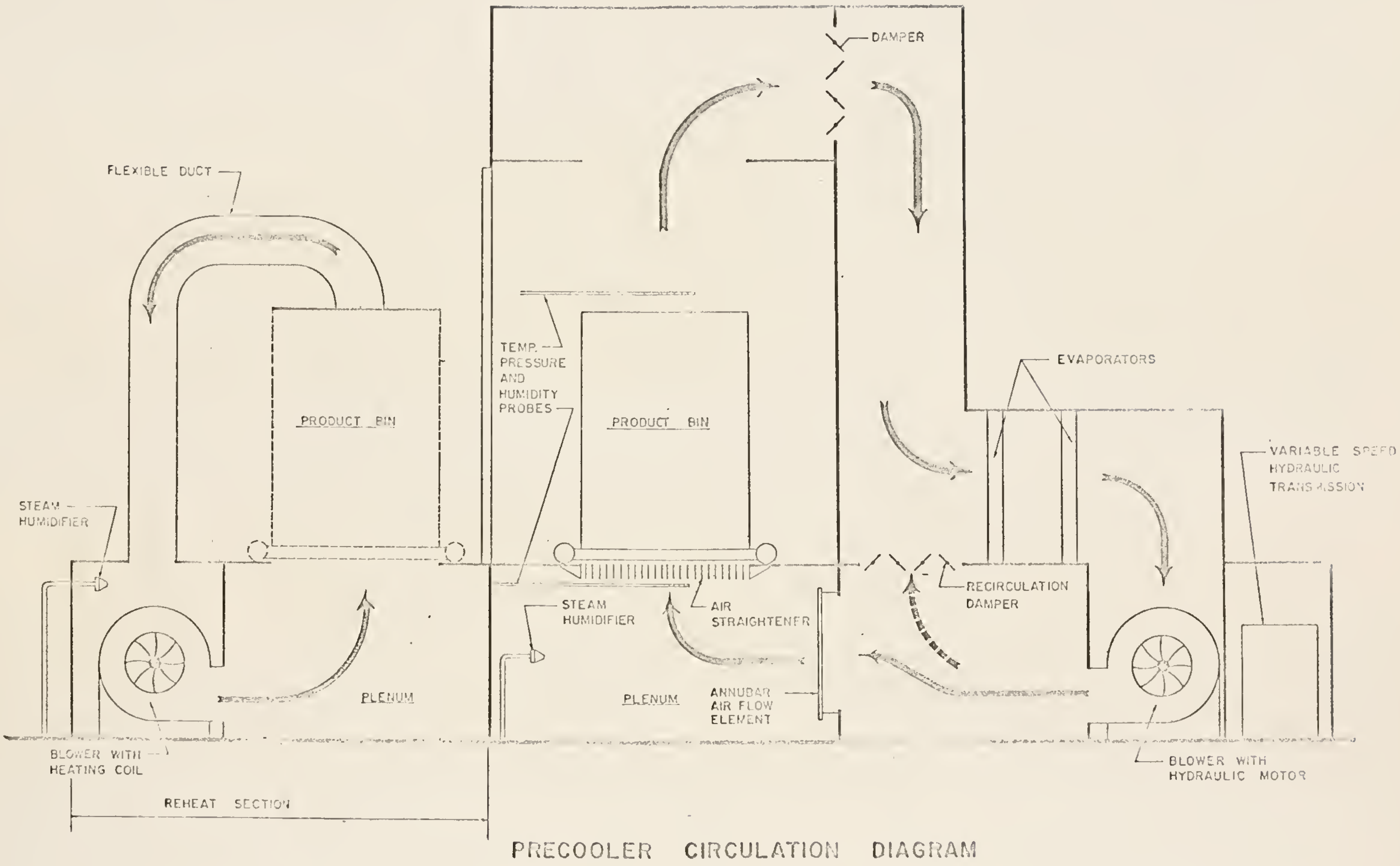

Figure 12. Elevation view of forced-air cooler

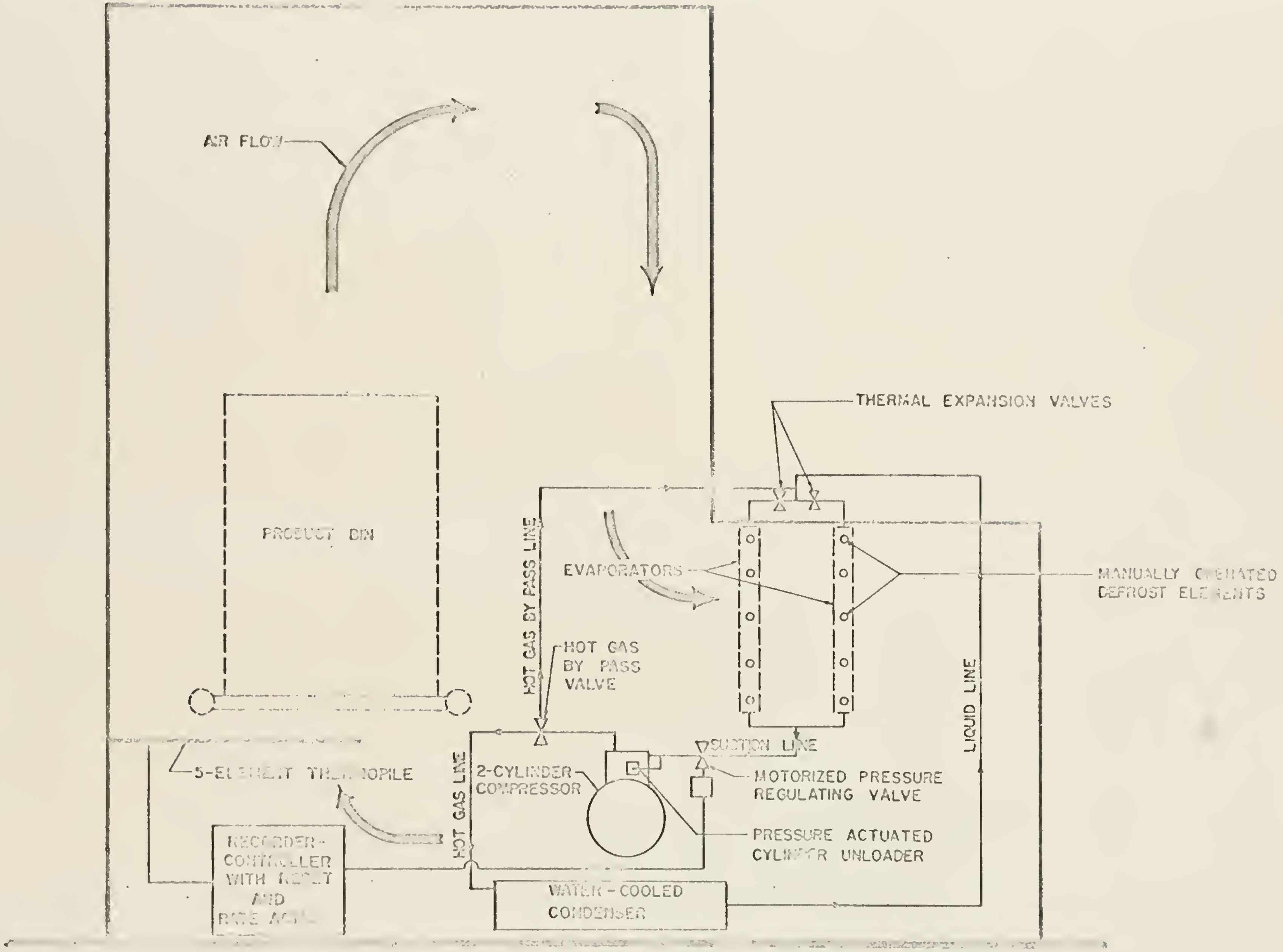

Figure 13. Precooler refrigeration components and controls

by a 7-1/2-hp motor and can accommodate up to 20-hp if more capacity is needed. The compressor is equipped with an automatic cylinder unloader which inactivates one of the cylinders when the suction pressure drops below an adjustable preset value. A belt-driven compressor is desirable when the system is to be used for various applications where the evaporator temperatures may vary over a wide range. The following example will illustrate this point.

Example illustrating capacity of system

Using Refrigerant 502 with a compressor rpm of 520, evaporator temperature of 30 F and a condenser temperature of 100 F, 7 tons of cooling will be produced, requiring 7-1/2-hp. If the evaporator temperature is increased to 55 F, with other conditions unchanged, approximately 11 tons of cooling will be produced requiring 6-1/2-hp. When the evaporator temperature is decreased to -20 F, approximately 2-1/2 tons of cooling will be produced, requiring 6 hp. Since cooling capacity and horsepower vary with compressor rpm, it may be necessary to change the compressor rpm in order to obtain the desired cooling capacity at a given evaporator temperature or to adjust the horsepower required at a certain evaporator temperature.

Components used for control

The refrigeration system is designed to allow continuous operation of the compressor. Intermittent operation would result in poor temperature control. Air temperature control is accomplished by adjusting the evaporator pressure with a motorized pressure regulating valve on the suction side of the evaporator. This valve is sometimes called a back-pressure regulator or an evaporator pressure regulator.

Since sometimes the cooling load varies over a wide range during a single test while the compressor is operating continuously, it is necessary to have a hot-gas bypass valve in addition to the cylinder unloader to provide for additional capacity reduction. As indicated in Figure 13, this valve recirculates hot gas from the compressor back through the evaporator when the suction pressure drops below an adjustable, preset level. The motorized pressure regulating valve is operated by an automatic controller which will be discussed in the next section.

Evaporator coils

The direct expansion evaporator coils shown in Figure 13 are standard models without housing or fan. They have wide-spaced fins (1/4 inch) so that a thin layer of ice collected during a test will not significantly affect the air flow rate. Both evaporators are equipped with defrosting heaters which can be actuated manually. The heaters can also be used to provide additional heat load on the refrigeration system which is sometimes desirable in order to achieve better control. Refrigerant 502 is used in this system since it allows a wide range of operating temperatures without changing the thermal expansion valves and other control components.

Air Temperature and Humidity

The automatic control of air temperature entering the product chamber is accomplished by the use of a proportional controller with reset and rate action, which regulates the motorized valve on the evaporator. The primary sensing element for the automatic controller is a thermocouple which is placed in the air stream at the entrance of the bed. The manipulated variable is the evaporator pressure which is regulated by the motorized valve.

For tests during which the inlet air temperature is to remain constant, the cooling load at the beginning of the test will be much greater than the average cooling load. Thus, it is desirable for a research facility to have a refrigeration system large enough to handle a temporary high cooling load for products that cool extremely fast.

Since the air is recirculated, the dew point of the cooling air will approach the evaporator temperature unless moisture is added. In some cases an undesirable drying effect is caused by a large water vapor pressure difference between air and the product surface. In order to minimize this effect, the cooler is equipped with a steam humidifier which injects steam into the air after it passes through the evaporator coils. Adding steam to the air in this manner results primarily in a latent heat increase, and very little sensible heating occurs. For example, when air at 30 F and 70% RH is saturated by adding 212 F steam, the air temperature is increased less than 0.4 F. This procedure presents no problem in controlling the air temperature since the temperature sensor is downstream from the humidifier. Using large evaporators, thus keeping the temperature difference between the coil and the air small, will result in higher humidities. However, the humidity will always be below 100% if moisture is not added back to the air after passing through the coils. Even when the air entering the product chamber is saturated, there is still a potential for drying in a product bed because the air is heated by the preceding layer of product.

In order to determine the amount of moisture loss during cooling, a load cell type of scale was mounted so that the entire product bin could be suspended and weighed before and after each test.

Air Flow

The location of the air handling unit and air flow patterns are shown in Figure 12. The air is circulated with a backward curved centrifugal blower having a capacity of 16,000 cfm when operating against 3 inches H_2O static pressure. The backward curved vanes produce a relatively high operating pressure and will provide approach velocities of up to 1000 fpm entering the product chamber.

The blower is driven by a hydraulic motor controlled by a variable speed hydraulic transmission which allows the air flow rate to be regulated by the rpm of the blower rather than by dampers. The transmission and electric motor are located outside of the cooler, which minimizes the heat produced inside the cooler. The blower was placed downstream from the evaporator coils so that the temperature of the air through the blower could remain constant throughout a test. If the blower were placed upstream from the evaporators, the temperature of air moving through the fan would vary during the test causing a variation in the velocity through the product chamber.

The air enters a large plenum and passes through an air-straightening section beneath the product chamber to ensure that the air entering the product is uniformly distributed as it enters the product chamber. In conjunction with the air-straightening vanes, small patches of screen wire were added to produce resistance in areas which have a high velocity. The velocity profile of the air entering the product chamber did not vary more than 5% when measured with a hot-wire anemometer probe at 6-inch intervals.

The air flow rate is measured to within ± 2 % through the use of an "annubar" flow element installed in a 1-foot-diameter PVC pipe. The flow rate is determined as a function of the difference between velocity and static pressure. The pressure difference is measured with an electronic differential pressure indicator which has a resolution of 0.001 mm Hg.

Reheat Section

The reheat section, as shown in Figure 12, is a self-contained unit which may be detached from the main structure or placed adjacent to the product chamber so that a container load of product can be rolled out and reheated for repeated tests on the same product load. It is also used to heat the product to a predetermined uniform temperature before the initial test. It is equipped with a blower, heater, temperature controller, and humidifier. Since the product is heated outside of the cooling chamber, the cooler can operate continuously and maintain the desired temperature while the product is being heated. The primary source of heat for the heating section is a steam-heated coil with secondary electric heaters used for fine control. The electric heaters are regulated by a proportional automatic controller.

Experimental Test Procedures

Ten tests were conducted on a 340-pound bulk load of

No. 100 Valencia oranges with superficial air velocities ranging from 25 to 400 fpm. These tests were conducted on two different bulk loads, five tests each, in order to get some information on the variability among bulk loads of oranges. Five tests were conducted on a 274-pound bulk load of No. 23 Marsh grapefruit with superficial air velocities ranging from 15 to 400 fpm.

Each cooling test was conducted using eight cartons (4/5 bushel each) of sized fruit which were weighed, counted, and placed into the bulk container. This container was 2x2x4 feet deep with an expanded metal floor. Thermocouples were placed in eight fruit which were positioned, two each, at four levels as indicated in Figure 14. These thermocouples were placed at the mass average temperature point and at the surface. Center temperatures were not measured since citrus fruit usually have a void space at the center. The thermocouples were constructed from 36-gage, insulated copper-constantan wire.

Figure 15 depicts the method used in placing the thermocouples in the product. The insulated thermocouple wire was first inserted into a hypodermic needle and then injected into the product to the desired location. Then the needle was carefully withdrawn leaving the thermocouple in place. The thermocouple was then sealed at the surface of the product. A reference mark, which always remains outside of the product, was placed on all thermocouple wires to indicate the thermocouple position in case of slippage.

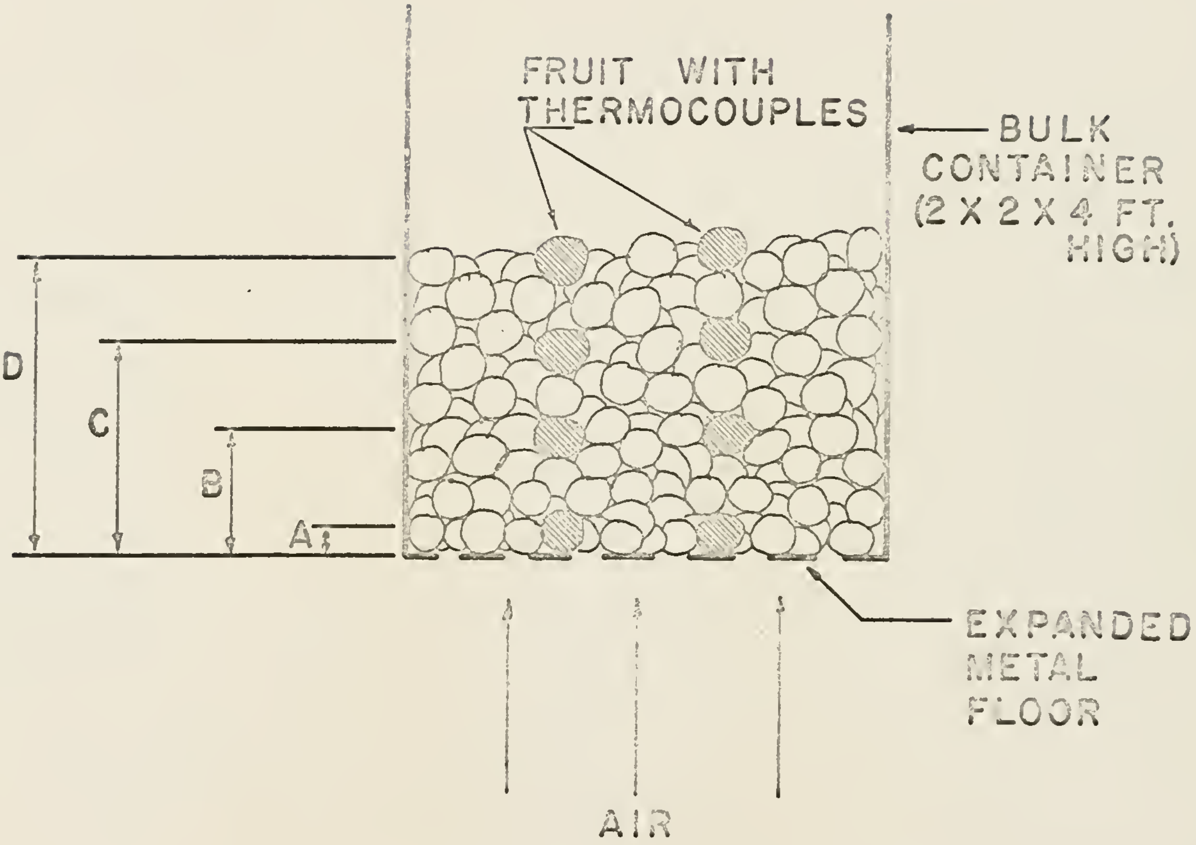

Figure 14. Bulk load of fruit showing the four levels at which product temperature was measured. Dimensions A, B, C, and D are indicated for each test

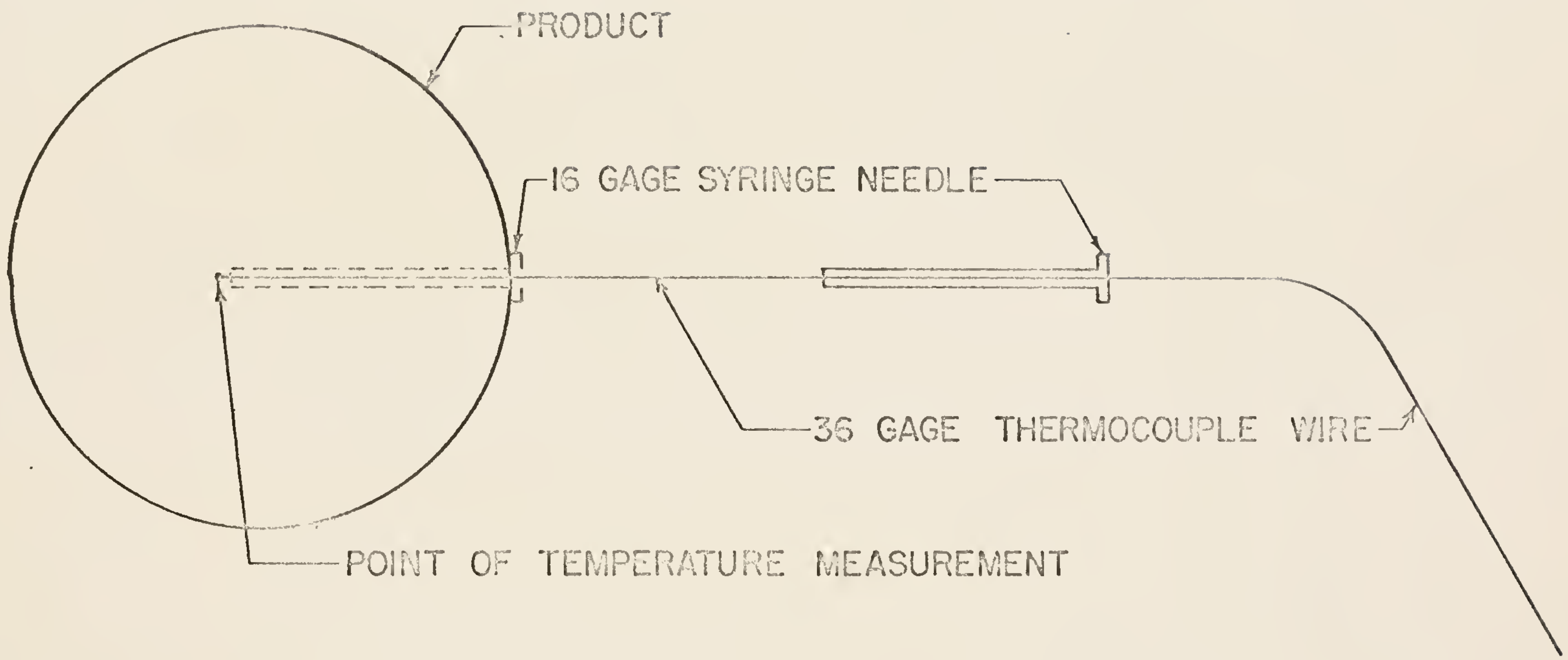

Figure 15. Method used for placing thermocouples in product

Bennett et al. (8) have suggested that errors due to conductance along the thermocouple wire from the surrounding cold air could be minimized if the thermocouple was always placed at least halfway through the product in order to produce a reverse temperature gradient in the thermocouple wire. This method was used for temperature measurement at the mass average point, but preliminary tests on plastic spheres indicated that a considerable error could result when surface temperatures were measured by inserting the thermocouple through the sphere and outward to the surface. The surface temperatures measured in this manner were always higher than those calculated by using the center or mass average temperatures and the theoretical solution for conduction in a sphere. This is probably due to the fact that the thermocouple is located in an outer layer of the sphere and not on the surface. The large temperature gradients in the outer layers of the sphere also could cause a conduction error along the wire near the junction. In an effort to improve this measurement, the conductors were twisted together for approximately 1/4 inch and imbedded along the surface of the fruit.

All thermocouple junctions were coated with a thin film of plastic to prevent possible corrosive or electrolytic action. The calibration of all thermocouples was checked at 32 F and 80 F and was found to have an error of less than 0.5 F.

Temperature was recorded on a multi-point potentiometer which read each point at two-minute intervals throughout the test. Each product load was brought to a uniform temperature just prior to placing the container into the cooling chamber.

Data and Results

Numerical Solution of Deep Bed Cooling

Figures 16 through 19 show typical output data from the numerical solution in graphical form. The computer program and sample output data are shown in Appendix B. It should be noted that only a small portion of the output can be indicated on any one figure and have the graphs remain legible. It is possible to produce a graph of the temperature at any point within the individual fruit and at any depth within the bed, as a function of time. The computer program provides the capability to vary the important thermal and physical properties of the cooling system such as: the size of product, thermal properties of product, air velocity, air temperature, and dimensions of the bed. A complete list of these variables is shown in Appendix B as input data.

The graphical results shown in this section are only samples from the complete range of tests. Additional results from the numerical model are shown in Appendix C in the form of a comparison between the numerical model and experimental data.

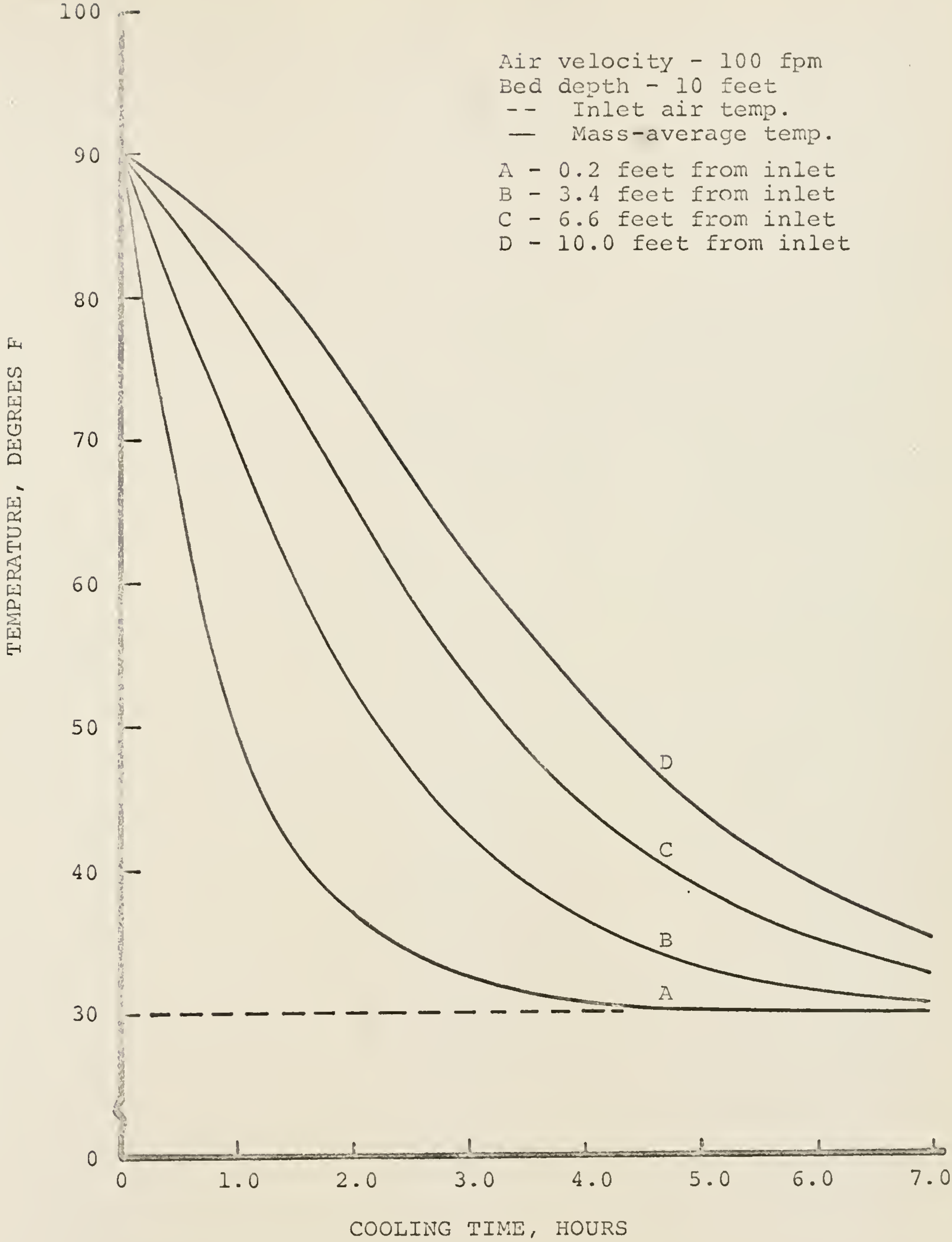

Figure 16. Theoretical mass-average temperature response of oranges to forced-air cooling as predicted by numerical model

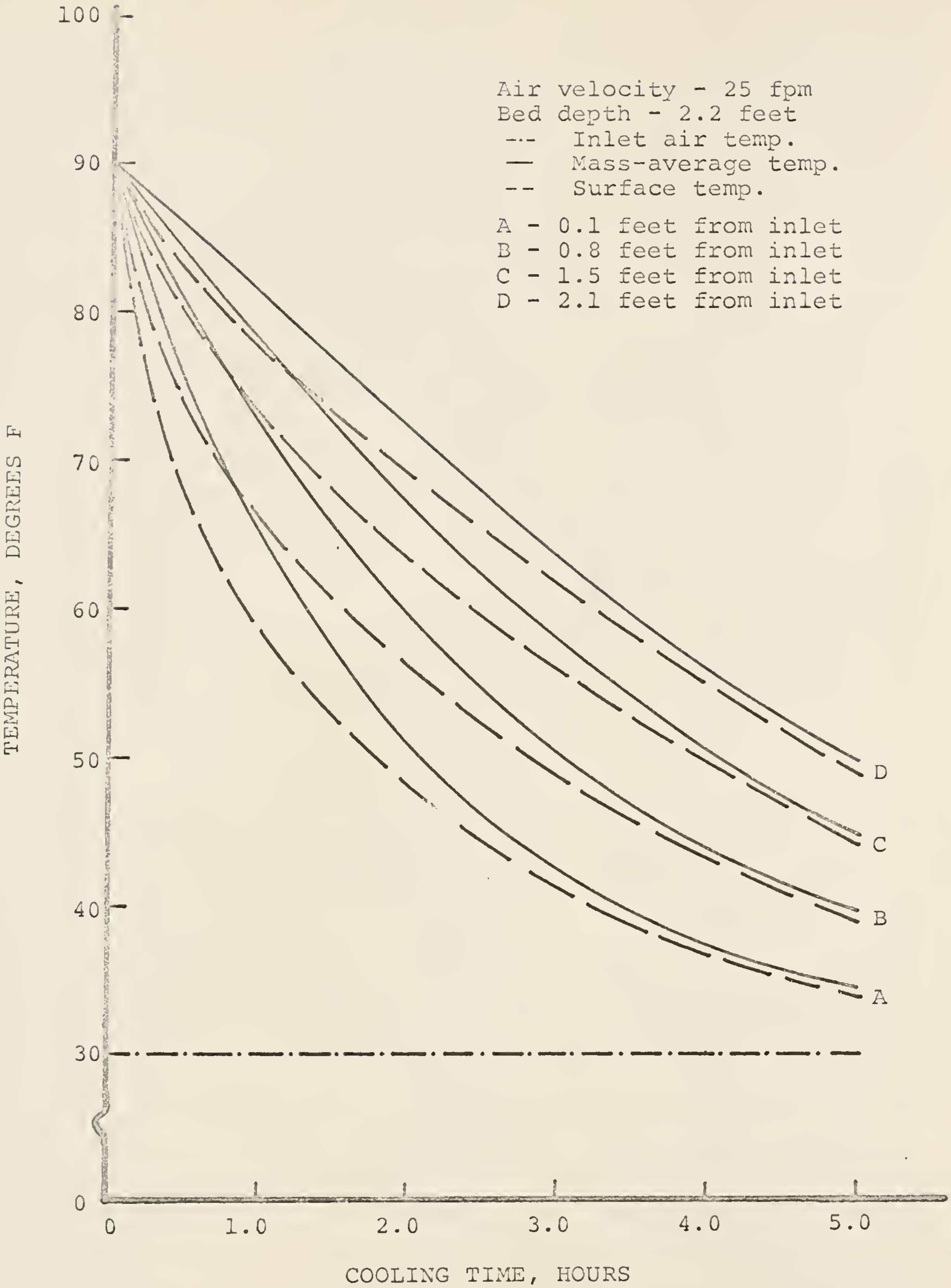

Figure 17. Theoretical mass-average and surface temperature response of oranges to forced-air cooling as predicted by numerical model

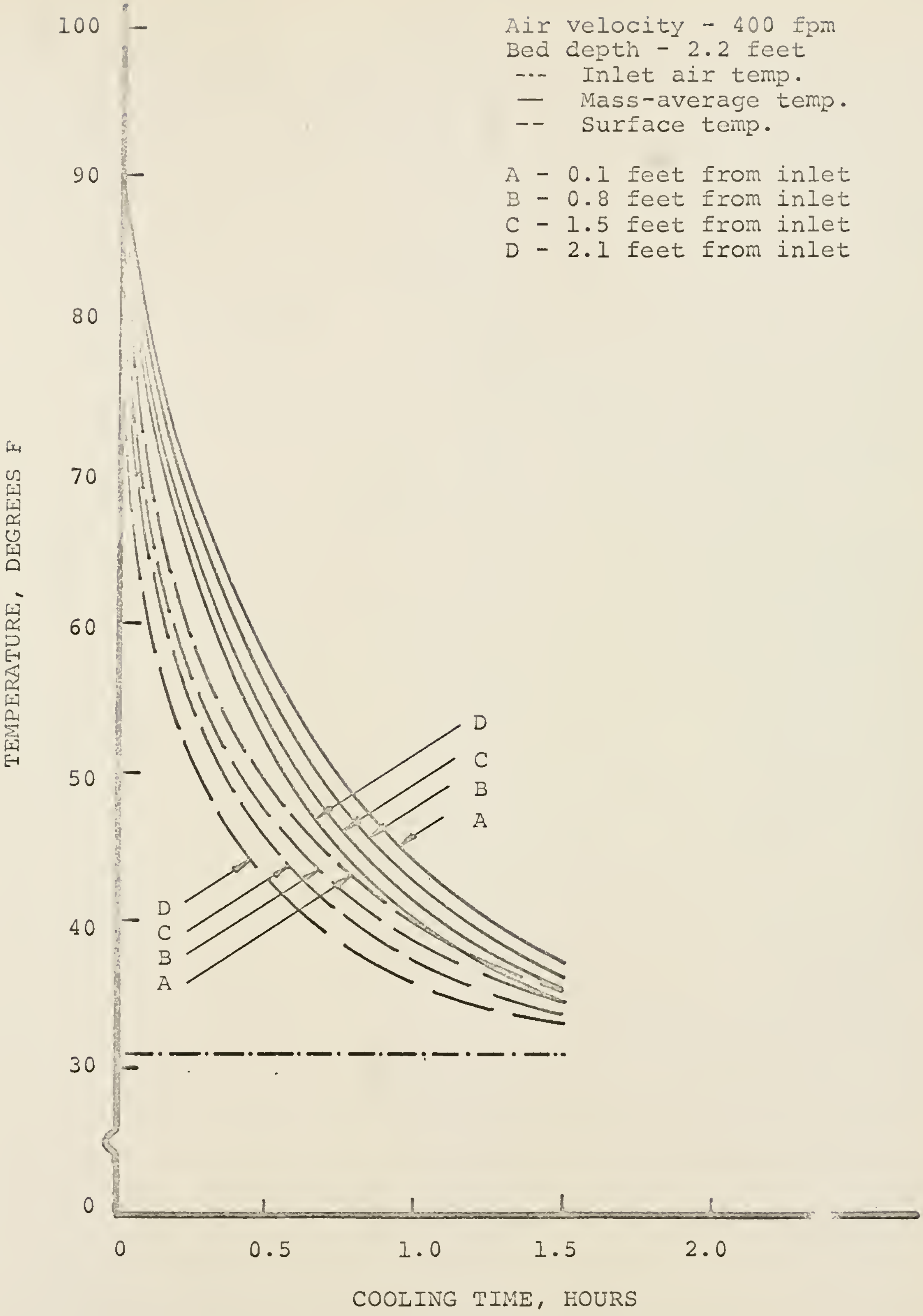

Figure 18. Theoretical mass-average and surface temperature response of oranges to forced-air cooling as predicted by numerical model

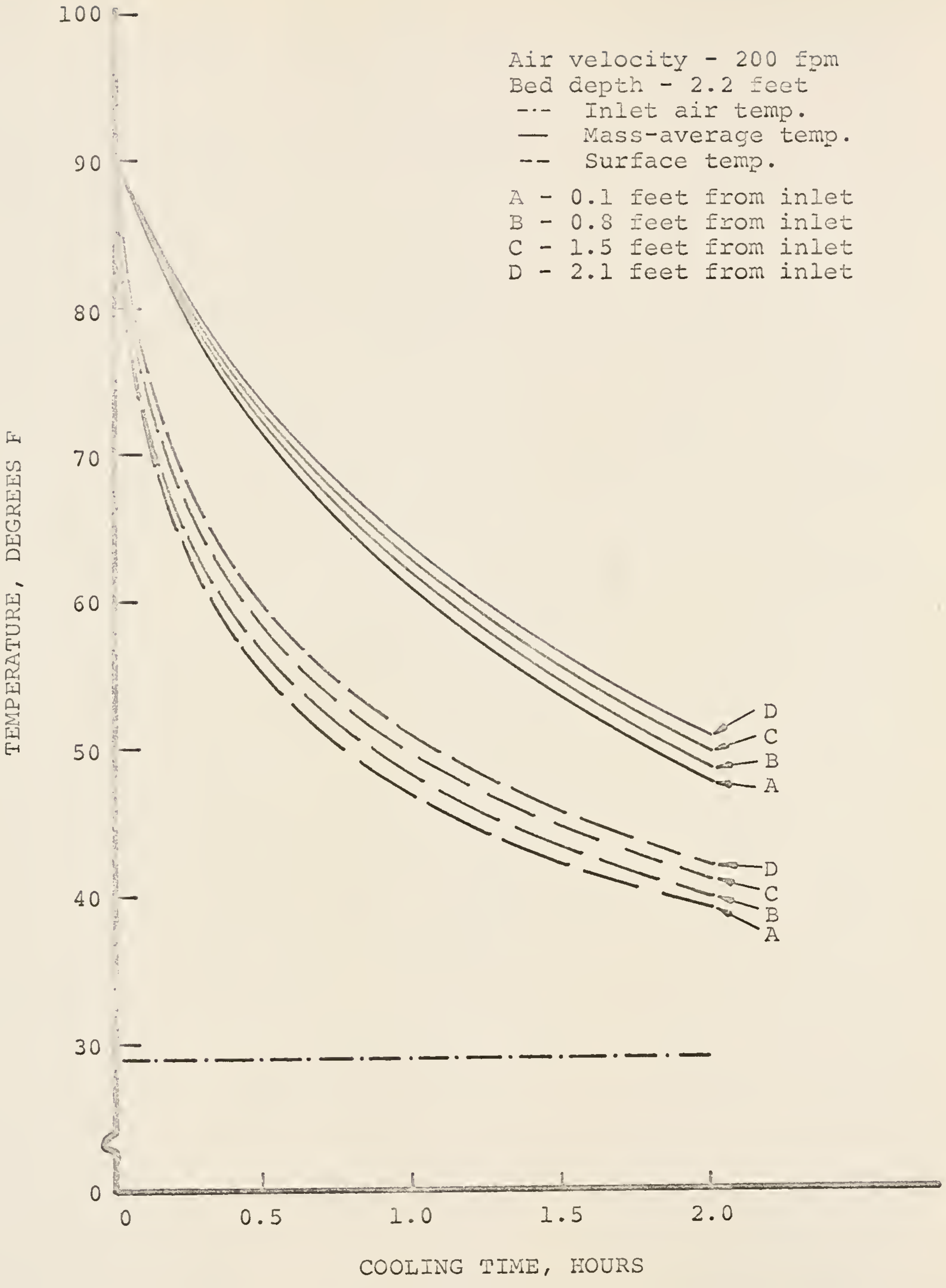

Figure 19. Theoretical mass-average and surface temperature response of grapefruit to forced-air cooling as predicted by numerical model

Convective Heat Transfer Coefficient (h)

A relationship for h in a deep bed of citrus fruit was determined in terms of Nusselt number versus Reynolds number as indicated by the following equation.

$$Nu = c(Re)^n$$

where

$Nu = hD/k$, Nusselt number

$Re = VD/\mu$, Reynolds number

A separate regression was made for each group of data as indicated in Figures 20, 21, 22, and Table 5.

Thermal Diffusivity (α)

Thermal diffusivity was determined experimentally for oranges and grapefruit using the method described by Smith *et al*. (47), which utilizes time-temperature data from fruit cooled in an agitated water bath. The thermal diffusivity (α) for oranges was found to be 0.00437 ft^2/hr with a standard deviation of 0.00010, based on five tests, while α for grapefruit was found to be 0.00362 ft^2/hr with a standard deviation of 0.00015, based on five tests.

Experimental Deep Bed Cooling Tests

The experimental temperature response from forced-air cooling tests conducted on bulk loads of Valencia oranges

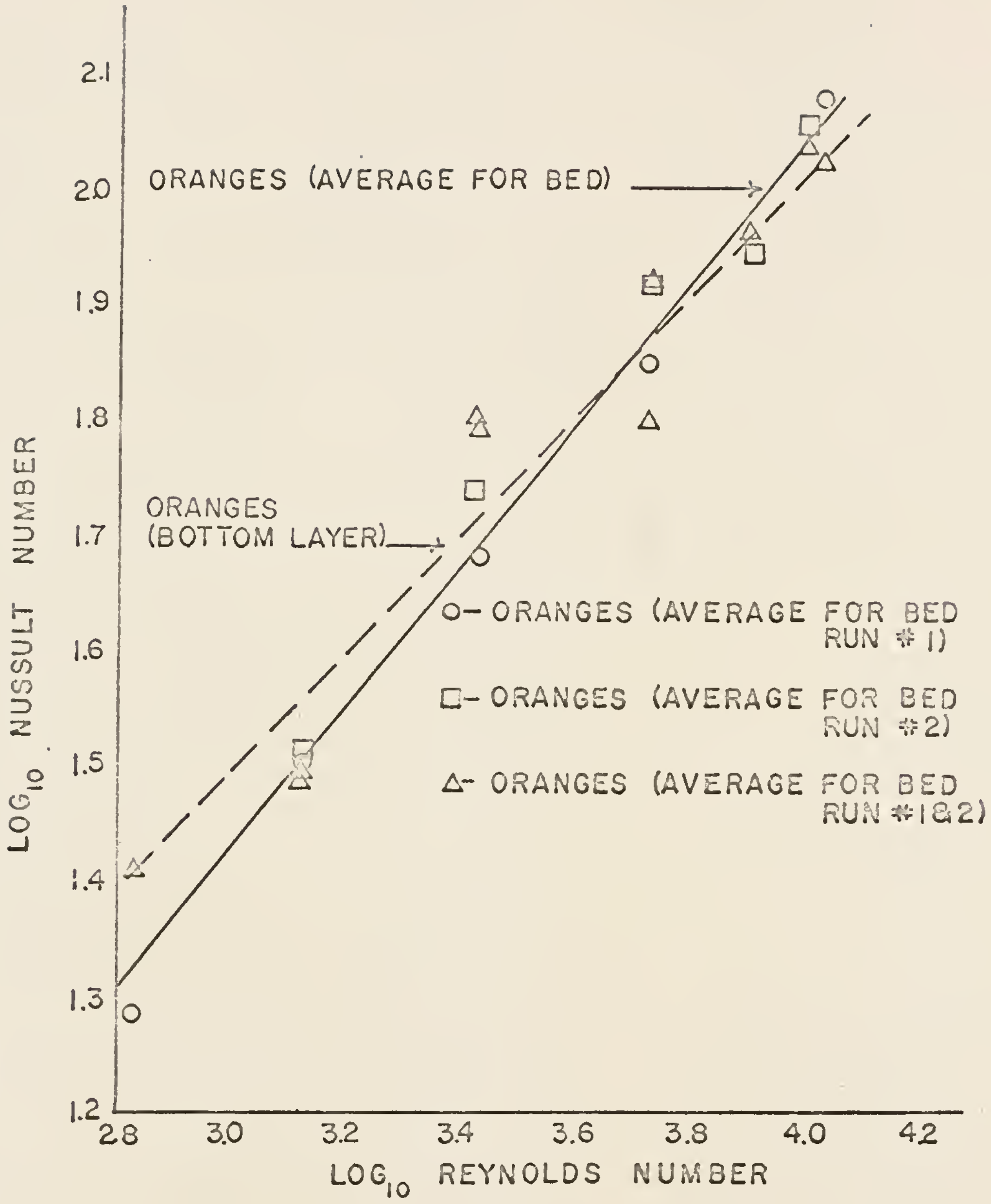

Figure 20. Linear regression relating Nusselt number and Reynolds number for forced-air cooling of oranges in bulk loads

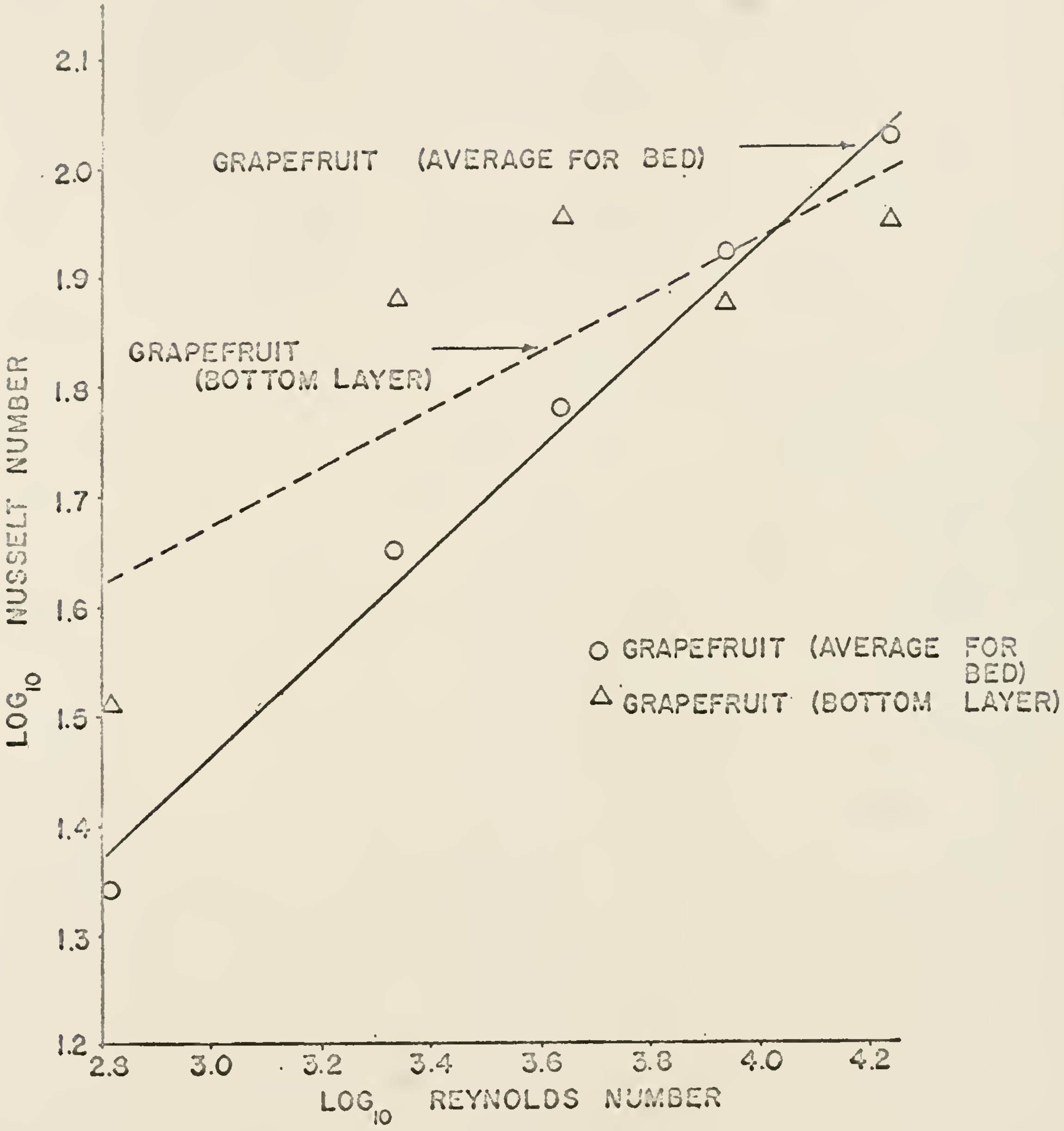

Figure 21. Linear regression relating Nusselt number and Reynolds number for forced-air cooling of grapefruit in bulk loads

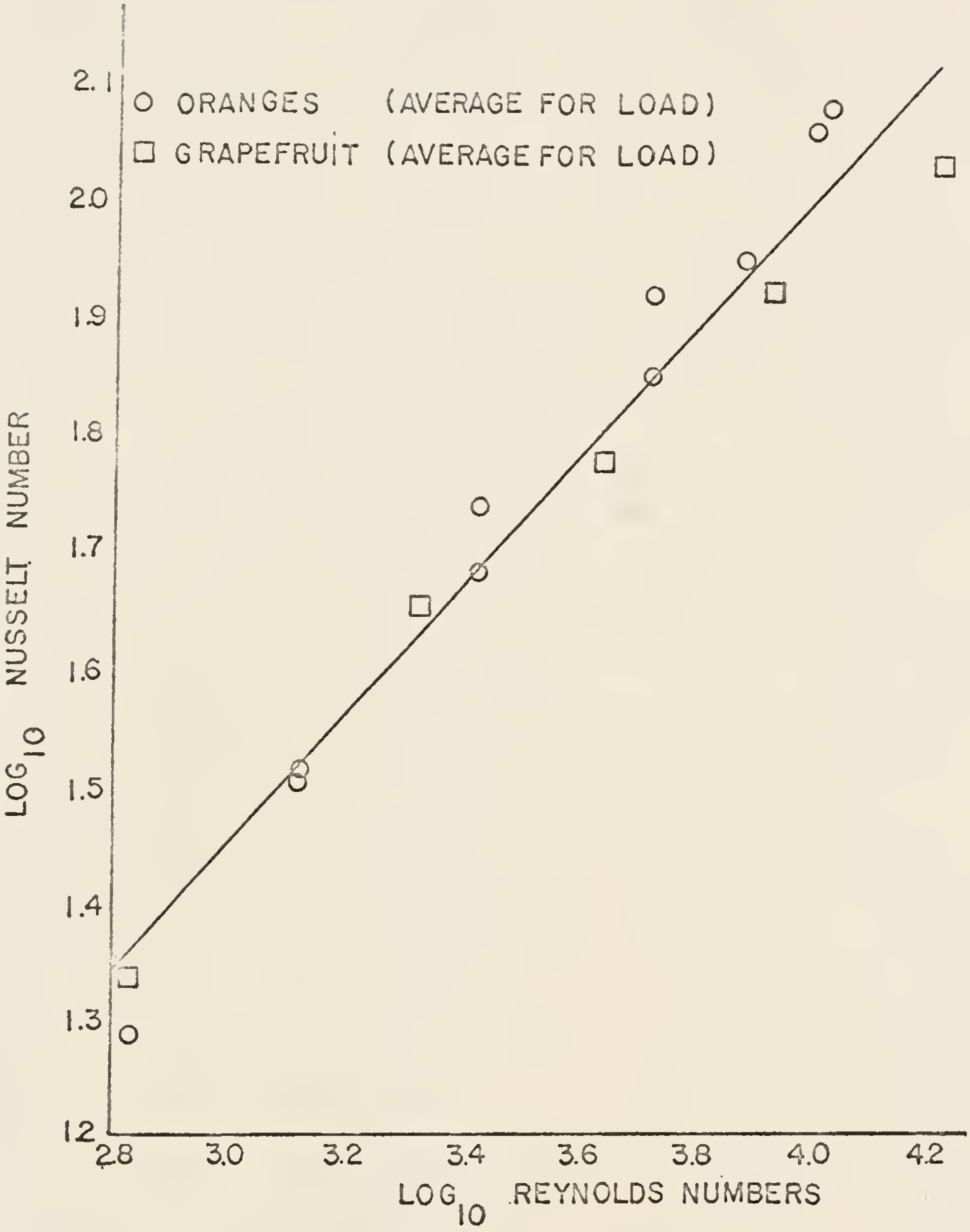

Figure 22. Linear regression relating Nusselt number and Reynolds number for forced-air cooling of oranges and grapefruit in bulk loads

and Marsh grapefruit are shown in Figure 23 through 26. Temperature was measured at the surface and mass average temperature point for fruit positioned in the bulk load as indicated in Figure 14. The dimensions A, B, C, and D indicated in Figure 14 are specified on each graph.

The results presented in this section (Figures 23 through 26) do not include all of the experimental tests. In all, there were fifteen tests run on oranges and grapefruit with superficial air velocities ranging from 15 to 400 fpm. The complete results of these tests are contained in Appendix C, in the form of a comparison between the numerical model and experimental data.

Table 6 gives the thermal and physical properties of the Valencia oranges and Marsh grapefruit used for the experimental tests. All of these properties were determined experimentally or calculated using experimental data, except specific heat (c), which was taken from reference (2).

Discussion

Comparison of Laplace Transform Solution for the Simplified Model and Numerical Solution for the Realistic Model

In order to obtain an analytical solution for cooling of a deep bed of citrus fruit, a simplifying assumption of no temperature gradient within the individual fruit was made. In the development of the numerical solution this assumption

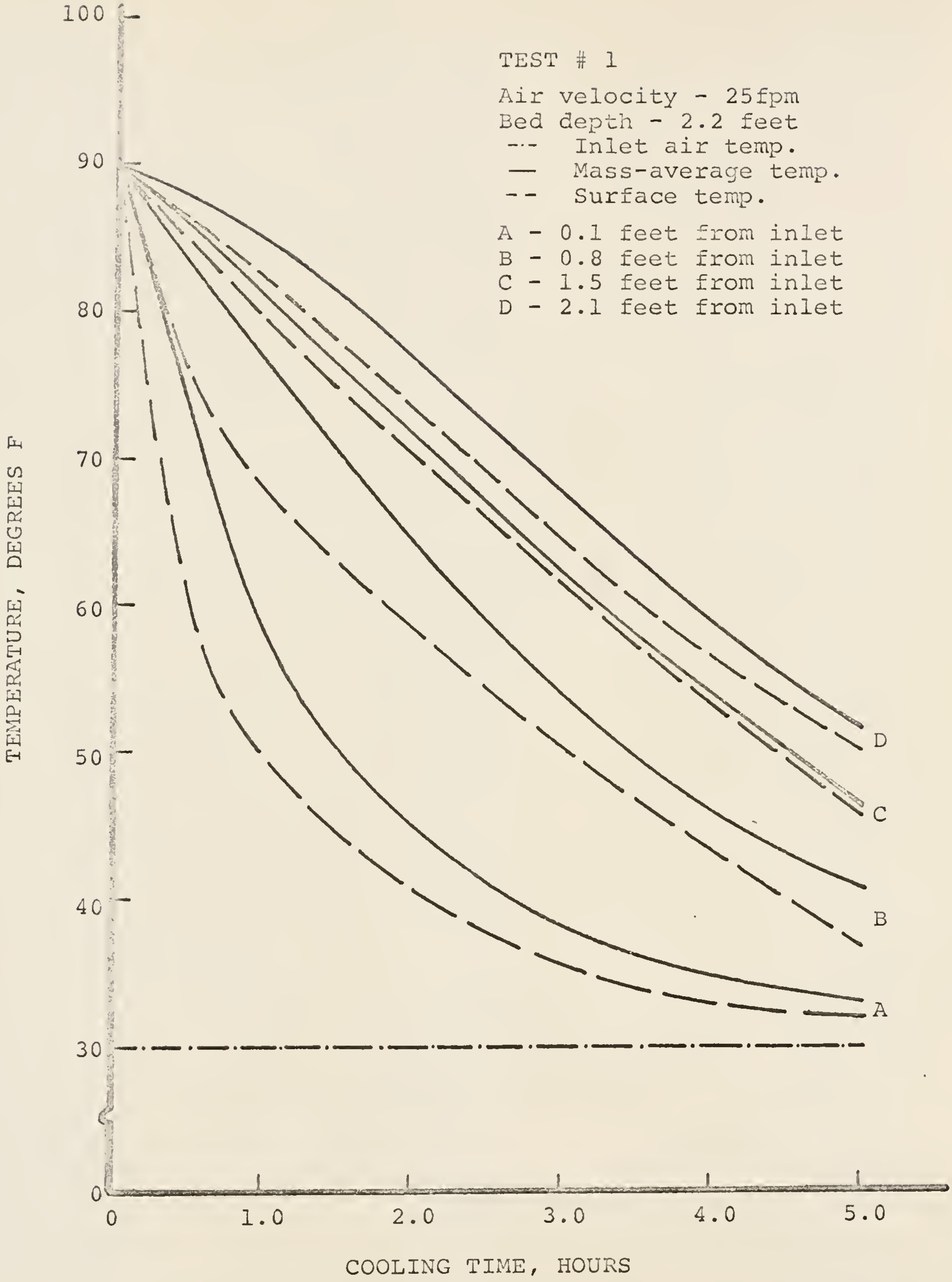

Figure 23. Experimental mass-average and surface temperature response of oranges to forced-air cooling

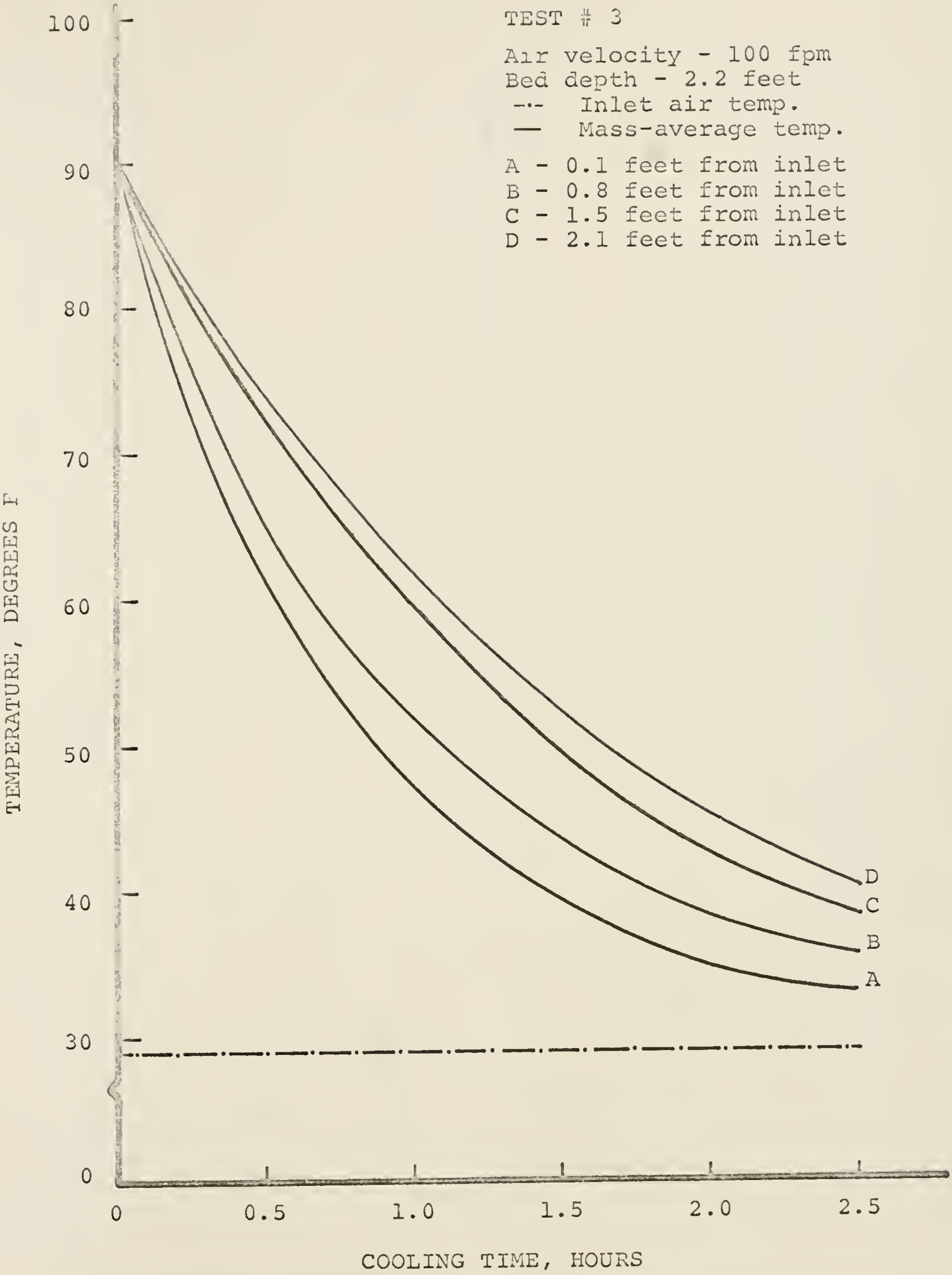

Figure 24. Experimental mass-average temperature response of oranges to forced-air cooling

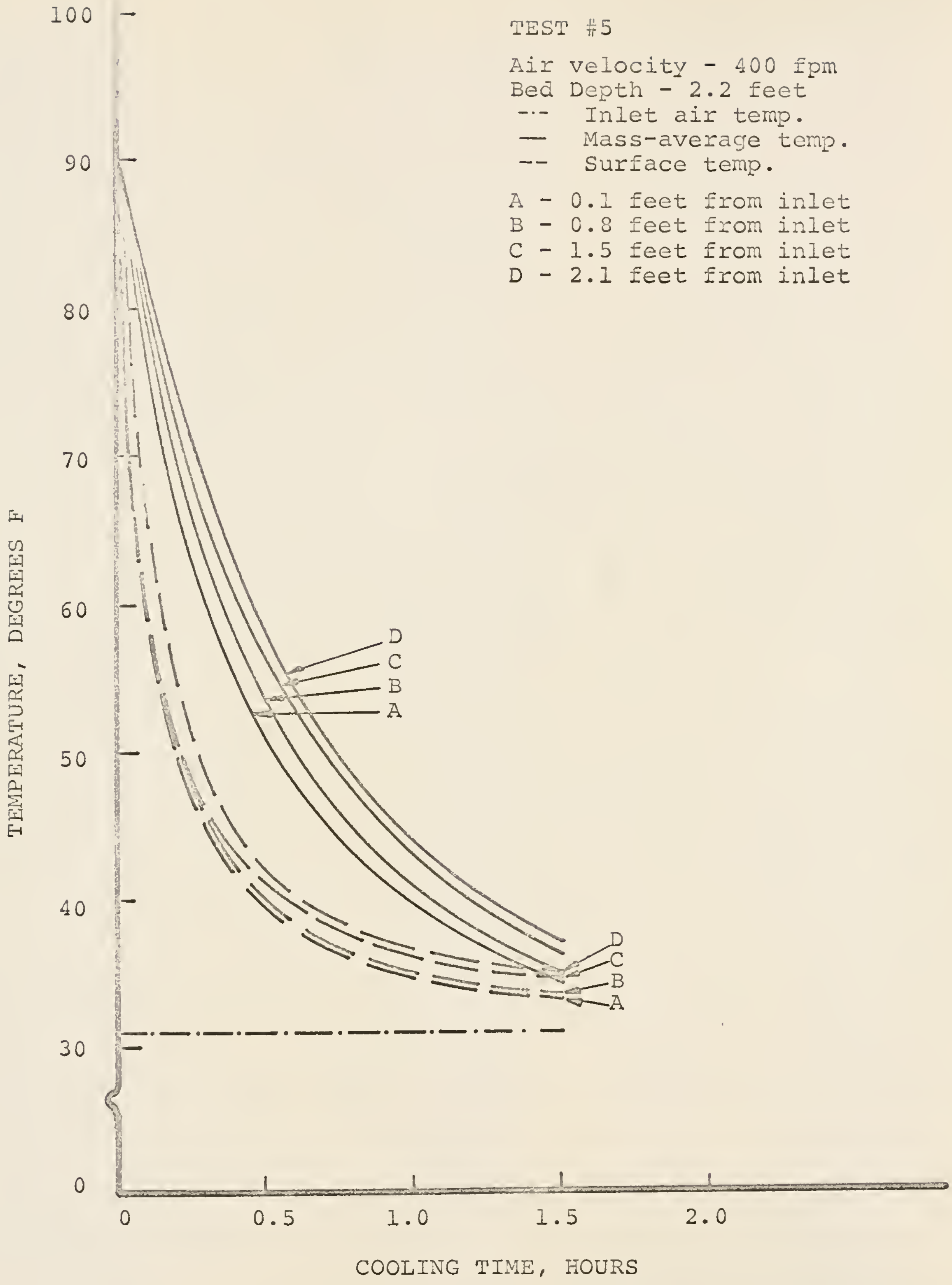

Figure 25. Experimental mass-average and surface temperature response of oranges to forced-air cooling

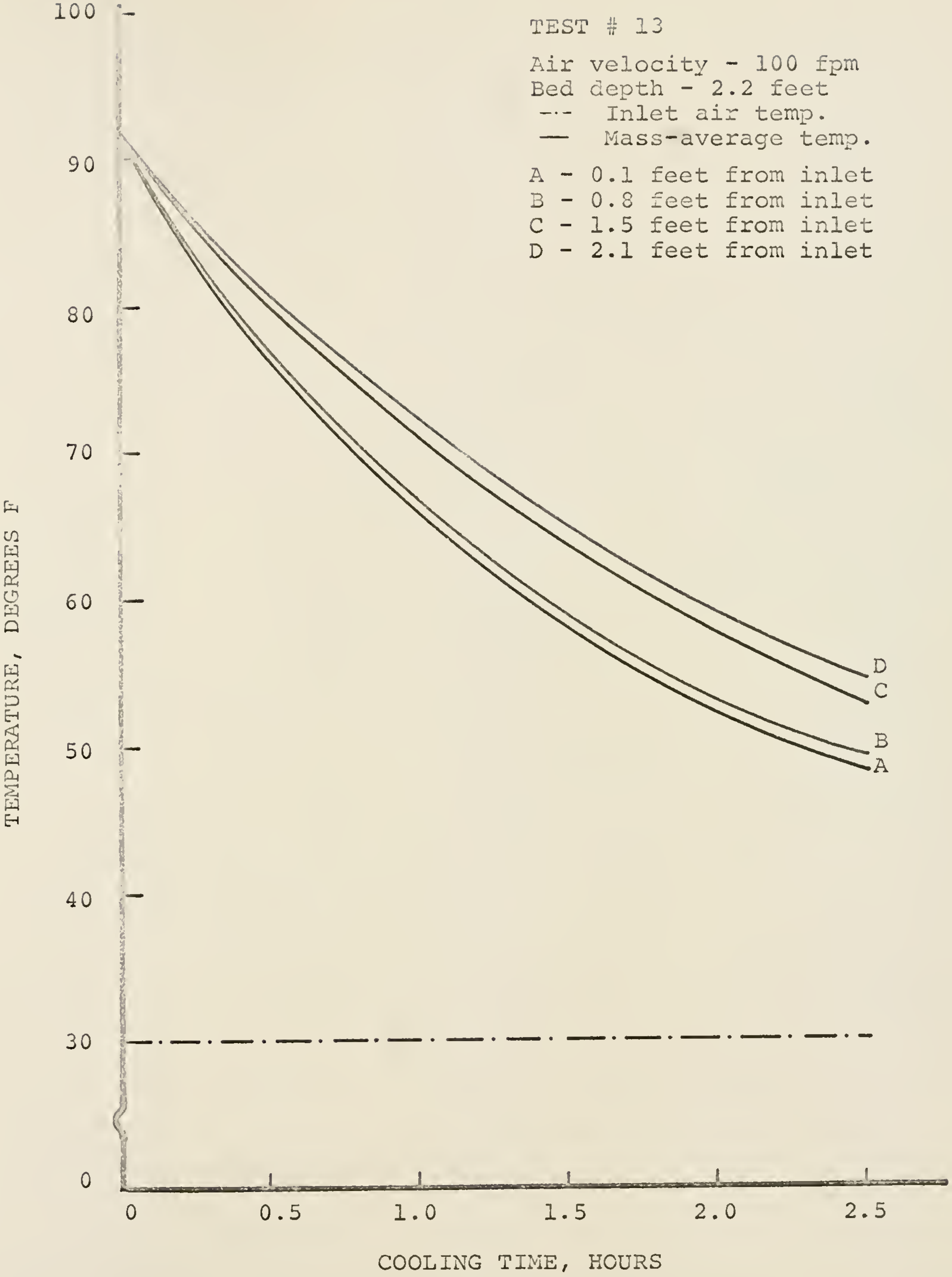

Figure 26. Experimental mass-average temperature response of grapefruit to forced-air cooling

Table 6. Thermal and Physical Properties of Valencia Oranges and Marsh Grapefruit Used in Cooling Tests.

	Valencia oranges	Marsh grapefruit
Total weight, lb	340	274
Total number of fruit	800	184
Bulk density, lb/ft^3	37.8	31.0
Specific gravity	1.016	0.843
Void space fraction	0.406	0.400
Equivalent diameter, ft	0.234	0.380
Surface area per volume, ft^2/ft^3	15.3	9.42
Thermal conductivity, BTU/hr-ft-°F	0.248	0.164
Specific heat, BTU/lb-°F	0.90	0.91
Thermal diffusivity, ft^2/hr	0.00437	0.00342

was lifted, thus, accounting for conduction heat transfer within the individual fruit. For very slow cooling rates, corresponding to low air flow rates, both solutions should agree since there will be a negligible temperature gradient within the individual fruit. Figure 27 shows that for an air flow rate of approximately 25 fpm there was no detectable difference between the two solutions.

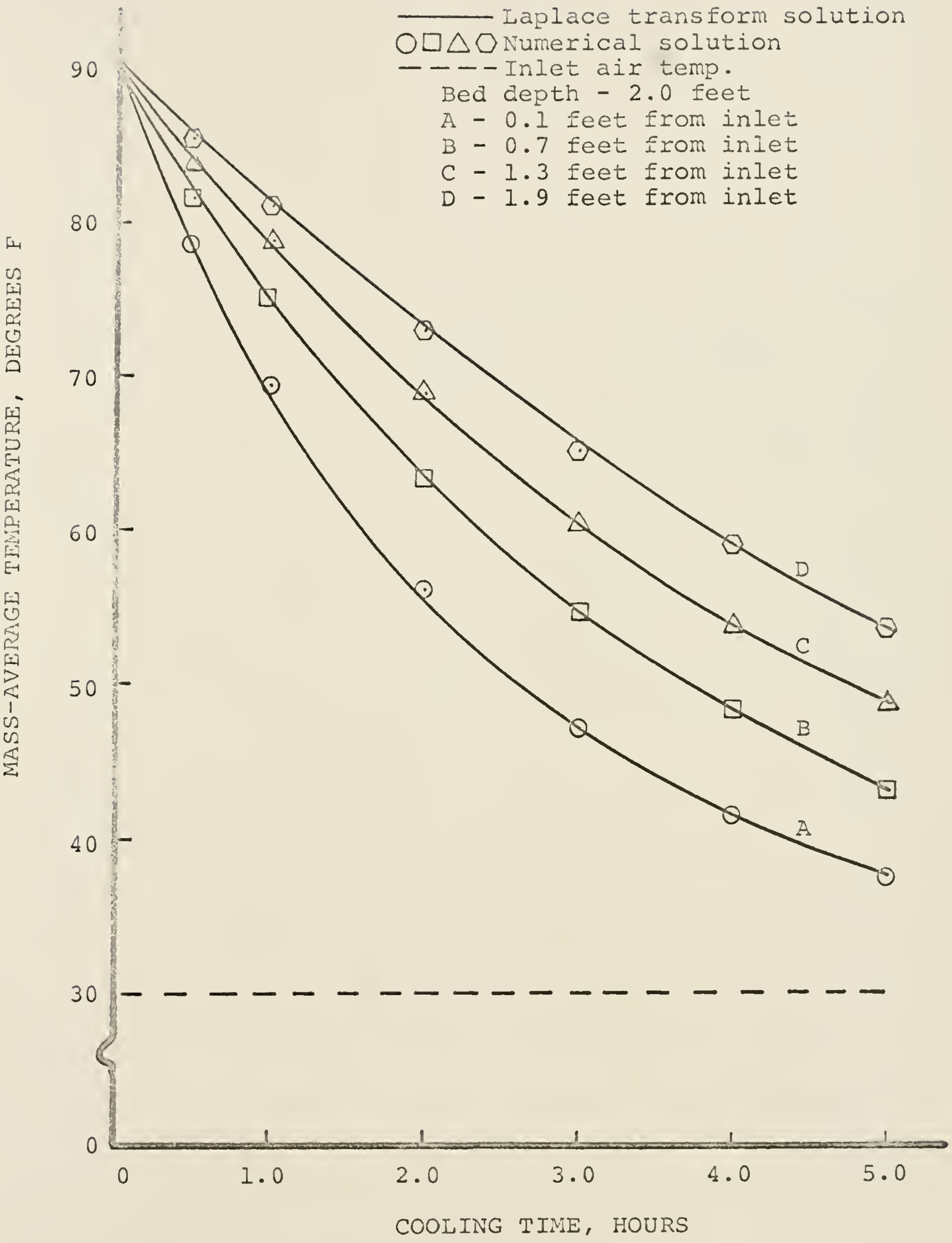

Figure 27. Comparison of Laplace transform solution of simplified model with numerical solution of realistic model for a slow cooling rate (25fpm)

This comparison indicates that the simplified model is valid for low air flow rates and also provides a check on the numerical solution. A similar comparison was made in the preceding chapter (Figure 4) which provided a check on the numerical solution for the case where conduction within the fruit was important.

In order to demonstrate the effect of significant temperature gradients within the individual fruit on the cooling rate, conditions corresponding to a faster cooling rate were used. Figure 28 gives this comparison for an air velocity of approximately 400 fpm. Thus, it is seen that the results are considerably different when the effect of temperature gradients within the individual fruit is considered.

The four curves on Figures 27 and 28 indicate the mass-average temperature at four levels within the bed of fruit as illustrated in Figure 14.

The accuracy of the numerical solution is obviously dependent upon the number of increments within the individual fruit, the number of increments within the bed and the number of time increments. As explained in the preceding chapter, the ratio of the number of time increments to the number of increments within the fruit has a lower limit in order to insure stability of the numerical solution. Therefore, the number of increments within the fruit is chosen first.

A series of tests was run using the computer program to determine the effect of the number of segments in the fruit

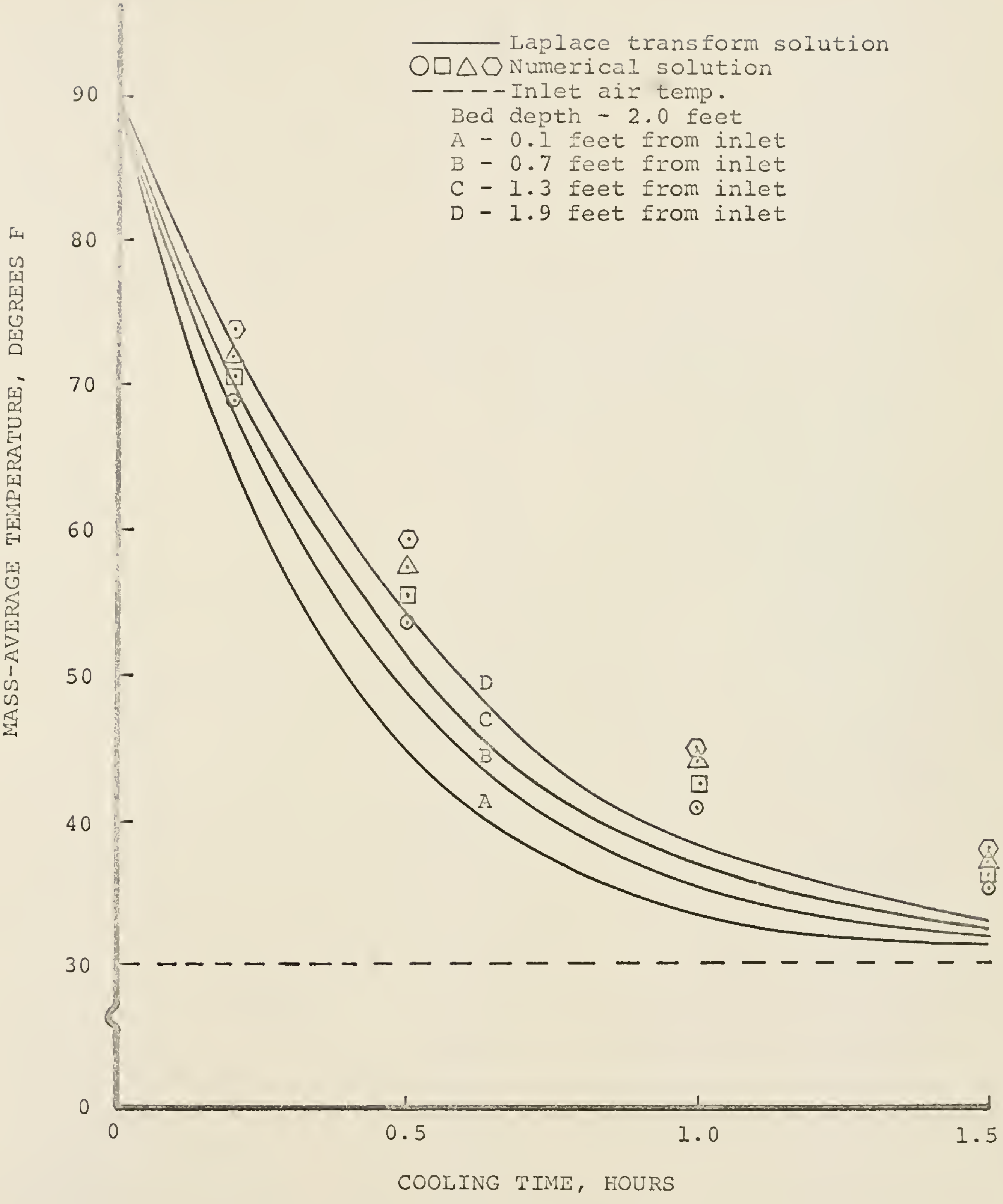

Figure 28. Comparison of Laplace transform solution of simplified model with numerical solution of realistic model for a fast cooling rate (400fpm)

and the number of layers in the bed, on the fruit temperature. The effect on the fruit temperature with respect to position in fruit, position in bed, and time was studied using the computer output. The largest change in fruit temperature as a function of number of layers in the bed and number of segments in the fruit was determined and is presented in Table 7. Using this information and considering the cost of computer time, the following number of increments was chosen: segments in fruit - 10, layers in bed - 5 per foot, and time increment - 0.005 hours. A decrease in the time increment below this value did not indicate a detectable increase in the accuracy. The results shown in Figures 27 and 28 and all other results from the prediction model were obtained using these increments. Using these increments for a cooling test on a 2-foot-deep bed, the computer time was less than 2 seconds per hour of cooling time when run on an IBM 370/165 model digital computer.

Convective Heat Transfer Coefficient (h)

A review of the prediction equations for h in packed beds (pages 50-52) indicates very little consistency among the numerous relationships. The problem of selecting the correct equation has perplexed many investigators who have studied heat transfer in packed beds. In many cases it

Table 7. The Effect of Increment Size on the Accuracy of the Numerical Solution.

No. of Layers in Bed	Product Surface Temperature for Top Layer (°F)
5	77.4
10	78.0
15	78.2

No. of Segments in Fruit	Product Mass Average Temperature for Bottom Layer (°F)
5	66.7
10	67.1
15	67.3

appears that too much effort was expended on one facet of the problem without due concern for how the results would be used in the solution of the total problem.

In this study the problem of selecting the correct equation for h was avoided by experimentally determining the relationship for h utilizing the prediction model developed in this study. This relationship, which was presented in terms of the Reynolds number and Nusselt number (equation [84]), compares favorably with relationships used by other investigators of heat transfer in beds of biological materials. The experimentally determined values for n (equation [84]) for oranges and grapefruit were 0.62 and 0.48 respectively as indicated in Table 5. Bakker-Arkema (5) and Huang et al. (29), in their work with heat transfer in beds of beets and onions, used a relationship with an n equal to 0.58 and obtained satisfactory results.

A relationship for h, valid only for the bottom layer of the bed, was determined using a completely different method as described by Smith et al. (27). Figure 20 shows a comparison of the relationship for the bottom layer and the average for the bed, indicating a close agreement.

Theoretically, h for oranges and grapefruit would be governed by the same equation if both were perfect spheres. Thus, a linear regression was made for all experimental tests conducted on oranges and grapefruit combined. Figure 20 shows that a good correlation was obtained with a correlation coefficient (r) equal to 0.977.

The fact that h determined for the bottom layer only and for the entire bed has similar values indicates that there was no significant variation of h through the bed. The value of h, of course, will vary through the bed due to the change in the air temperature as it moves through the bed. However, calculations based on a change in film temperature of 60 F through the bed would result in a variation in h of only 1%. Since this is an upper limit on the variation, this effect can be neglected.

One might propose that there could be a variation in h through the bed caused by a change in flow characteristics, similar to that which occurs for flow over tube banks in heat exchangers (31). However, there are no indications of this phenomenon in any of the literature which was reviewed on heat transfer in deep beds of particles. All such studies used an average h for the entire bed and in most cases obtained satisfactory results.

Comparison of Experimental Data With Numerical Solution

The experimental results of forced-air cooling tests on Valencia oranges and Marsh grapefruit are presented in graphical form along with corresponding results from the prediction model. Individual mass average and surface temperatures are indicated as a function of time and position within the bed for each air flow rate. Appendix C contains a complete set of these comparison curves, including all experimental data. Selected curves from this set will be included in this section to support discussion.

The thermal and physical properties of Valencia oranges and Marsh grapefruit, as listed in Table 6, were used to determine input data for the numerical solution. The convective heat transfer coefficient (h) used in the numerical solution was calculated from equation [84]. Values of "c" and "n" for oranges and grapefruit were taken from Table 6 as 0.374, 0.620, 1.04 and 0.482 respectively.

Experimental data

The consistency of the experimental data, with respect to between-fruit differences and between-bulk-load differences, was considered to be exceptionally good when compared to experimental temperature data collected by other investigators. Tests No. 2 and No. 6 (Figures 29 and 30) were conducted on two different bulk loads of oranges under similar conditions. Very little difference in temperature response can be detected between the tests, and both sets of experimental data agree equally well with the theoretical prediction curve.

Each experimental data point is an average of two values taken from two fruit which were located at the same level in the bed. An indication of the between-fruit variation can be obtained by noting the average difference between these values taken at the approximate half-cooling time. The average difference was approximately two degrees Fahrenheit.

Analyses of the differences between experimental and theoretical data

Evaporative cooling.--The mass-average temperatures indicated by the prediction model fit the experimental data reasonably well. However, in most cases, the difference in temperature between the top and bottom layers of the bed was greater for the experimental data than it was for the theoretical data (Figure 31). The primary reason

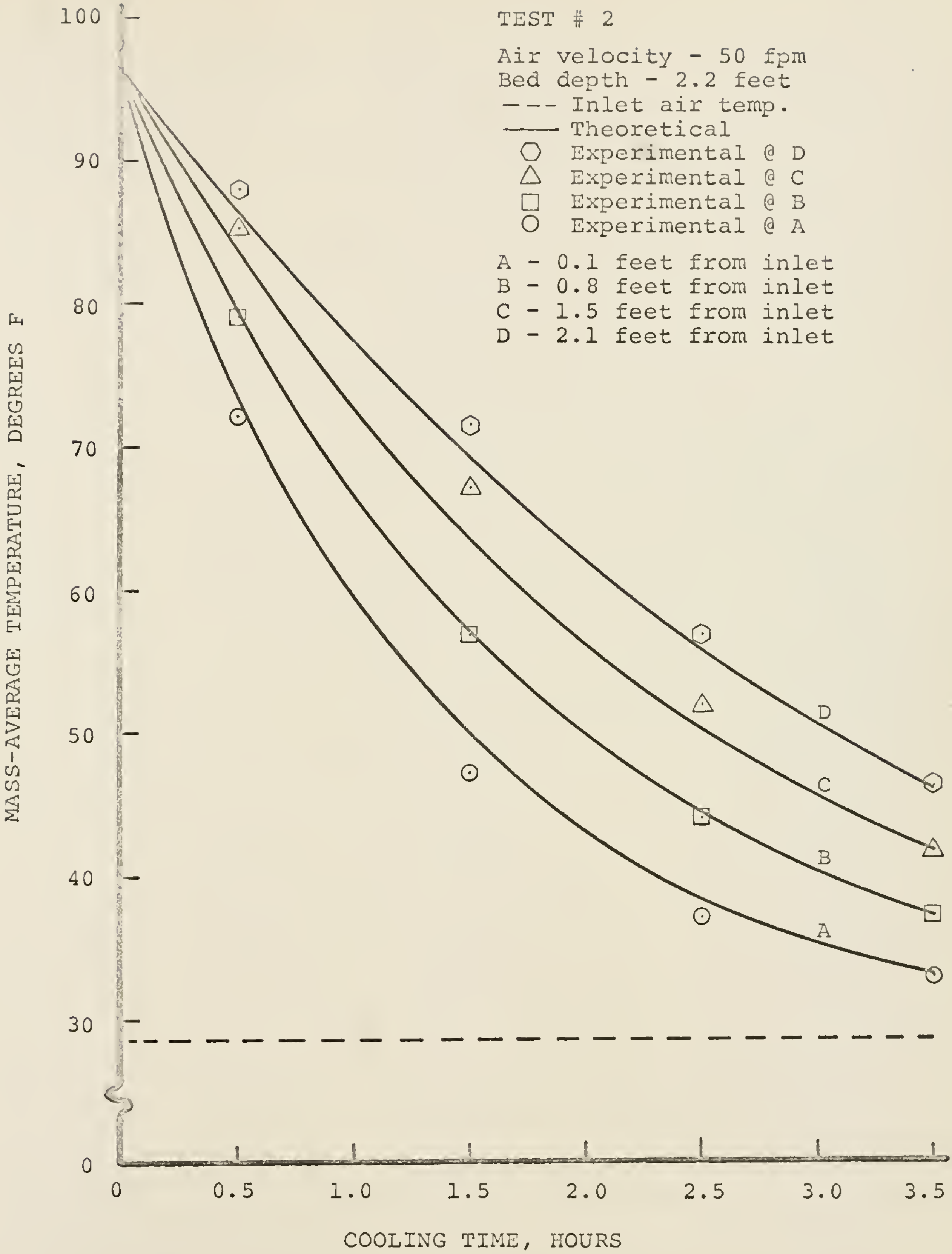

Figure 29. Comparison of experimental and theoretical temperature response of oranges to forced-air cooling

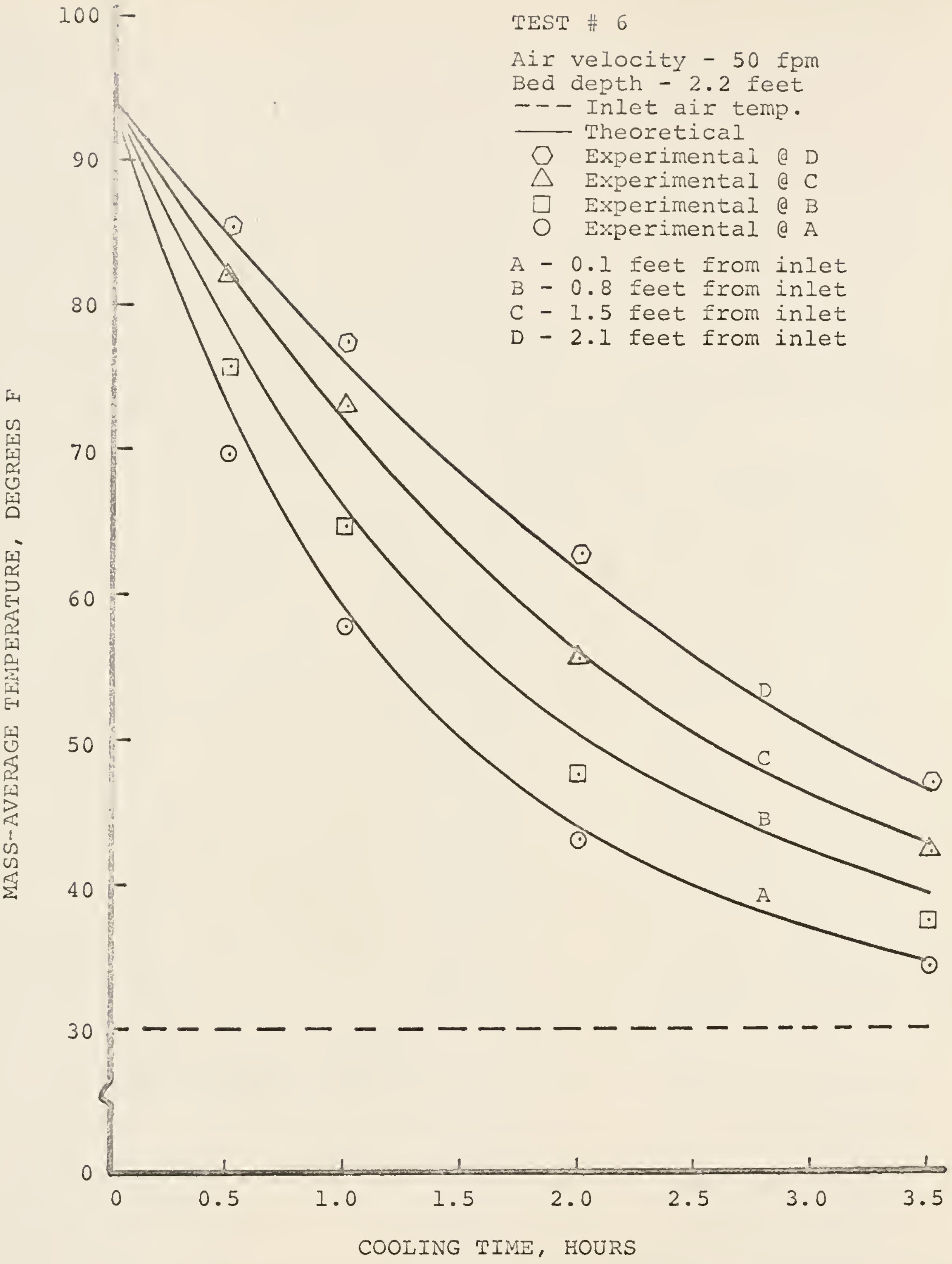

Figure 30. Comparison of experimental and theoretical temperature response of oranges to forced-air cooling

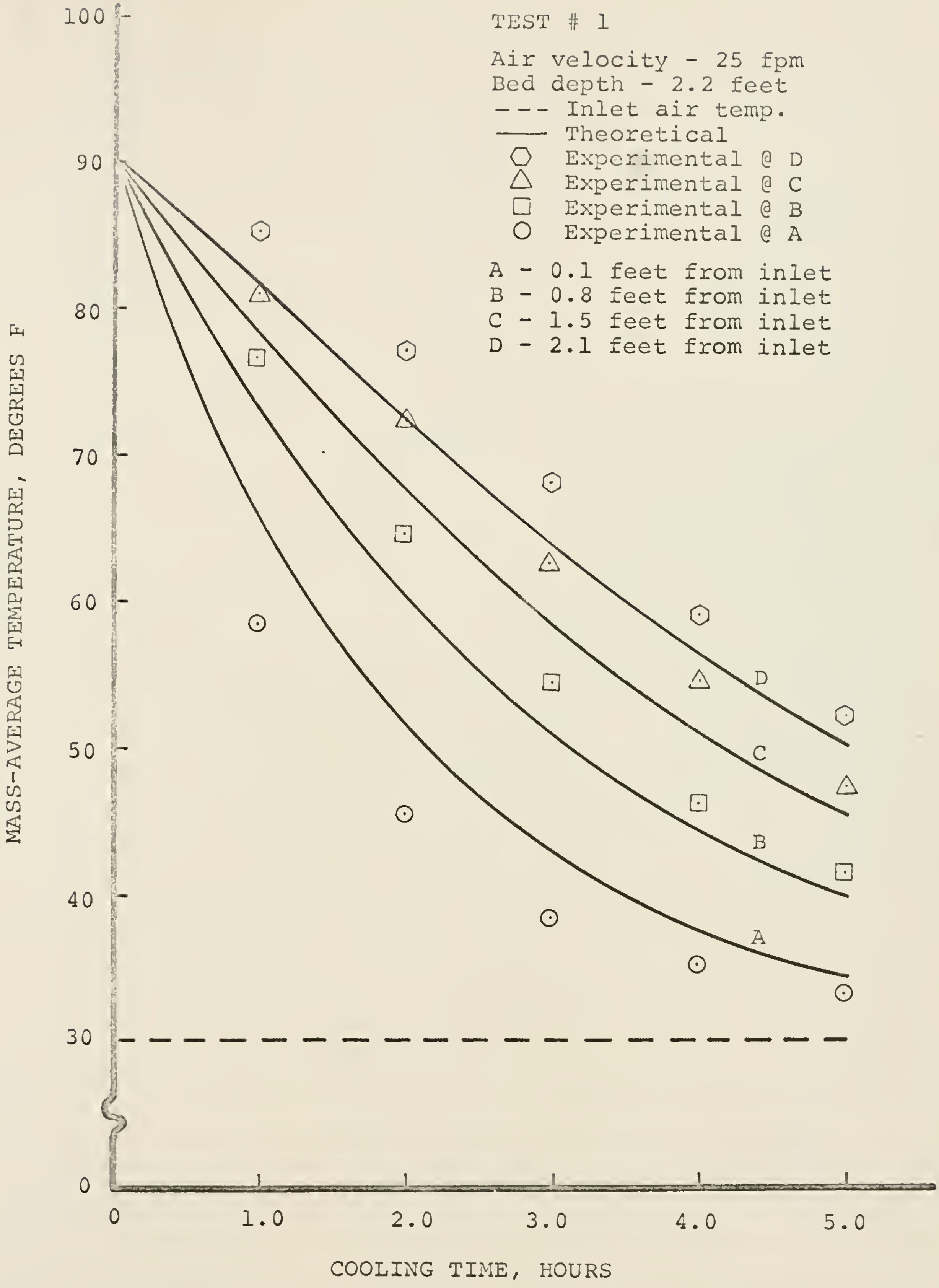

Figure 31. Comparison of experimental and theoretical temperature response of oranges to forced-air cooling

for this is probably due to a variation in h through the bed caused by evaporative cooling on the surface of the fruit. Figure 31 indicates that the bottom two layers cooled faster than predicted while the top two layers cooled slower than predicted. This means that the h for the bottom two layers was greater than that for the top two layers, since the prediction curves were generated using a constant h through the bed. This could be attributed to evaporative cooling since the humidity of the air increases as it moves through the bed, causing less evaporative cooling in each succeeding layer of the bed. An estimate of the upper limit for the amount of cooling produced by mass transfer can be made by considering the total amount of moisture loss during cooling. The average amount of moisture lost during a cooling test amounted to 0.53%. If all of the heat for vaporization came from the fruit, the temperature of the entire bed would be reduced by approximately 6 F. However, a large portion of the heat comes from the air and in turn leaves the bed without significantly cooling the fruit. Several investigators have observed that, in some cases, the temperature of the air leaving the bed was cooler than that entering.

Radiation heat transfer--Heat was transferred from the top and bottom layers of the bed to the cold inside surfaces of the cooler by radiation. However, assuming black bodies and a maximum temperature difference, radiation could account for only about 2 F of cooling during an average cooling test. The perforated top and bottom of the box reduced the exposed surface area; thus the amount of cooling by radiation would be reduced proportionally.

Conduction along the thermocouple wire--Heat will be conducted away from the measuring junction in the warm fruit because the thermocouple wire leading from the measuring junction is exposed to the cold air surrounding the fruit. This will result in a reading lower than the true value. Using basic heat transfer relationships, the dimensions of the wire, and average operating conductions; the maximum deviation was estimated to be -2 F.

Insulating effect of rind--The comparison curves (Appendix C) indicate that the experimental surface temperatures are consistently lower than the predicted theoretical values. Although some of this difference could be attributed to the foregoing reasons, it is believed that the major portion of it must be attributed to some other cause. Since the difference was so much more pronounced on the grapefruit than on the oranges, the effect of the rind on the temperature gradient was further investigated. The effect of the different thermal properties of the rind had previously been neglected based upon experimental data in the literature.

In order to investigate the effect of the rind on the temperature profile in citrus fruit a solution for heat conduction in a composite sphere was needed. Such a solution with convection boundary conditions at the surface would provide a comparison of surface temperatures for identical conditions. A solution with convection boundary conditions was not found in the literature. However, Carslaw and Jaeger (11) give the following solution for a composite sphere initially at a temperature, T_1, and the outer surface (r=b) suddenly lowered to zero temperature and held constant. It is assumed that there is no contact resistance between layers (r=a).

$$T_{inner} = 2bT_1/r \sum_{n=1}^{\infty} [1/\phi(\lambda_n)] \sin r\lambda_n \sin a\lambda_n \sin p(b-a)\lambda_n \, e^{-\alpha_i \lambda_n^2 t} \qquad [85]$$

$$T_{outer} = 2bT_1/r \sum_{n=1}^{\infty} [1/\phi(\lambda_n)] \sin^2 a\lambda_n \sin p(b-r)\lambda_n \, e^{-\alpha_i \lambda_n^2 t} \qquad [86]$$

$$\phi(\lambda_n) = \sigma a\lambda_n \sin^2 p\lambda_n (b-a) + p(b-a)\lambda_n \sin^2 a\lambda_n + [(1-p\sigma)/pa\lambda_n] \sin^2 a\lambda_n \sin^2 p(b-a)\lambda_n \qquad [87]$$

where

$\pm\lambda_n$, n = 1, 2, ..., are the roots of equation [87]

$p = \sqrt{\alpha_i/\alpha_o}$

$\sigma = k_i/pk_o$

a = radius of inner core

b = radius of outer core

T_{inner} = temperature of inner core

T_{outer} = temperature of outer shell

k_i = thermal conductivity of inner core

k_o = thermal conductivity of outer shell

α_i = thermal diffusivity of inner core

α_o = thermal diffusivity of outer shell

T_1 = initial uniform temperature of sphere

Equations [85] through [87] were evaluated using a digital computer and typical constants for grapefruit.

Figure 32 gives a comparison of the temperature profile in a homogeneous sphere with average properties of a grapefruit and the temperature profile in a composite sphere. For the composite sphere, the inner-core properties were set equal to those of the juice vesicles and the outer-shell properties were set equal to those of the rind. These curves represent the temperature profile after 0.5 hours of exposure time. The solid line represents the temperature profile in the composite sphere using $\alpha_{inner} = \alpha_{outer}$, but with the thermal conductivity (k) differing by a factor of two. The dashed

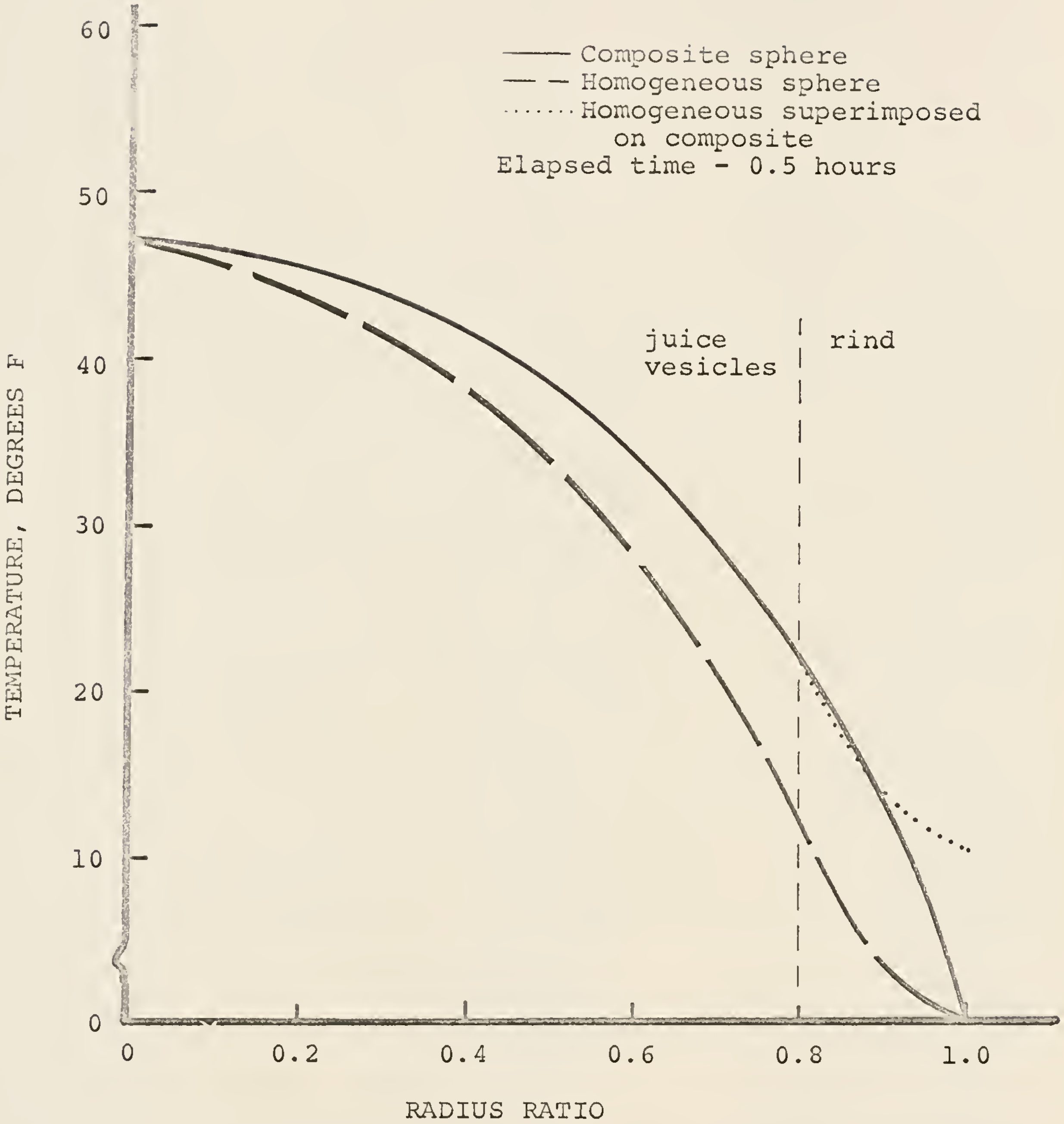

Figure 32. Comparison of the temperature profile in a homogeneous sphere with average properties of a grapefruit and the temperature profile in a composite sphere with properties corresponding to the rind and juice vesicles

line represents the temperature profile using the same equation, but with $\alpha_{inner} = \alpha_{outer}$ and $k_{inner} = k_{outer}$.

The temperature drop through the rind region is much greater for the composite sphere than it is for the homogeneous sphere (without rind). Although an actual comparison of surface temperatures cannot be made, an estimate can be obtained by superimposing the profile of one curve on the other, starting at the innerface between the juice vesicles and the rind. Thus, it is seen that the surface temperature may be as much as 10 F lower when the effect of the rind is considered. For actual air-cooling tests the effect of the rind on the temperature profile will not be as great as it was in this example, since the cooling rate will be less. However, it will no doubt account for most of the difference between the experimental and predicted surface temperatures.

Suggestions for Further Study

Optimum design and operating conditions

The results of this study provide a basis for making an economic analysis of the cooling system. By assuming certain cost figures and certain limitations based upon the physiological response of the product; the optimum air flow rate, air temperature, arrangement of product, etc., can be determined. The results of this study could be in the form of a computer program so that the designer or operator could plug in current input data based on his particular application.

Modification of numerical model

The results of this study are believed to be sufficiently accurate for engineering application, except for the predicted surface temperatures for grapefruit. Further work is necessary in order to model heat transfer in a bed of composite spheres.

In order to apply the numerical model to other products, it will be necessary to account for water-vapor transfer from the product and heat conduction in irregularly shaped bodies.

CONCLUSIONS

1. The numerical model can be used to predict the temperature distribution in an individual orange or grapefruit and within the bulk load as a function of time.
2. For slow cooling rates (25 fpm or less), the temperature gradients within the individual fruit can be neglected without significantly affecting the predicted mass-average temperature. However, for faster cooling rates the effect becomes significant.
3. The average convective heat transfer coefficient (h) can be predicted for a bed of oranges or grapefruit by using the Nusselt number - Reynolds number relationship as indicated in equation [84]. The constants in equation [84] can be evaluated by comparing experimental data with data from the numerical solution, thus providing a new and direct method for evaluating h in packed beds.
4. An average thermal diffusivity (α) for oranges or grapefruit can be determined experimentally by utilizing a fast cooling method, such as an agitated water bath. Since $\alpha \equiv \rho c/k$, all necessary properties

can be determined with adequate accuracy for engineering calculations when α and ρ are determined experimentally, and c is calculated as a function of moisture content. This allows k to be calculated, thus eliminating the tedious job of experimentally determining k.

5. The presence of the thick rind on grapefruit significantly affects the temperature gradient near the surface.
6. Radiation heat transfer does not significantly affect the cooling rate for the normal range of temperature used in precooling.

REFERENCES

1. Allen, F. W. and L. R. McKinnon. 1935. Precooling investigations with deciduous fruits. Univ. of Calif. Agr. Exp. Sta. Bul. 590. Berkeley.

2. American Society of Heating, Refrigerating and Air Conditioning Engineers. 1972. Handbook of Fundamentals. ASHRAE. N. Y.

3. Arpaci, V. S. 1966. Conduction Heat Transfer. Addison-Wesley Publishing Co., Reading, Mass.

4. Awberry, J. H. 1927. The flow of heat in a body generating heat. Phil. Mag. 4(7): 629-638.

5. Bakker-Arkema, F. W. and W. G. Bickert. 1966. A deep-bed computational cooling procedure for biological products. Transaction of the ASAE. 9(6): 834-836, 845.

6. Barker, J. J. 1965. Heat transfer in packed and fluidized beds I and II. Ind. Eng. Chem. 57(4): 43-51, 57(5): 33-39.

7. Bennett, A. H., W. G. Chace Jr., and R. H. Cubbedge. 1964. Thermal conductivity of Valencia orange and Marsh grapefruit rind and juice vesicles. ASHRAE Transactions. 70: 256-259.

8. Bennett, A. H., W. G. Chace Jr., and R. H. Cubbedge. 1970. Thermal properties and heat transfer characteristics of Marsh grapefruit. USDA Technical Bul. 1413. U. S. Government Printing Office, Washington, D. C.

9. Bennett, A. H., J. Soule, and G. E. Yost. 1966. Temperature response of Florida citrus to forced-air precooling. ASHRAE Journ. 8(4): 48-54, 66.

10. Businger, J. A. 1954. Luchtbehandeling var producten in gestorte toestand. Medelingen Institut voor Tuinbouwtechnik, Wageningen. 11, 31.

11. Carslaw, H. S. and J. C. Jaeger. 1959. Conduction of Heat in Solids. 2d. Ed. Oxford University Press, London.

12. Churchhill, R. V. 1958. Operational Mathematics. 2d. Ed. McGraw-Hill Book Co. N. Y.

13. Daizo, K. and S. Motoyuki. 1967. Particle to fluid heat and mass transfer in packed beds of fine particles. Ind. Eng. Chem. 59(2): 89-95.

14. Eaks, I. L. 1956. Effect of Hydrocooling on Oranges. Citrus Leaves. 6(2): 2, 33.

15. Earle, R. L. 1966. Unit Operations in Food Processing. pp. 334. Pergamon Press, N. Y.

16. Eckert, E. R. G. 1950. Introduction to the Transfer of Heat and Mass. McGraw-Hill Book Co., N. Y.

17. Florida Department of Agriculture and Consumer Services. 1972. Fla. Agr. Statistics - Citrus Summary.

18. Fourier, J. B. J. 1822. Theorie analytique de la Chaleur, Paris. English translation by A. Freeman, Cambridge. 1878.

19. Furnas, C. C. 1930. Heat transfer from a gas stream to a bed of broken solids. Ind. Eng. Chem. 22(7): 721-731.

20. Gane, R. 1936. The thermal conductivity of the tissue of fruits. Report of the Food Investigation Board for the year 1936: 211-212, London.

21. Grierson, W. 1957. Preliminary studies on cooling Florida oranges prior to packing. Fla. State Hort. Soc. Proc. 70: 264-272.

22. Guillou, R. 1960. Coolers for fruits and vegetables. Agr. Exp. Sta. Bul. 773, Univ. Calif., Berkeley.

23. Gurney, H. P. and J. Lurie. 1923. Charts for estimating temperature distributions in heating or cooling solid shapes. Ind. Eng. Chem. 15: 1170-1172.

24. Hayakawa, K. 1971. A parameter for evaluating initial cooling treatments for fresh foods. Can. Inst. Food Technol. J. 4(2): 58-61.

25. Heisler, M. P. 1947. Temperature charts for induction and constant-temperature heating. Trans. ASME. 69: 227-236.

26. Hendrickson, H. M. and J. R. RacRill. 1947. Refrigeration of oranges in California. Refrigerating Engineering. Sept.

27. Hood, C. E. 1964. Temperature progression during cooling of pickling cucumbers. Ph.D. thesis. Depart. of Agr. Eng., N. C. State, Raleigh.

28. Hopkins, E. F. and K. W. Loucks. 1951. The Dowicide A-Hexamine treatment of citrus fruits for the control of mold and stem-end rot decay. Citrus Mag. 13(12): 22-26.

29. Huang, R. and W. W. Gunkel. 1972. Theoretical and experimental studies of the heating front in a deep bed hygroscopic product. Paper presented at 1972 summer meeting of ASAE, Hot Springs, Arkansas.

30. Kethley, T. W., W. B. Cown, and F. Bellinger. 1950. An estimate of the thermal conductivities of fruits and vegetables. Refrigerating Engineering. 58(1): 49-50.

31. Kreith, F. 1958. Principles of Heat Transfer. International Textbook Co., Scranton, Pa.

32. Lebedev, P. D. and V. G. Petror-Denison. 1964. Hydrodynamics, heat and mass transfer in a bed of fine non-porous particles. Int. J. Heat Mass Transfer. 7: 1033-1045.

33. Leggett, J. T. and G. E. Sutton. 1951. Precooling of citrus fruits. Engineering Progress. 5(5): 1-31. (Bul. Ser. No. 43).

34. Maxie, E. C., N. F. Sommer, and F. G. Mitchell. 1967. The postharvest scientist's view of some problems in perishables handling. Proc. Fruit and Veg. Perrish. Handling Conf., Univ. of Calif., Davis, March 20-23.

35. McAdams, W. H. 1954. Heat Transmission. McGraw-Hill Book Co., N. Y.

36. Ming, T. V., J. S. Perry, and A. H. Bennett. 1969. Forced-air precooling of white potatoes in bulk. ASHRAE Transactions.

37. Perry, R. L., F. M. Turrell, and S. W. Austin. 1964. Thermal diffusivity of citrus fruits. Heat-Mass Transfer and Thermodynamics. pp. 242-246.

38. Pflug, I. J., J. L. Blaisdell, and I. J. Kopelman. 1965. Developing temperature-time curves for objects that can be approximated by a sphere, infinite plate, or infinite cylinder. Paper presented at semi-annual meeting of ASHRAE. Jan. 25-28. Chicago, Ill.

39. Poppendick, H. F. 1953. Transient and steady-state heat transfer in irradiated citrus fruit, ASME Transactions. 75: 421-425.

40. Powell, G. H. 1908. The Decay of Oranges while in transit from California. U.S.D.A. Bur. Plant Indus. Bul. 123, 79 pp.

41. Ramsey, H. J. 1915. Handling and Shipping Citrus Fruits in the Gulf States. U.S.D.A. Farmer's Bul. 696, 28 pp.

42. Redit, W. H. and A. A. Hamer. 1961. Protection of rail shipments of fruits and vegetables. U.S.D.A. Handbook No. 195, U. S. Govt. Printing Office. Washington, D. C.

43. Sainsbury, G. F. 1951. Improved fruit cooling methods. Refrigerating Engineering. 59(1): 464-469.

44. Schneider, P. J. 1955. Conduction heat transfer. Addison-Wesley Pub. Co., Reading, Mass.

45. Schumann, T. E. W. 1929. Heat Transfer: A liquid flowing through a porous prism. J. Franklin Inst. 208(3): 405-416.

46. Smith, R. E. and A. H. Bennett. 1965. Mass-average temperature of fruits and vegetables during transient cooling. Transactions of the ASAE.

47. Smith, R. E., G. L. Nelson, and R. L. Hendrickson. 1968. Applications of geometry analysis of anomalous shapes to problems in transient heat transfer. Transactions of the ASAE. 11(2): 296-302.

48. Soule, J., G. E. Yost, and A. H. Bennett. 1969. Experimental forced-air precooling of Florida citrus fruit. U.S.D.A. Marketing Research Report No. 845. U. S. Government Printing Office, Washington, D. C.

49. Thevenot, R. 1955. Precooling. Proceedings of International Congress of Refrigeration. 1: 0052-0071.

50. Turrell, F. M. and R. L. Perry. 1957. Specific heat and heat conductivity of citrus fruit. Proc. Amer. Soc. Hort. Science. 70: 261-265.

51. Vanecck, C. V., M. Markvart, and R. Drbohlav. 1964. Fluidized bed drying. CRC Press, Int. Scientific Series. London.

52. Wadsworth, J. 1961. An experimental investigation of the local packing and heat transfer processes in packed beds of homogeneous spheres. Intern. Heat Transfer Conf. ASME. N. Y.

53. Wang, J. and P. Wang. 1967. A computational technique for deep-bed forced-air precooling of tomatoes. Paper presented at 1967 winter meeting of ASAE, Detroit, Michigan.

APPENDIX A

COMPUTER PROGRAM AND SAMPLE OUTPUT FOR CONDUCTION IN A SPHERE WITH SPECIFIED SURROUNDING TEMPERATURE

```
      DIMENSION ATEMP(21),PRSNT(21),PREC(21),TESTNO(3)
   99 READ (5,1,END=1000) ALPHA,CONDTY, HTC,RADIUS,NPOINT,
     *TPINIT,TIMINC,THETA,INC,(TESTNO(I),I=1,3)
    1 FORMAT (F5.5,F5.3,F5.1,F5.3,I5,F5.1,F5.3,F5.2,I5,23X,3A4
     *)
      READ (5,2) (ATEMP(L),L=1,11)
    2 FORMAT (11F5.1)
      PRINT 70,(TESTNO(I),I=1,3)
   70 FORMAT (1H1,'UNIVERSITY OF FLORIDA AGRICULTURAL ENGINE',
     *'ERING DEPARTMENT--COOLING TEST NUMBER ',3A4,//)
      PRINT 80, ALPHA,CONDTY,HTC,RADIUS,NPOINT,TPINIT,TIMINC,
     *THETA,INC,(ATEMP(L),L=1.11)
   80 FORMAT (35X,'THERMAL DIFFUSIVITY',F11.5//,35X,'THERMAL',
     *' CONDUCTIVITY',F8.3//,35X,'CONVECTIVE COEFFICIENT',
     *F5.1//,35X,'RADIUS',F22.3//,35X,'NUMBER OF POINTS',I9//,
     *F14.3//,35X,'TOTAL TIME',F17.2//,35X,'PRINT FREQUENCY',
     *I10/////,1X,'AIR TEMPERATURES:',11F6.1)
      SEGMNT=NPOINT-1
      RINC=RADIUS/SEGMNT
      D=1.0-3.0*ALPHA*TIMINC*((RADIUS-RINC/2.0)**2/RIND+RADIU
     *S**2*HTC/CONDTY)/(RADIUS**3-(RADIUS-RINC/2.0)**)
      IF (D .LT. 0.0) GO TO 100
      B=3.0*ALPHA*TIMINC*(RADIUS-RINC/2.0)**2/RINC/(RADIUS**3
     *-(RADIUS-RINC/2.0)**3)
      H=6.0*ALPHA*TIMINC/RINC**2
      P=1.0-H
      NDIV=THETA/TIMINC/10.0
      TIME=0.0
      NO=0
      N=1
      NUM=1
      TAIR=ATEMP(1)
      DO 3 J=1,NPOINT
    3 PRSNT(J)=TPINIT
      PRINT 70,(TESTNO(I),I=1,3
      PRINT 300
  300 FORMAT (1H ,' TIME  AIR  **************** PRODUCT TEMP',
     *'ERATURE AT R/RADIUS ****************'/,1X,' (HR)  TEM',
     *'P',31X, '(F)'/,6X'  (F)   1.0   0.9   0.8   0.7   0.6',
     *'   0.5   0.4   0.3   0.2   0.1   0.0'//)
      PRINT 4, TIME,TAIR,(PRSNT(J),J=1,NPOINT)
    4 FORMAT (1H ,F6.3,F5.1,11F6.2)
    9 N=N+1
      NCT=0
      DAIR=(ATEMP(N)-ATEMP(N-1))/THETA*(TIMINC*10.0)
    5 TIME=TIME+TIMINC
      NCT=NCT+1
      NUM=NUM+1
      DO 15 J=1,NPOINT
   15 PREC(J)=PRSNT(J)
      PRSNT(1)=B*PREC(2)+C*TAIR+PREC(1)
      TAIR=TAIR+DAIR
      M=NPOINT-1
      DO 7 J=2,M
      R=RADIUS-RINC*(J-1)
      E=1.0-ALPHA*TIMINC*(2.0+((RINC/R)**2/2.0))/RINC**2
      IF (E .LT. 0.0) GO TO 101
      F=ALPHA*TIMINC*(1.0-RINC/2.0/R)**2/RINC**2
      G=ALPHA*TIMINC*(1.0+RINC/2.0/R)**2/RINC**2
    7 PRSNT(J)=E*PREC(J)+F*PREC(J+1)+G*PREC(J-1)
      J=NPOINT
      PRSNT(J)=H*PREC(J-1)+P*PREC(J)
      IF (NUM-INC)40,40,20
   20 PRINT 6, TIME, TAIR,(PRSNT(J),J=1,NPOINT)
    6 FORMAT (1H , F6.3, F5.1,11F6.2)

      NO=NO+1
      NUM=1
   40 IF (NO-50) 90,10,10
   10 NO=0
      PRINT 70,(TESTNO(I),I=1,3)
      PRINT 300
   90 IF (THETA-TIME) 99,99,8
    8 IF (NDIV-NCT) 5,9,5
  100 PRINT 50
   50 FORMAT (1H1,'D IS LESS THAN ZERO')
      GO TO 99
 1000 PRINT 1001
 1001 FORMAT ('1')
      STOP
      END
```

```
                INPUT DATA

     THERMAL DIFFUSIVITY      0.0051

     THERMAL CONDUCTIVITY     0.256

     CONVECTIVE COEFFICIENT   11.7

     RADIUS                   0.113

     NUMBER OF POINTS         11

     INITIAL FRUIT TEMP.      90.0

     TIME INCREMENT           0.005

     TOTAL TIME               2.00

     PRINT FREQUENCY          20


AIR TEMPERATURES:  30.0  30.0  30.0  30.0  30.0  30.0  30.0  30.0  30.0  30.0  30.0
```

```
TIME   AIR   **************** PRODUCT TEMPERATURE AT R/RADIUS ***************
(HR)   TEMP                              (F)
       (F)   1.0    0.9    0.8    0.7    0.6    0.5    0.4    0.3    0.2    0.1    0.0


0.0    30.0 90.00  90.00  90.00  90.00  90.00  90.00  90.00  90.00  90.00  90.00  90.00
0.100  30.0 50.77  61.36  70.60  77.84  82.97  86.23  88.12  89.11  89.57  89.77  89.93
0.200  30.0 43.89  51.21  58.34  64.91  70.63  75.36  79.06  81.76  83.55  84.54  84.89
0.300  30.0 40.07  45.44  50.86  56.11  69.97  65.26  68.88  71.72  73.74  74.91  75.33
0.400  30.0 37.53  41.57  45.70  49.77  53.62  57.12  60.13  62.55  64.31  65.33  65.70
0.500  30.0 35.71  38.77  41.92  45.05  48.04  50.77  53.15  55.07  56.48  57.31  57.61
0.600  30.0 34.34  36.68  39.08  41.48  43.77  45.88  47.72  49.22  50.31  50.96  51.19
0.700  30.0 33.31  35.09  36.93  38.76  40.52  42.14  43.55  44.70  45.54  46.04  46.22
0.800  30.0 32.53  33.89  35.29  36.69  38.04  39.27  40.35  41.23  41.88  42.26  42.40
0.900  30.0 31.93  32.97  34.04  35.11  36.14  37.08  37.91  38.58  39.08  39.37  39.47
1.000  30.0 31.48  32.27  33.09  33.90  34,69  35.41  36.04  36.56  36.93  37.16  37.24
1.100  30.0 31.13  31.73  32.36  32.98  33.58  34.13  34.16  35.01  35.30  35.47  35.53
1.200  30.0 30.86  31.32  31.80  32.28  32.73  33.16  33.52  33.82  34.05  34.17  34.22
1.300  30.0 30.66  31.01  31.38  31.74  32.09  32.41  32.69  32.92  33.09  33.19  33.22
1.400  30.0 30.50  30.77  31.05  31.33  31.59  31.84  32.06  32.23  32.36  32.43  32.46
1.500  30.0 30.38  30.59  30.80  31.01  31.22  31.41  31.57  31.70  31.80  31.86  31.88
1.600  30.0 30.29  30.45  30.61  30.77  30.93  31.07  31.20  31.30  31.38  31.42  31.44
1.700  30.0 30.22  30.34  30.47  30.59  30.71  30.82  30.91  30.99  31.05  31.08  31.10
1.800  30.0 30.17  30.26  30.36  30.45  30.54  30.63  30.70  30.76  30.80  30.83  30.84
1.900  30.0 30.13  30.20  30.27  30.34  30.41  30.48  30.53  30.58  30.61  30.63  30.64
2.000  30.0 30.10  30.15  30.21  30.26  30.32  30.36  30.41  30.44  30.47  30.48  30.49
```

APPENDIX B - COMPUTER PROGRAM AND SAMPLE OUTPUT FOR COOLING A DEEP BED OF CITRUS FRUIT

```
      DIMENSION PRSNT(21,25),PREC(21,25),TESTNO(3),VOL(21),
     *TPSECA(21),TPLSUP(21),PRSFAV(25),PREPAV(25)
   99 READ (5,1,END=1000) ALPHA,CONDTY, HTC,RADIUS,NPOINT,TPIN
     *IT,TIMINC,THETA,INC,(TESTNO(I),I=1,3)
    1 FORMAT (F5.5,F5.3,F5.2,F5.3,I5,F5.1,F5.3,F5.2,I5,23X,3A4
     *)
      READ (5,2) SHA,SHP,TOTWT,AIRWTF,NUMLAY,BHGHT,ATEMP,AIRVE
     *L,KPROD
    2 FORMAT (F5.3,F5.3,F5.1,F5.0,I5,F5.2,F5.1,F5.0,I1)
      PRINT 70,(TESTNO(I),I=1,3)
   70 FORMAT (1H1,'                                                   ',
     *'                                                   ',3A4,/////////)
      PRINT 80, ALPHA,CONDTY,HTC,RADIUS,NPOINT,TPINIT,TIMINC,T
     *HETA,INC,SHA,SHP,TOTWT,AIRWTF,NUMLAY,BHGHT,ATEMP,AIRVEL
   80 FORMAT (35X,'THERMAL DIFFUSIVITY',F11.5//,35X,'THERMAL',
     *' CONDUCTIVITY',F8.3//,35X,'CONVECTIVE COEFFICIENT',
     *F6.3//,35X,'RADIUS',F22.3//,35X,'NUMBER OF POINTS',
     *I9//,35X,'INITIAL FRUIT TEMP.',F8.1//,35X,'TIME INCREME',
     *'NT',F14.3//,35X,'TOTAL TIME',F17.2//,35X,'PRINT FRE',
     *'QUENCY',I10//,35X,'SPECIFIC HEAT AIR',F12.4//,35X,
     *'SPECIFIC HEAT PRODUCT',F7.3//,35X,'WEIGHT PRODUCT',
     *F14.1//,35X,'AIR FLOW RATE',F14.0//,35X,'LAYERS IN BED',
     *I12//,35X,'BED DEPTH',F19.3//,35X,'ENTERING AIR TEMP.',
     *F10.1//,35X,'AIR VELOCITY',F15.0/)
      IF (KPROD-1) 350,350,360
  350 PRINT 351
  351 FORMAT (35X,'PRODUCT',16X,'GRAPEFRUIT')
      GO TO 352
  360 PRINT 361
  361 FORMAT (35X,'PRODUCT',16X,'ORANGES')
  352 SEGMNT=NPOINT-1
      RINC=RADIUS/SEGMNT
      D=1.0-3.0*ALPHA*TIMINC*((RADIUS-RINC/2.0)**2/RINC+RADIUS
     ***2*HTC/CONDTY)/(RADIUS**3-(RADIUS-RINC/2.0)**3)
      IF (D .LT. 0.0) GO TO 100
      B=3.0*ALPHA*TIMINC*(RADIUS-RINC/2.0)**2/RINC/(RADIUS**3-
     *(RADIUS-RINC/2.0)**3)
      C=3.0*RADIUS**2*HTC*ALPHA*TIMINC/CONDTY/(RADIUS**3-(RADI
     *US-RINC/2.0)**3)
      H=6.0*ALPHA*TIMINC/RINC**2
      P=1.0-H
      NSEG=NPOINT-1
      WTPL=TOTWT/NUMLAY
      DO 31 J=1,NSEG
      A=J
      SEG=NSEG
   31 VOL(J)=(1.-(A-1.)/SEG)**3-(1.-A/SEG)**3
      IF (KPROD-1) 250,250,260
  250 VOLO=VOL(1)*30.0+VOL(2)*30.0
      VOLI=0.0
      DO 200 L=3,NSEG
  200 VOLI=VOLI+VOL(L)*57.2
      TVOL=VOLI+VOLO
      VOL(1)=VOL(1)*(30.0/TVOL)
      VOL(2)=VOL(2)*(30.0/TVOL)
      DO 201 L=3,NSEG
  201 VOL(L)=VOL(L)*(57.2/TVOL)
      GO TO 270
  260 VOLO=VOL(1)*23.7
      VOLI=0.0
      DO 261 L=2,NSEG
  261 VOLI=VOLI+VOL(L)*57.6
      TVOL=VOLI+VOLO
      VOL(1)=VOL(1)*(23.7/TVOL)
      DO 262 L=2,NSEG
  262 VOL(L)=VOL(L)*(57.6/TVOL)
  270 TIME=0.0
      NO=0
      N=1
      TAIR=ATEMP
      DO 3 J=1,NPCINT
      DO 3 K=1,NUMLAY
    3 PRSNT(J,K)=TPINIT
      PRINT 70,(TESTNO(I),I=1.3)
      K=1
      PRINT 300
  300 FORMAT (15X,'DISTANCE  TIME  AIR  ***************** PRO',
     *'DUCT TEMPERATURES AT R/RADIUS ***************** MASS'/,
     *15X,'FROM',6X,'(HR)  TEMP',31X,'(F)',33X,'AVG'/,15X,
     *'INLET',11X,'(F)   1.0   0.9   0.8   0.7   0.6   0.5',
     *'   0.4   0.3   0.2   0.1   0.0  TEMP'/,15X,'(FT)')
      PRINT 4, TIME,TAIR,(PRSNT(J,K),J=1,NPCINT),TPINIT
    4 FORMAT (15X,9X,F6.3,F5.1,11F6.2,F6.2)
      DO 37 K=1,NUMLAY
   37 PREPAV(K)=TPINIT
   43 NPRINT=1
   42 NUM=1
   41 TIME=TIME+TIMINC
      K=0
      NUM=NUM+1
    5 K=K+1
      AK=K
      ANUMLY=NUMLAY
      IF (K-1) 301,301,302
  301 DFINLT=(BHGHT/ANUMLY)/2.0
      GO TO 303
  302 DFINLT=AK*(BHGHT/ANUMLY)-(BHGHT/ANUMLY)/2.0
  303 DO 15 J=1.NPCINT
   15 PREC(J,K)=PRSNT(J,K)
      PRSNT(1,K)=B*PREC(2.K)+C*TAIR+D*PREC(1,K)
      M=NPCINT-1
      DO 7 J=2,M
      R=RADIUS-RINC*(J-1)
      E=1.0-ALPHA*TIMINC*(2.0+((RINC/R)**2/2.0))/RINC**2
      IF (E .LT. 0.0) GO TO 101
      F=ALPHA*TIMINC*(1.0-RINC/2.0/R)**2/RINC**2
      G=ALPHA*TIMINC*(1.0+RINC/2.0/R)**2/RINC**2
    7 PRSNT(J,K)=E*PREC(J,K)+F*PREC(J+1,K)+G*PREC(J-1,K)
```

```
      J=NPOINT
      PRSNT(J,K)=H*PREC(J-1,K)+P*PREC(J,K)
      DO 30 J=1,NSEG
   30 TPSECA(J)=(PRSNT(J+1,K)-PRSNT(J,K))*0.5300+PRSNT(J,K)
      DO 32 J=1,NSEG
   32 TPLSUB(J)=TPSECA(J)*VOL(J)
      PRSPAV(K)=0.0
      DO 33 J=1,NSEG
   33 PRSPAV(K)=PRSPAV(K)+TPLSUB(J)
      IF (NUM-INC) 40,40,20
   20 PRINT 6,DFINLT,TIME,TAIR,(PRSNT(J,K),J=1,NPOINT),PRSPAV(
     *K)
    6 FORMAT (15X,F5.2,4X,F6.3,F5.1,11F6.2,F6.2)
      NPRINT=NPRINT+1
      NO=NC+1
   40 IF (NC-33) 89,10,10
   10 NO=0
      PRINT 70,(TESTNO(I),I=1,3)
      PRINT 300
   89 DTAIR=WTPL*SHP*(PREPAV(K)-PRSPAV(K))/(AIRWTF*TIMINC*SHA)
      TAIR=TAIR+DTAIR
      IF (K-NUMLAY) 5,90,90
   90 IF (THETA-TIME) 99,99,38
   38 DO 39 K=1,NUMLAY
   39 PREPAV(K)=PRSPAV(K)
      TAIR=ATEMP
      IF (NUMLAY-NPRINT) 43,41,41
  100 PRINT 50
   50 FORMAT (1H1,'D IS LESS THAN ZERO')
      GO TO 99
  101 PRINT 60
   60 FORMAT (1H1,'E IS LESS THAN ZERO')
      GO TO 99
 1000 PRINT 1001
 1001 FORMAT ('1')
      STOP
      END
```

INPUT DATA

```
THERMAL DIFFUSIVITY     0.00437

THERMAL CONDUCTIVITY    0.249

CONVECTIVE COEFFICIENT 3.060

RADIUS                  0.117

NUMBER OF POINTS        11

INITIAL FRUIT TEMP.     91.0

TIME INCREMENT          0.005

TOTAL TIME              2.50

PRINT FREQUENCY         20

SPECIFIC HEAT AIR       0.2400

SPECIFIC HEAT PRODUCT   0.900

WEIGHT PRODUCT          340.0

AIR FLOW RATE          1930.

LAYERS IN BED           11

BED DEPTH               2.200

ENTERING AIR TEMP.       32.0

AIR VELOCITY            100.

PRODUCT                 ORANGES
```

```
DISTANCE  TIME  AIR   *************** PRODUCT TEMPERATURES AT R/RADIUS ************** MASS
FROM      (HR)  TEMP                                    (F)                           AVG
INLET           (F)   1.0    0.9    0.8    0.7    0.6    0.5    0.4    0.3    0.2    0.1    0.0   TEMP
(FT)
          0.0   32.0 91.00  91.00  91.00  91.00  91.00  91.00  91.00  91.00  91.00  91.00  91.00 91.00
  0.10    0.100 32.0 75.00  80.63  84.85  87.69  89.38  90.28  90.71  90.89  90.96  90.98  90.99 85.71
  0.30    0.100 35.3 75.89  81.19  85.18  87.86  89.46  90.32  90.72  90.89  90.96  90.98  90.99 85.99
  0.50    0.100 38.5 76.72  81.73  85.49  88.02  89.54  90.35  90.74  90.90  90.96  90.98  90.99 86.26
  0.70    0.100 41.4 77.51  82.23  85.78  88.18  89.62  90.38  90.75  90.90  90.96  90.98  90.99 86.51
  0.90    0.100 44.2 78.26  82.71  86.06  88.33  89.69  90.41  90.76  90.91  90.96  90.98  90.99 86.76
  1.10    0.100 46.9 78.96  83.16  86.33  88.46  89.75  90.44  90.77  90.91  90.97  90.98  90.99 86.98
  1.30    0.100 49.4 79.63  83.59  86.58  88.60  89.82  90.47  90.78  90.92  90.97  90.99  90.99 87.20
  1.50    0.100 51.7 80.26  83.99  86.81  88.72  89.88  90.50  90.79  90.92  90.97  90.99  90.99 87.40
  1.70    0.100 53.9 80.85  84.37  87.03  88.84  89.93  90.52  90.80  90.92  90.97  90.99  90.99 87.60
  1.90    0.100 56.0 81.41  84.73  87.25  88.95  89.99  90.54  90.81  90.93  90.97  90.99  90.99 87.78
  2.10    0.100 58.0 81.94  85.08  87.45  89.06  90.04  90.57  90.82  90.93  90.97  90.99  90.99 87.95
  0.10    0.200 32.0 68.94  74.00  78.38  81.97  84.76  86.82  88.25  89.19  89.75  90.04  90.14 80.40
  0.30    0.200 35.0 70.12  74.92  79.07  82.46  85.10  87.04  88.40  89.28  89.82  90.09  90.19 80.97
  0.50    0.200 37.9 71.24  75.79  79.71  82.93  85.42  87.26  88.53  89.37  89.88  90.14  90.23 81.51
  0.70    0.200 40.7 72.29  76.61  80.33  83.37  85.72  87.46  88.67  89.46  89.94  90.18  90.27 82.02
  0.90    0.200 43.3 73.30  77.39  80.91  83.78  86.01  87.65  88.79  89.54  89.99  90.23  90.31 82.51
  1.10    0.200 45.7 74.24  78.13  81.46  84.17  86.28  87.83  88.91  89.62  90.05  90.27  90.34 82.97
  1.30    0.200 48.1 75.14  78.82  81.97  84.54  86.53  88.00  89.02  89.69  90.10  90.30  90.37 83.40
  1.50    0.200 50.3 75.99  79.48  82.46  84.89  86.77  88.16  89.12  89.76  90.14  90.34  90.41 83.81
  1.70    0.200 52.4 76.79  80.10  82.93  85.22  87.00  88.31  89.22  89.82  90.19  90.37  90.44 84.20
  1.90    0.200 54.4 77.55  80.69  83.37  85.54  87.22  88.46  89.32  89.89  90.23  90.41  90.47 84.57
  2.10    0.200 56.3 78.27  81.25  83.78  85.83  87.42  88.59  89.41  89.94  90.27  90.44  90.49 84.92
  0.10    0.300 32.0 64.52  69.06  73.18  76.80  79.86  82.34  84.27  85.69  86.64  87.17  87.36 75.58
  0.30    0.300 34.8 65.86  70.19  74.12  77.55  80.45  82.81  84.64  85.98  86.88  87.38  87.56 76.39
  0.50    0.300 37.4 67.13  71.27  75.00  78.27  81.02  83.25  84.98  86.25  87.10  87.57  87.74 77.15
  0.70    0.300 39.9 68.34  72.28  75.84  78.94  81.55  83.66  85.30  86.50  87.31  87.76  87.91 77.88
  0.90    0.300 42.3 69.48  73.25  76.64  79.58  82.06  84.06  85.61  86.74  87.51  87.93  88.08 78.56
  1.10    0.300 44.6 70.57  74.17  77.39  80.19  82.53  84.43  85.90  86.97  87.69  88.09  88.24 79.21
  1.30    0.300 46.7 71.60  75.04  78.10  80.76  82.99  84.78  86.17  87.19  87.87  88.25  88.38 79.83
  1.50    0.300 48.8 72.58  75.86  78.78  81.30  83.42  85.12  86.43  87.39  88.04  88.40  88.52 80.42
  1.70    0.300 50.8 73.51  76.64  79.42  81.82  83.82  85.43  86.68  87.59  88.20  88.54  88.66 80.97
  1.90    0.300 52.7 74.40  77.38  80.03  82.31  84.20  85.73  86.91  87.77  88.35  88.67  88.78 81.49
  2.10    0.300 54.5 75.24  78.08  80.60  82.77  84.57  86.01  87.13  87.95  88.49  88.79  88.90 81.99
```

```
DISTANCE  TIME   AIR   *************** PRODUCT TEMPERATURES AT R/RADIUS ************** MASS
FROM      (HR)   TEMP                              (F)                                  AVG
INLET            (F)    1.0    0.9    0.8    0.7    0.6    0.5    0.4    0.3    0.2    0.1    0.0   TEMP
(FT)
 0.10     0.400  32.0  60.95  65.02  68.81  72.23  75.23  77.77  79.83  81.41  82.51  83.14  83.36  71.24
 0.30     0.400  34.5  62.37  66.28  69.91  73.19  76.05  78.46  80.42  81.92  82.97  83.56  83.77  72.23
 0.50     0.400  36.9  63.73  67.49  70.97  74.09  76.82  79.12  80.98  82.40  83.39  83.96  84.16  73.17
 0.70     0.400  39.2  65.02  68.64  71.97  74.95  77.55  79.74  81.51  82.86  83.80  84.33  84.52  74.06
 0.90     0.400  41.4  66.25  69.73  72.92  75.77  78.25  80.33  82.01  83.29  84.18  84.69  84.87  74.91
 1.10     0.400  43.5  67.43  70.77  73.82  76.55  78.91  80.89  82.48  83.70  84.55  85.03  85.20  75.72
 1.30     0.400  45.5  68.55  71.76  74.68  77.28  79.53  81.42  82.93  84.09  84.89  85.35  85.51  76.48
 1.50     0.400  47.5  69.62  72.70  75.50  77.98  80.12  81.92  83.36  84.46  85.22  85.65  85.80  77.21
 1.70     0.400  49.3  70.64  73.59  76.27  78.64  80.69  82.39  83.76  84.80  85.52  85.93  86.08  77.90
 1.90     0.400  51.1  71.61  74.45  77.01  79.27  81.22  82.84  84.14  85.13  85.82  86.20  86.34  78.56
 2.10     0.400  52.8  72.53  75.26  77.71  79.87  81.73  83.27  84.51  85.44  86.09  86.46  86.59  79.18
 0.10     0.500  32.0  57.90  61.56  65.01  68.17  70.99  73.42  75.43  77.00  78.11  78.75  78.98  67.33
 0.30     0.500  34.2  59.37  62.91  66.24  69.28  71.98  74.30  76.23  77.72  78.78  79.39  79.61  68.46
 0.50     0.500  36.4  60.77  64.20  67.41  70.33  72.92  75.14  76.98  78.41  79.41  79.99  80.20  69.53
 0.70     0.500  38.5  62.12  65.44  68.52  71.33  73.81  75.94  77.69  79.05  80.01  80.57  80.76  70.55
 0.90     0.500  40.5  63.40  66.61  69.59  72.29  74.66  76.70  78.37  79.67  80.59  81.11  81.30  71.53
 1.10     0.500  42.5  64.64  67.74  70.60  73.19  75.47  77.42  79.02  80.25  81.13  81.63  81.81  72.46
 1.30     0.500  44.4  65.81  68.81  71.57  74.06  76.24  78.10  79.63  80.81  81.64  82.12  82.29  73.34
 1.50     0.500  46.2  66.94  69.84  72.50  74.88  76.97  78.75  80.21  81.33  82.13  82.58  82.74  74.19
 1.70     0.500  47.9  68.02  70.82  73.38  75.67  77.67  79.37  80.76  81.83  82.59  83.02  83.17  74.99
 1.90     0.500  49.6  69.05  71.75  74.21  76.41  78.33  79.96  81.28  82.31  83.02  83.43  83.58  75.76
 2.10     0.500  51.3  70.04  72.65  75.01  77.12  78.96  80.51  81.78  82.75  83.44  83.83  83.97  76.49
 0.10     0.600  32.0  55.24  58.54  61.66  64.54  67.13  69.39  71.27  72.76  73.81  74.42  74.64  63.81
 0.30     0.600  34.0  56.73  59.94  62.96  65.75  68.26  70.43  72.24  73.66  74.67  75.26  75.47  65.03
 0.50     0.600  36.0  58.15  61.28  64.22  66.92  69.33  71.42  73.16  74.52  75.49  76.05  76.25  66.21
 0.70     0.600  37.9  59.52  62.57  65.42  68.02  70.35  72.36  74.03  75.34  76.27  76.80  77.00  67.33
 0.90     0.600  39.7  60.84  63.80  66.56  69.08  71.33  73.26  74.86  76.12  77.01  77.52  77.70  68.40
 1.10     0.600  41.5  62.10  64.98  67.66  70.10  72.26  74.12  75.65  76.86  77.71  78.20  78.37  69.43
 1.30     0.600  43.3  63.32  66.12  68.71  71.06  73.14  74.93  76.41  77.56  78.37  78.84  79.01  70.41
 1.50     0.600  45.0  64.48  67.20  69.71  71.98  73.99  75.71  77.12  78.23  79.01  79.46  79.62  71.35
 1.70     0.600  46.7  65.60  68.24  70.67  72.86  74.79  76.44  77.80  78.86  79.61  80.04  80.19  72.24
 1.90     0.600  48.3  66.68  69.24  71.59  73.70  75.56  77.15  78.45  79.46  80.18  80.59  80.74  73.10
 2.10     0.600  49.8  67.71  70.20  72.47  74.51  76.29  77.82  79.07  80.04  80.72  81.12  81.26  73.92
```

```
DISTANCE   TIME   AIR   *************** PRODUCT TEMPERATURES AT R/RADIUS *************** MASS
FROM       (HR)   TEMP                              (F)                                   AVG
INLET             (F)    1.0    0.9    0.8    0.7    0.6    0.5    0.4    0.3    0.2    0.1    0.0   TEMP
(FT)
  0.10     0.700  32.0  52.89  55.85  58.67  61.28  63.64  65.71  67.44  68.81  69.78  70.35  70.56  60.63
  0.30     0.700  33.8  54.37  57.28  60.03  62.57  64.87  66.87  68.54  69.86  70.80  71.35  71.55  61.93
  0.50     0.700  35.6  55.79  58.65  61.33  63.81  66.04  67.97  69.59  70.86  71.77  72.30  72.49  63.18
  0.70     0.700  37.3  57.17  59.97  62.59  65.00  67.16  69.03  70.59  71.82  72.69  73.20  73.38  64.37
  0.90     0.700  39.0  58.50  61.23  63.79  66.13  68.23  70.04  71.55  72.73  73.57  74.06  74.24  65.52
  1.10     0.700  40.7  59.78  62.45  64.95  67.22  69.25  71.00  72.46  73.60  74.41  74.88  75.05  66.61
  1.30     0.700  42.3  61.01  63.63  66.06  68.27  70.23  71.92  73.33  74.43  75.21  75.66  75.82  67.67
  1.50     0.700  43.9  62.20  64.76  67.12  69.27  71.17  72.80  74.16  75.22  75.97  76.40  76.56  68.68
  1.70     0.700  45.5  63.35  65.84  68.14  70.22  72.06  73.64  74.95  75.97  76.69  77.11  77.26  69.64
  1.90     0.700  47.0  64.45  66.88  69.12  71.14  72.92  74.45  75.71  76.69  77.38  77.78  77.93  70.57
  2.10     0.700  48.5  65.52  67.89  70.06  72.01  73.74  75.21  76.43  77.37  78.04  78.43  78.56  71.46
  0.10     0.800  32.0  50.79  53.46  56.00  58.36  60.49  62.37  63.94  65.19  66.08  66.60  66.79  57.78
  0.30     0.800  33.6  52.25  54.88  57.38  59.70  61.79  63.61  65.15  66.36  67.22  67.73  67.91  59.12
  0.50     0.800  35.2  53.66  56.26  58.72  60.98  63.03  64.81  66.30  67.47  68.31  68.80  68.97  60.41
  0.70     0.800  36.8  55.03  57.59  60.01  62.22  64.22  65.95  67.40  68.54  69.35  69.82  69.99  61.65
  0.90     0.800  38.4  56.35  58.88  61.25  63.41  65.36  67.04  68.45  69.56  70.35  70.80  70.97  62.85
  1.10     0.800  39.9  57.63  60.12  62.44  64.56  66.45  68.09  69.46  70.53  71.29  71.74  71.90  64.00
  1.30     0.800  41.5  58.87  61.32  63.59  65.66  67.50  69.10  70.42  71.46  72.20  72.63  72.78  65.10
  1.50     0.800  42.9  60.07  62.47  64.70  66.72  68.51  70.06  71.34  72.35  73.07  73.48  73.63  66.17
  1.70     0.800  44.4  61.24  63.59  65.76  67.73  69.48  70.98  72.23  73.20  73.89  74.29  74.44  67.19
  1.90     0.800  45.8  62.36  64.66  66.79  68.71  70.40  71.86  73.07  74.01  74.68  75.07  75.21  68.17
  2.10     0.800  47.2  63.44  65.70  67.77  69.64  71.29  72.71  73.88  74.79  75.43  75.81  75.94  69.12
  0.10     0.900  32.0  48.91  51.31  53.60  55.72  57.65  59.35  60.78  61.91  62.72  63.19  63.36  55.21
  0.30     0.900  33.5  50.34  52.72  54.99  57.09  58.99  60.65  62.05  63.16  63.95  64.41  64.57  56.57
  0.50     0.900  34.9  51.72  54.10  56.34  58.41  60.28  61.91  63.27  64.35  65.12  65.57  65.73  57.89
  0.70     0.900  36.4  53.07  55.43  57.64  59.68  61.51  63.11  64.45  65.50  66.25  66.69  66.85  59.16
  0.90     0.900  37.8  54.38  56.71  58.90  60.91  62.70  64.27  65.57  66.60  67.33  67.76  67.91  60.38
  1.10     0.900  39.2  55.65  57.96  60.12  62.09  63.85  65.38  66.65  67.66  68.37  68.78  68.93  61.57
  1.30     0.900  40.6  56.89  59.17  61.29  63.23  64.95  66.45  67.69  68.67  69.36  69.76  69.91  62.71
  1.50     0.900  42.0  58.09  60.34  62.43  64.33  66.01  67.47  68.69  69.64  70.31  70.70  70.84  63.81
  1.70     0.900  43.4  59.26  61.47  63.52  65.38  67.04  68.46  69.64  70.57  71.22  71.60  71.74  64.87
  1.90     0.900  44.8  60.38  62.57  64.58  66.40  68.02  69.41  70.56  71.45  72.09  72.46  72.60  65.90
  2.10     0.900  46.1  61.48  63.63  65.60  67.38  68.96  70.31  71.43  72.31  72.93  73.29  73.41  66.89
```

```
DISTANCE  TIME   AIR   *************** PRODUCT TEMPERATURES AT R/RADIUS ************** MASS
FROM      (HR)   TEMP                             (F)                                  AVG
INLET            (F)   1.0   0.9   0.8   0.7   0.6   0.5   0.4   0.3   0.2   0.1   0.0   TEMP
(FT)
 0.10     1.000 32.0 47.22 49.38 51.44 53.36 55.10 56.63 57.92 58.94 59.67 60.09 60.25 52.89
 0.30     1.000 33.3 48.61 50.77 52.82 54.73 56.45 57.97 59.24 60.24 60.96 61.38 61.53 54.26
 0.50     1.000 34.6 49.96 52.12 54.17 56.06 57.77 59.26 60.51 61.49 62.20 62.61 62.76 55.59
 0.70     1.000 36.0 51.28 53.44 55.47 57.35 59.03 60.50 61.73 62.70 63.39 63.80 63.94 56.87
 0.90     1.000 37.3 52.57 54.72 56.74 58.59 60.25 61.70 62.91 63.86 64.54 64.93 65.08 58.11
 1.10     1.000 38.6 53.82 55.96 57.96 59.80 61.43 62.86 64.04 64.98 65.64 66.03 66.17 59.31
 1.30     1.000 39.9 55.05 57.17 59.15 60.96 62.57 63.97 65.13 66.05 66.70 67.08 67.21 60.48
 1.50     1.000 41.2 56.24 58.35 60.30 62.08 63.67 65.04 66.18 67.08 67.72 68.08 68.22 61.61
 1.70     1.000 42.5 57.40 59.49 61.42 63.17 64.73 66.08 67.19 68.07 68.69 69.05 69.18 62.69
 1.90     1.000 43.8 58.53 60.59 62.50 64.22 65.75 67.07 68.16 69.02 69.63 69.98 70.10 63.75
 2.10     1.000 45.0 59.63 61.66 63.54 65.24 66.74 68.03 69.10 69.93 70.53 70.87 70.99 64.77
 0.10     1.100 32.0 45.70 47.64 49.50 51.23 52.79 54.17 55.33 56.26 56.92 57.30 57.44 50.81
 0.30     1.100 33.2 47.04 49.00 50.86 52.59 54.16 55.53 56.68 57.59 58.25 58.62 58.76 52.17
 0.50     1.100 34.4 48.35 50.33 52.19 53.92 55.48 56.84 57.98 58.88 59.53 59.90 60.04 53.49
 0.70     1.100 35.6 49.64 51.62 53.49 55.21 56.75 58.10 59.23 60.13 60.76 61.13 61.27 54.77
 0.90     1.100 36.8 50.90 52.88 54.74 56.46 57.99 59.33 60.45 61.33 61.95 62.32 62.45 56.01
 1.10     1.100 38.0 52.13 54.11 55.97 57.67 59.19 60.51 61.61 62.48 63.10 63.46 63.59 57.22
 1.30     1.100 39.2 53.33 55.31 57.16 58.85 60.35 61.66 62.74 63.60 64.21 64.56 64.69 58.40
 1.50     1.100 40.4 54.51 56.48 58.32 59.99 61.47 62.76 63.83 64.67 65.27 65.62 65.74 59.54
 1.70     1.100 41.6 55.66 57.62 59.44 61.09 62.56 63.83 64.88 65.71 66.30 66.64 66.76 60.64
 1.90     1.100 42.8 56.78 58.73 60.53 62.16 63.61 64.86 65.90 66.71 67.28 67.62 67.74 61.72
 2.10     1.100 44.0 57.87 59.81 61.59 63.20 64.63 65.86 66.87 67.67 68.24 68.56 68.68 62.75
 0.10     1.200 32.0 44.33 46.08 47.75 49.31 50.72 51.96 53.01 53.84 54.43 54.78 54.91 48.93
 0.30     1.200 33.1 45.62 47.40 49.09 50.65 52.07 53.32 54.36 55.19 55.78 56.13 56.25 50.27
 0.50     1.200 34.2 46.89 48.69 50.39 51.97 53.39 54.63 55.67 56.49 57.08 57.43 57.55 51.57
 0.70     1.200 35.3 48.14 49.95 51.66 53.24 54.66 55.90 56.94 57.76 58.34 58.68 58.81 52.84
 0.90     1.200 36.4 49.36 51.19 52.91 54.49 55.90 57.14 58.17 58.98 59.56 59.90 60.02 54.08
 1.10     1.200 37.5 50.56 52.40 54.12 55.70 57.11 58.34 59.36 60.17 60.74 61.07 61.19 55.29
 1.30     1.200 38.6 51.74 53.58 55.30 56.88 58.28 59.50 60.51 61.31 61.88 62.21 62.33 56.46
 1.50     1.200 39.7 52.90 54.74 56.46 58.02 59.42 60.62 61.63 62.42 62.98 63.30 63.42 57.60
 1.70     1.200 40.9 54.03 55.87 57.58 59.14 60.52 61.71 62.71 63.49 64.04 64.36 64.48 58.71
 1.90     1.200 42.0 55.13 56.97 58.67 60.22 61.59 62.77 63.75 64.52 65.06 65.38 65.49 59.80
 2.10     1.200 43.1 56.22 58.05 59.74 61.27 62.63 63.79 64.76 65.52 66.05 66.36 66.48 60.85
```

```
DISTANCE  TIME  AIR   *************** PRODUCT TEMPERATURES AT R/RADIUS *************** MASS
FRCM      (HR)  TEMP                                    (F)                                AVG
INLET           (F)   1.0   0.9   0.8   0.7   0.6   0.5   0.4   0.3   0.2   0.1   0.0   TEMP
(FT)
 0.10     1.300 32.0 43.10 44.68 46.18 47.58 48.85 49.97 50.91 51.66 52.20 52.51 52.62 47.24
 0.30     1.300 33.0 44.34 45.95 47.48 48.90 50.18 51.31 52.26 53.01 53.55 53.86 53.97 48.55
 0.50     1.300 33.9 45.56 47.20 48.75 50.18 51.48 52.61 53.56 54.32 54.85 55.17 55.28 49.83
 0.70     1.300 35.0 46.76 48.43 50.00 51.44 52.75 53.88 54.84 55.59 56.12 56.44 56.55 51.08
 0.90     1.300 36.0 47.94 49.63 51.22 52.67 53.98 55.12 56.07 56.82 57.36 57.67 57.78 52.30
 1.10     1.300 37.0 49.11 50.82 52.41 53.87 55.18 56.32 57.27 58.02 58.55 58.86 58.97 53.49
 1.30     1.300 38.0 50.26 51.98 53.58 55.04 56.35 57.49 58.43 59.18 59.71 60.01 60.12 54.66
 1.50     1.300 39.1 51.39 53.12 54.72 56.18 57.49 58.62 59.56 60.30 60.83 61.13 61.24 55.79
 1.70     1.300 40.1 52.50 54.23 55.84 57.30 58.60 59.72 60.66 61.39 61.91 62.21 62.32 56.90
 1.90     1.300 41.2 53.59 55.32 56.93 58.38 59.68 60.79 61.72 62.45 62.96 63.26 63.37 57.99
 2.10     1.300 42.3 54.66 56.39 57.99 59.44 60.73 61.83 62.75 63.47 63.98 64.27 64.38 59.04
 0.10     1.400 32.0 41.99 43.41 44.77 46.03 47.17 48.18 49.03 49.70 50.18 50.46 50.57 45.72
 0.30     1.400 32.9 43.17 44.63 46.02 47.31 48.47 49.49 50.35 51.03 51.52 51.80 51.91 46.99
 0.50     1.400 33.8 44.34 45.84 47.25 48.56 49.74 50.78 51.64 52.33 52.82 53.11 53.21 48.23
 0.70     1.400 34.7 45.50 47.03 48.46 49.79 50.99 52.03 52.90 53.59 54.09 54.37 54.48 49.46
 0.90     1.400 35.6 46.64 48.20 49.66 51.00 52.20 53.25 54.13 54.82 55.32 55.60 55.71 50.65
 1.10     1.400 36.6 47.77 49.35 50.83 52.18 53.39 54.45 55.33 56.02 56.52 56.80 56.91 51.83
 1.30     1.400 37.5 48.89 50.48 51.97 53.34 54.55 55.61 56.49 57.19 57.68 57.97 58.07 52.98
 1.50     1.400 38.5 49.99 51.60 53.10 54.47 55.69 56.75 57.63 58.32 58.81 59.10 59.20 54.10
 1.70     1.400 39.5 51.07 52.69 54.20 55.57 56.80 57.85 58.73 59.42 59.91 60.19 60.30 55.20
 1.90     1.400 40.5 52.14 53.77 55.28 56.65 57.87 58.93 59.80 60.49 60.98 61.26 61.36 56.28
 2.10     1.400 41.5 53.19 54.82 56.34 57.71 58.93 59.98 60.85 61.53 62.01 62.29 62.39 57.33
 0.10     1.500 32.0 41.00 42.27 43.49 44.63 45.66 46.57 47.33 47.94 48.37 48.62 48.71 44.35
 0.30     1.500 32.8 42.12 43.44 44.70 45.86 46.92 47.85 48.62 49.24 49.68 49.94 50.03 45.58
 0.50     1.500 33.6 43.23 44.60 45.89 47.08 48.16 49.10 49.89 50.52 50.97 51.22 51.32 46.78
 0.70     1.500 34.4 44.34 45.74 47.06 48.28 49.37 50.33 51.13 51.76 52.22 52.48 52.57 47.97
 0.90     1.500 35.3 45.44 46.87 48.22 49.46 50.57 51.54 52.34 52.98 53.44 53.70 53.80 49.14
 1.10     1.500 36.2 46.53 47.99 49.36 50.61 51.74 52.71 53.53 54.17 54.63 54.90 54.99 50.29
 1.30     1.500 37.0 47.61 49.09 50.48 51.75 52.88 53.87 54.69 55.33 55.79 56.06 56.15 51.41
 1.50     1.500 38.0 48.68 50.18 51.58 52.86 54.00 54.99 55.82 56.46 56.92 57.19 57.29 52.52
 1.70     1.500 38.9 49.73 51.25 52.67 53.96 55.10 56.09 56.92 57.57 58.03 58.29 58.39 53.61
 1.90     1.500 39.8 50.77 52.31 53.73 55.03 56.18 57.17 57.99 58.64 59.10 59.37 59.46 54.68
 2.10     1.500 40.7 51.80 53.35 54.78 56.08 57.23 58.22 59.04 59.69 60.15 60.41 60.51 55.72
```

```
DISTANCE    TIME  AIR  *************** PRODUCT TEMPERATURES AT R/RADIUS **************** MASS
FROM        (HR)  TEMP                                (F)                                AVG
INLET             (F)   1.0   0.9   0.8   0.7   0.6   0.5   0.4   0.3   0.2   0.1   0.0  TEMP
(FT)
  0.10      1.600 32.0 40.10 41.25 42.35 43.37 44.30 45.11 45.80 46.35 46.74 46.97 47.05 43.12
  0.30      1.600 32.7 41.16 42.36 43.50 44.56 45.51 46.35 47.06 47.62 48.02 48.25 48.33 44.30
  0.50      1.600 33.4 42.23 43.47 44.64 45.73 46.71 47.57 48.29 48.87 49.27 49.51 49.60 45.46
  0.70      1.600 34.2 43.28 44.57 45.78 46.89 47.90 48.77 49.51 50.09 50.50 50.74 50.83 46.61
  0.90      1.600 35.0 44.34 45.66 46.90 48.04 49.06 49.95 50.70 51.29 51.71 51.95 52.04 47.74
  1.10      1.600 35.8 45.39 46.74 48.00 49.16 50.20 51.11 51.86 52.46 52.88 53.13 53.22 48.86
  1.30      1.600 36.6 46.43 47.81 49.09 50.27 51.33 52.24 53.01 53.61 54.04 54.28 54.37 49.96
  1.50      1.600 37.5 47.46 48.86 50.17 51.37 52.43 53.36 54.12 54.73 55.16 55.41 55.50 51.05
  1.70      1.600 38.3 48.48 49.91 51.23 52.44 53.52 54.45 55.22 55.83 56.26 56.51 56.60 52.12
  1.90      1.600 39.2 49.49 50.94 52.28 53.49 54.58 55.51 56.29 56.90 57.33 57.58 57.67 53.17
  2.10      1.600 40.1 50.50 51.96 53.31 54.53 55.62 56.56 57.34 57.95 58.38 58.63 58.72 54.20
  0.10      1.700 32.0 39.29 40.33 41.31 42.23 43.07 43.80 44.42 44.92 45.27 45.47 45.55 42.01
  0.30      1.700 32.6 40.30 41.38 42.42 43.37 44.24 45.00 45.64 46.15 46.51 46.72 46.80 43.14
  0.50      1.700 33.3 41.31 42.44 43.51 44.50 45.40 46.18 46.84 47.36 47.73 47.95 48.02 44.26
  0.70      1.700 34.0 42.32 43.49 44.60 45.62 46.54 47.35 48.02 48.55 48.93 49.15 49.23 45.36
  0.90      1.700 34.7 43.32 44.54 45.68 46.73 47.67 48.49 49.18 49.72 50.11 50.33 50.41 46.46
  1.10      1.700 35.4 44.33 45.58 46.75 47.82 48.78 49.62 50.32 50.87 51.27 51.49 51.58 47.54
  1.30      1.700 36.2 45.33 46.61 47.81 48.90 49.88 50.73 51.44 52.00 52.40 52.63 52.71 48.61
  1.50      1.700 37.0 46.32 47.63 48.85 49.97 50.96 51.83 52.54 53.11 53.51 53.74 53.83 49.67
  1.70      1.700 37.8 47.31 48.65 49.89 51.02 52.03 52.90 53.63 54.20 54.60 54.84 54.92 50.72
  1.90      1.700 38.6 48.30 49.65 50.91 52.06 53.07 53.95 54.69 55.26 55.67 55.90 55.99 51.75
  2.10      1.700 39.4 49.27 50.65 51.92 53.08 54.10 54.99 55.72 56.30 56.71 56.95 57.03 52.76
  0.10      1.800 32.0 38.56 39.50 40.38 41.21 41.97 42.63 43.18 43.63 43.94 44.13 44.19 41.01
  0.30      1.800 32.6 39.51 40.50 41.43 42.30 43.09 43.78 44.35 44.81 45.14 45.33 45.40 42.09
  0.50      1.800 33.2 40.47 41.50 42.48 43.38 44.20 44.91 45.51 45.99 46.32 46.52 46.59 43.16
  0.70      1.800 33.8 41.43 42.51 43.52 44.46 45.30 46.04 46.65 47.14 47.49 47.69 47.77 44.22
  0.90      1.800 34.5 42.39 43.51 44.56 45.52 46.39 47.15 47.78 48.28 48.64 48.84 48.92 45.28
  1.10      1.800 35.1 43.35 44.51 45.59 46.58 47.47 48.25 48.89 49.40 49.77 49.98 50.06 46.32
  1.30      1.800 35.8 44.31 45.50 46.61 47.63 48.54 49.33 49.99 50.51 50.88 51.09 51.17 47.36
  1.50      1.800 36.6 45.27 46.49 47.63 48.67 49.59 50.40 51.07 51.60 51.97 52.19 52.27 48.39
  1.70      1.800 37.3 46.22 47.47 48.63 49.69 50.63 51.45 52.13 52.67 53.05 53.27 53.35 49.41
  1.90      1.800 38.1 47.17 48.45 49.63 50.70 51.66 52.49 53.18 53.72 54.10 54.32 54.40 50.41
  2.10      1.800 38.9 48.12 49.41 50.61 51.70 52.67 53.51 54.20 54.75 55.13 55.36 55.44 51.41
```

```
DISTANCE  TIME  AIR   ************** PRODUCT TEMPERATURES AT R/RADIUS ************** MASS
FROM      (HR)  TEMP                              (F)                                  AVG
INLET           (F)    1.0   0.9   0.8   0.7   0.6   0.5   0.4   0.3   0.2   0.1   0.0  TEMP
(FT)
  0.10    1.900 32.0 37.91 38.75 39.55 40.29 40.97 41.57 42.07 42.47 42.75 42.92 42.98 40.11
  0.30    1.900 32.5 38.80 39.70 40.54 41.33 42.04 42.66 43.19 43.61 43.90 44.08 44.14 41.14
  0.50    1.900 33.1 39.71 40.65 41.54 42.36 43.11 43.76 44.30 44.73 45.04 45.22 45.29 42.16
  0.70    1.900 33.6 40.62 41.60 42.53 43.39 44.16 44.84 45.40 45.85 46.17 46.35 46.42 43.17
  0.90    1.900 34.2 41.53 42.56 43.53 44.42 45.21 45.91 46.49 46.95 47.28 47.47 47.54 44.19
  1.10    1.900 34.9 42.45 43.52 44.52 45.43 46.26 46.97 47.57 48.05 48.38 48.58 48.65 45.20
  1.30    1.900 35.5 43.37 44.47 45.50 46.45 47.29 48.03 48.64 49.12 49.47 49.67 49.74 46.20
  1.50    1.900 36.2 44.29 45.42 46.48 47.45 48.32 49.07 49.69 50.19 50.54 50.74 50.81 47.20
  1.70    1.900 36.9 45.20 46.37 47.46 48.45 49.33 50.10 50.73 51.23 51.59 51.79 51.87 48.18
  1.90    1.900 37.6 46.12 47.32 48.42 49.43 50.33 51.11 51.76 52.26 52.63 52.83 52.91 49.16
  2.10    1.900 38.3 47.04 48.25 49.38 50.41 51.32 52.11 52.77 53.28 53.65 53.86 53.93 50.13
  0.10    2.000 32.0 37.32 38.07 38.80 39.47 40.08 40.61 41.06 41.42 41.68 41.83 41.88 39.30
  0.30    2.000 32.5 38.16 38.97 39.74 40.45 41.09 41.66 42.13 42.51 42.78 42.94 42.99 40.27
  0.50    2.000 33.0 39.01 39.87 40.68 41.43 42.11 42.70 43.20 43.59 43.87 44.04 44.10 41.24
  0.70    2.000 33.5 39.87 40.78 41.63 42.41 43.12 43.74 44.26 44.67 44.96 45.13 45.19 42.22
  0.90    2.000 34.0 40.74 41.69 42.58 43.40 44.13 44.77 45.31 45.73 46.04 46.21 46.27 43.19
  1.10    2.000 34.6 41.61 42.60 43.53 44.37 45.14 45.80 46.35 46.79 47.10 47.28 47.35 44.15
  1.30    2.000 35.2 42.49 43.52 44.47 45.35 46.14 46.82 47.39 47.83 48.15 48.34 48.41 45.12
  1.50    2.000 35.8 43.37 44.43 45.42 46.32 47.13 47.83 48.41 48.87 49.20 49.38 49.45 46.08
  1.70    2.000 36.5 44.25 45.34 46.36 47.29 48.11 48.83 49.42 49.89 50.22 50.42 50.49 47.04
  1.90    2.000 37.1 45.14 46.26 47.30 48.24 49.09 49.82 50.42 50.90 51.24 51.44 51.51 47.99
  2.10    2.000 37.8 46.02 47.17 48.23 49.20 50.05 50.80 51.41 51.90 52.24 52.44 52.51 48.93
  0.10    2.100 32.0 36.79 37.47 38.12 38.72 39.27 39.75 40.16 40.48 40.71 40.85 40.90 38.58
  0.30    2.100 32.4 37.58 38.31 39.01 39.65 40.23 40.75 41.18 41.52 41.76 41.91 41.96 39.49
  0.50    2.100 32.9 38.38 39.16 39.90 40.58 41.20 41.74 42.19 42.55 42.81 42.96 43.01 40.41
  0.70    2.100 33.3 39.19 40.02 40.80 41.52 42.17 42.73 43.21 43.58 43.85 44.01 44.06 41.34
  0.90    2.100 33.8 40.02 40.89 41.70 42.46 43.13 43.72 44.22 44.61 44.89 45.05 45.11 42.27
  1.10    2.100 34.4 40.85 41.76 42.61 43.40 44.10 44.71 45.22 45.63 45.91 46.08 46.14 43.19
  1.30    2.100 34.9 41.68 42.63 43.52 44.33 45.06 45.69 46.22 46.64 46.93 47.11 47.17 44.12
  1.50    2.100 35.5 42.52 43.51 44.43 45.27 46.02 46.67 47.21 47.64 47.95 48.12 48.19 45.05
  1.70    2.100 36.1 43.37 44.39 45.34 46.20 46.97 47.64 48.20 48.64 48.95 49.13 49.19 45.97
  1.90    2.100 36.7 44.22 45.27 46.24 47.13 47.92 48.60 49.17 49.62 49.94 50.12 50.19 46.89
  2.10    2.100 37.4 45.07 46.14 47.14 48.05 48.86 49.56 50.14 50.60 50.92 51.11 51.17 47.81
```

```
DISTANCE  TIME  AIR  *************** PRODUCT TEMPERATURES AT R/RADIUS ************** MASS
FROM      (HR)  TEMP                          (F)                                     AVG
INLET           (F)   1.0   0.9   0.8   0.7   0.6   0.5   0.4   0.3   0.2   0.1   0.0  TEMP
(FT)
 0.10     2.200 32.0 36.31 36.92 37.51 38.05 38.54 38.98 39.35 39.64 39.84 39.97 40.01 37.92
 0.30     2.200 32.4 37.05 37.71 38.34 38.93 39.46 39.92 40.31 40.62 40.84 40.97 41.02 38.78
 0.50     2.200 32.8 37.81 38.52 39.19 39.81 40.37 40.87 41.28 41.61 41.84 41.98 42.02 39.66
 0.70     2.200 33.2 38.57 39.33 40.04 40.70 41.29 41.81 42.25 42.59 42.84 42.98 43.03 40.53
 0.90     2.200 33.7 39.35 40.15 40.90 41.60 42.22 42.76 43.21 43.57 43.83 43.98 44.03 41.42
 1.10     2.200 34.2 40.14 40.98 41.77 42.49 43.14 43.71 44.18 44.55 44.82 44.97 45.03 42.30
 1.30     2.200 34.7 40.93 41.81 42.64 43.39 44.07 44.65 45.14 45.53 45.80 45.96 46.02 43.19
 1.50     2.200 35.2 41.74 42.65 43.51 44.29 44.99 45.60 46.10 46.50 46.78 46.95 47.01 44.08
 1.70     2.200 35.8 42.54 43.49 44.38 45.19 45.91 46.53 47.05 47.46 47.75 47.92 47.98 44.97
 1.90     2.200 36.4 43.36 44.34 45.25 46.08 46.83 47.47 48.00 48.42 48.72 48.89 48.95 45.86
 2.10     2.200 37.0 44.17 45.19 46.12 46.98 47.74 48.40 48.94 49.37 49.68 49.85 49.92 46.75
 0.10     2.300 32.0 35.88 36.43 36.96 37.45 37.89 38.28 38.61 38.87 39.06 39.17 39.21 37.33
 0.30     2.300 32.3 36.57 37.17 37.74 38.27 38.75 39.17 39.53 39.81 40.01 40.12 40.17 38.14
 0.50     2.300 32.7 37.28 37.93 38.54 39.11 39.62 40.07 40.45 40.74 40.96 41.08 41.12 38.97
 0.70     2.300 33.1 38.00 38.70 39.35 39.95 40.50 40.97 41.37 41.68 41.91 42.04 42.08 39.80
 0.90     2.300 33.5 38.74 39.47 40.16 40.80 41.37 41.87 42.29 42.62 42.86 42.99 43.04 40.64
 1.10     2.300 34.0 39.48 40.26 40.99 41.66 42.26 42.78 43.22 43.56 43.81 43.95 44.00 41.48
 1.30     2.300 34.4 40.24 41.05 41.82 42.52 43.14 43.69 44.14 44.50 44.75 44.90 44.96 42.33
 1.50     2.300 34.9 41.00 41.86 42.65 43.38 44.03 44.59 45.06 45.43 45.70 45.85 45.91 43.19
 1.70     2.300 35.5 41.78 42.66 43.49 44.24 44.92 45.50 45.99 46.37 46.64 46.80 46.85 44.04
 1.90     2.300 36.0 42.56 43.47 44.33 45.11 45.80 46.40 46.90 47.30 47.57 47.74 47.80 44.90
 2.10     2.300 36.6 43.34 44.29 45.17 45.97 46.68 47.30 47.82 48.22 48.50 48.67 48.73 45.75
 0.10     2.400 32.0 35.49 35.99 36.46 36.90 37.30 37.66 37.95 38.19 38.36 38.45 38.49 36.80
 0.30     2.400 32.3 36.14 36.68 37.20 37.68 38.11 38.49 38.82 39.07 39.25 39.36 39.39 37.56
 0.50     2.400 32.6 36.80 37.39 37.95 38.47 38.93 39.34 39.69 39.96 40.15 40.26 40.30 38.34
 0.70     2.400 33.0 37.48 38.12 38.71 39.27 39.76 40.20 40.56 40.85 41.05 41.17 41.22 39.13
 0.90     2.400 33.4 38.18 38.85 39.49 40.07 40.60 41.06 41.44 41.75 41.96 42.09 42.13 39.92
 1.10     2.400 33.8 38.88 39.60 40.27 40.89 41.44 41.92 42.33 42.64 42.87 43.00 43.05 40.73
 1.30     2.400 34.2 39.60 40.35 41.06 41.71 42.29 42.79 43.21 43.54 43.78 43.92 43.97 41.54
 1.50     2.400 34.7 40.33 41.12 41.86 42.53 43.14 43.66 44.10 44.44 44.69 44.83 44.88 42.35
 1.70     2.400 35.2 41.06 41.89 42.66 43.36 43.99 44.53 44.99 45.34 45.60 45.74 45.80 43.17
 1.90     2.400 35.7 41.81 42.66 43.46 44.19 44.84 45.40 45.87 46.24 46.50 46.65 46.71 44.00
 2.10     2.400 36.2 42.56 43.45 44.27 45.03 45.70 46.27 46.76 47.14 47.40 47.56 47.62 44.82
```

```
DISTANCE  TIME  AIR   *************** PRODUCT TEMPERATURES AT R/RADIUS ************** MASS
FROM      (HR)  TEMP                               (F)                                AVG
INLET           (F)   1.0    0.9    0.8    0.7    0.6    0.5    0.4    0.3    0.2    0.1    0.0   TEMP
(FT)
 0.10     2.500 32.0 35.14  35.59  36.02  36.41  36.77  37.09  37.36  37.57  37.72  37.81  37.84  36.32
 0.30     2.500 32.3 35.75  36.24  36.71  37.14  37.54  37.88  38.17  38.40  38.57  38.66  38.70  37.04
 0.50     2.500 32.6 36.37  36.91  37.41  37.88  38.31  38.68  38.99  39.24  39.42  39.52  39.56  37.77
 0.70     2.500 32.9 37.01  37.59  38.13  38.64  39.09  39.49  39.82  40.09  40.28  40.38  40.42  38.51
 0.90     2.500 33.3 37.66  38.28  38.86  39.40  39.89  40.31  40.66  40.94  41.14  41.25  41.30  39.27
 1.10     2.500 33.6 38.33  38.99  39.61  40.18  40.69  41.13  41.50  41.80  42.01  42.13  42.17  40.03
 1.30     2.500 34.0 39.00  39.70  40.36  40.96  41.49  41.96  42.35  42.66  42.88  43.01  43.05  40.80
 1.50     2.500 34.5 39.70  40.43  41.12  41.75  42.31  42.80  43.20  43.52  43.75  43.88  43.93  41.58
 1.70     2.500 34.9 40.40  41.17  41.88  42.54  43.12  43.63  44.06  44.39  44.63  44.76  44.81  42.37
 1.90     2.500 35.4 41.11  41.91  42.66  43.34  43.94  44.47  44.91  45.25  45.50  45.64  45.69  43.16
 2.10     2.500 35.9 41.82  42.66  43.43  44.14  44.77  45.31  45.76  46.12  46.37  46.52  46.57  43.95
```

APPENDIX C

GRAPHICAL RESULTS SHOWING COMPARISON OF EXPERIMENTAL DATA WITH NUMERICAL SOLUTION

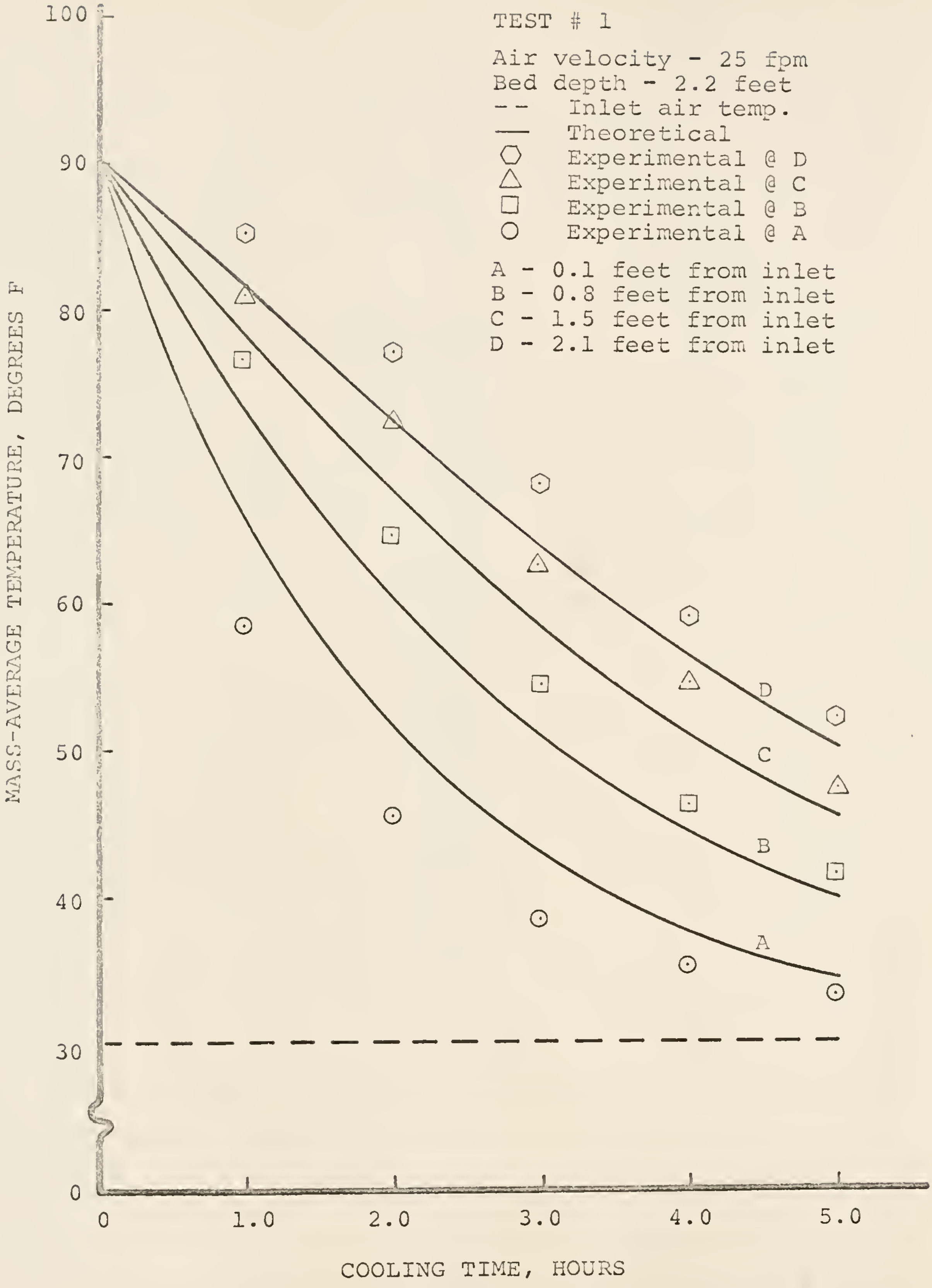

Figure 33. Theoretical and experimental temperature response of oranges to forced-air cooling

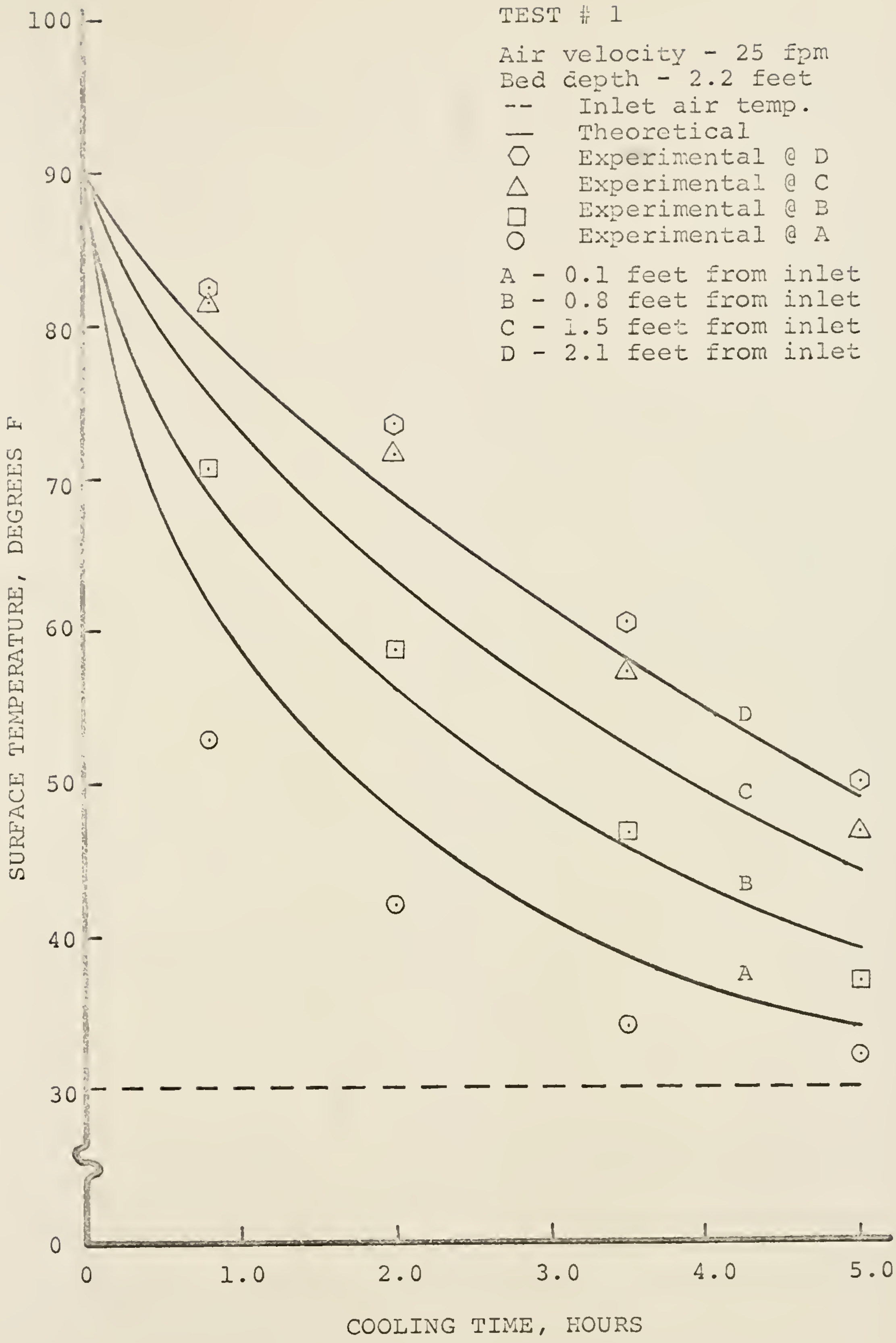

Figure 34. Theoretical and experimental temperature response of oranges to forced- air cooling

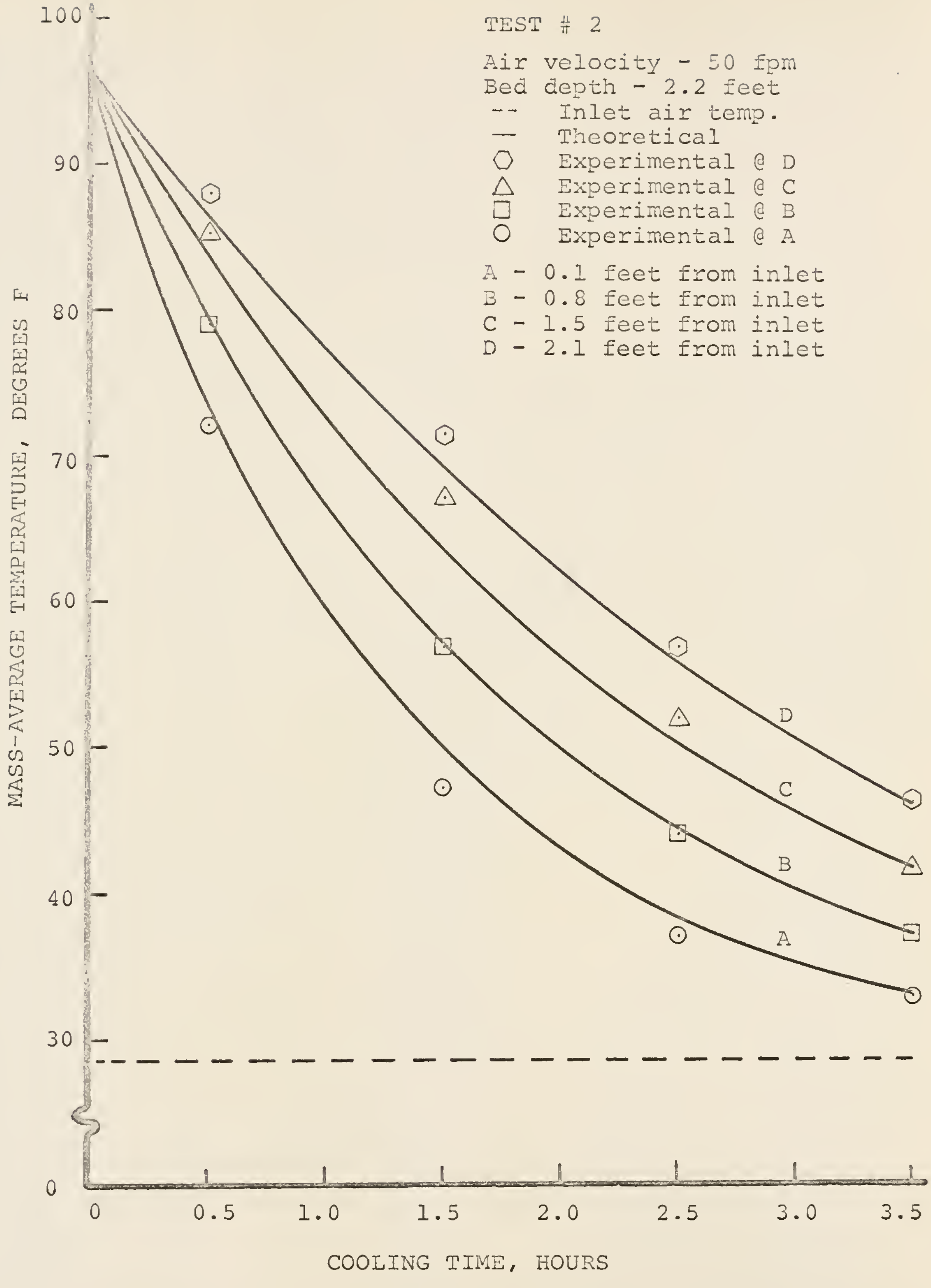

Figure 35. Theoretical and experimental temperature response of oranges to forced-air cooling

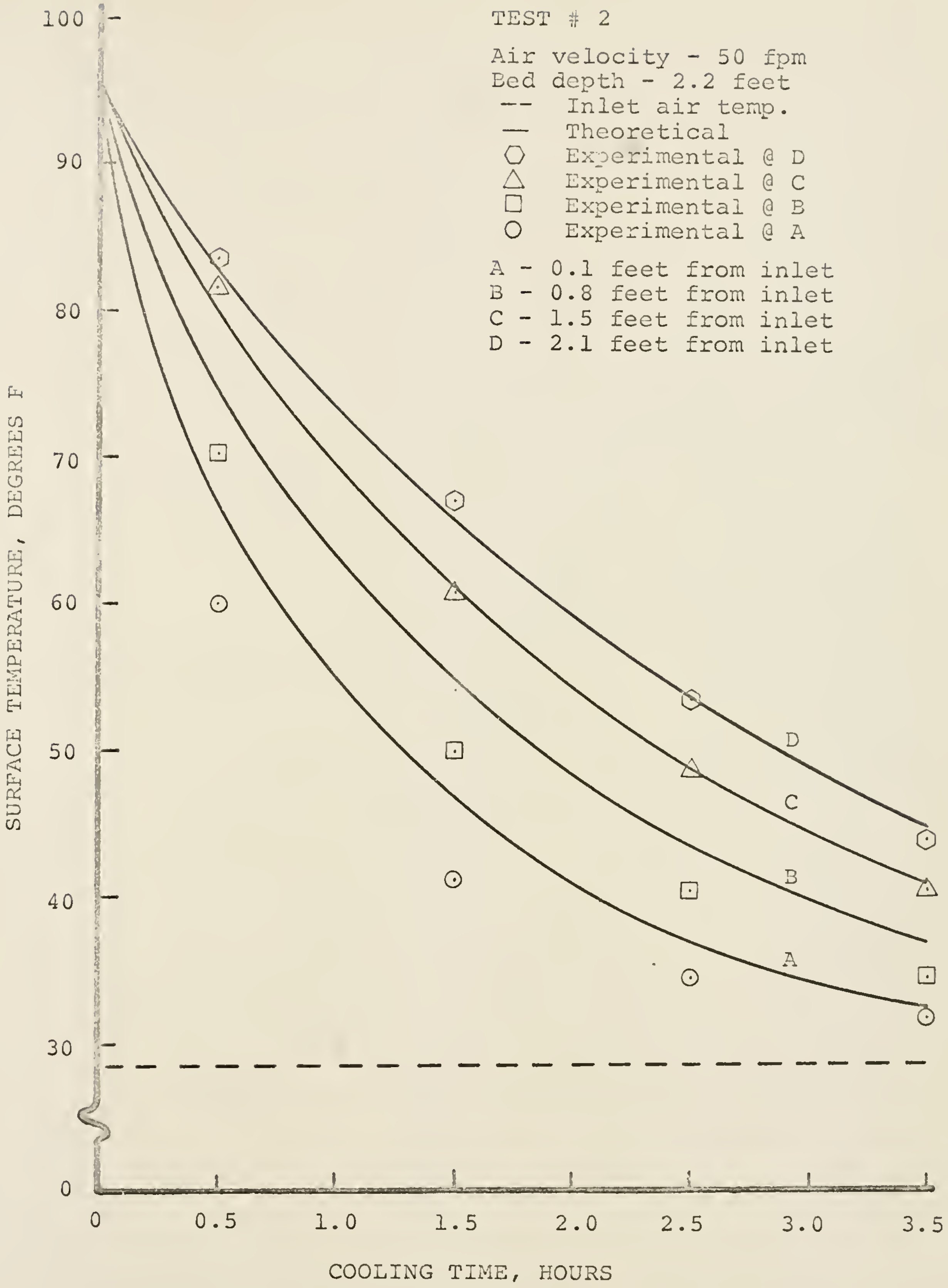

Figure 36. Theoretical and experimental temperature response of oranges to forced-air cooling

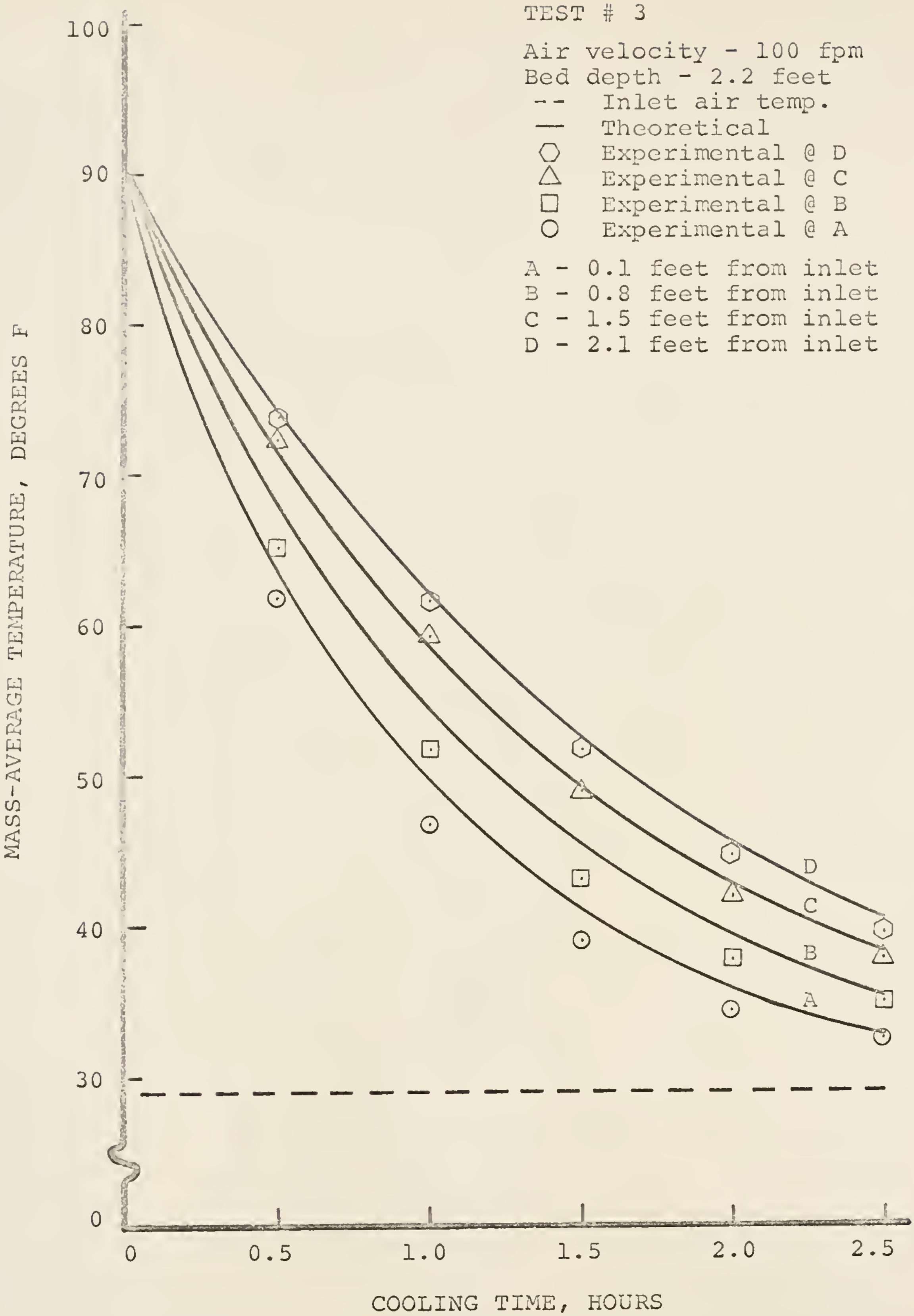

Figure 37. Theoretical and experimental temperature response of oranges to forced-air cooling

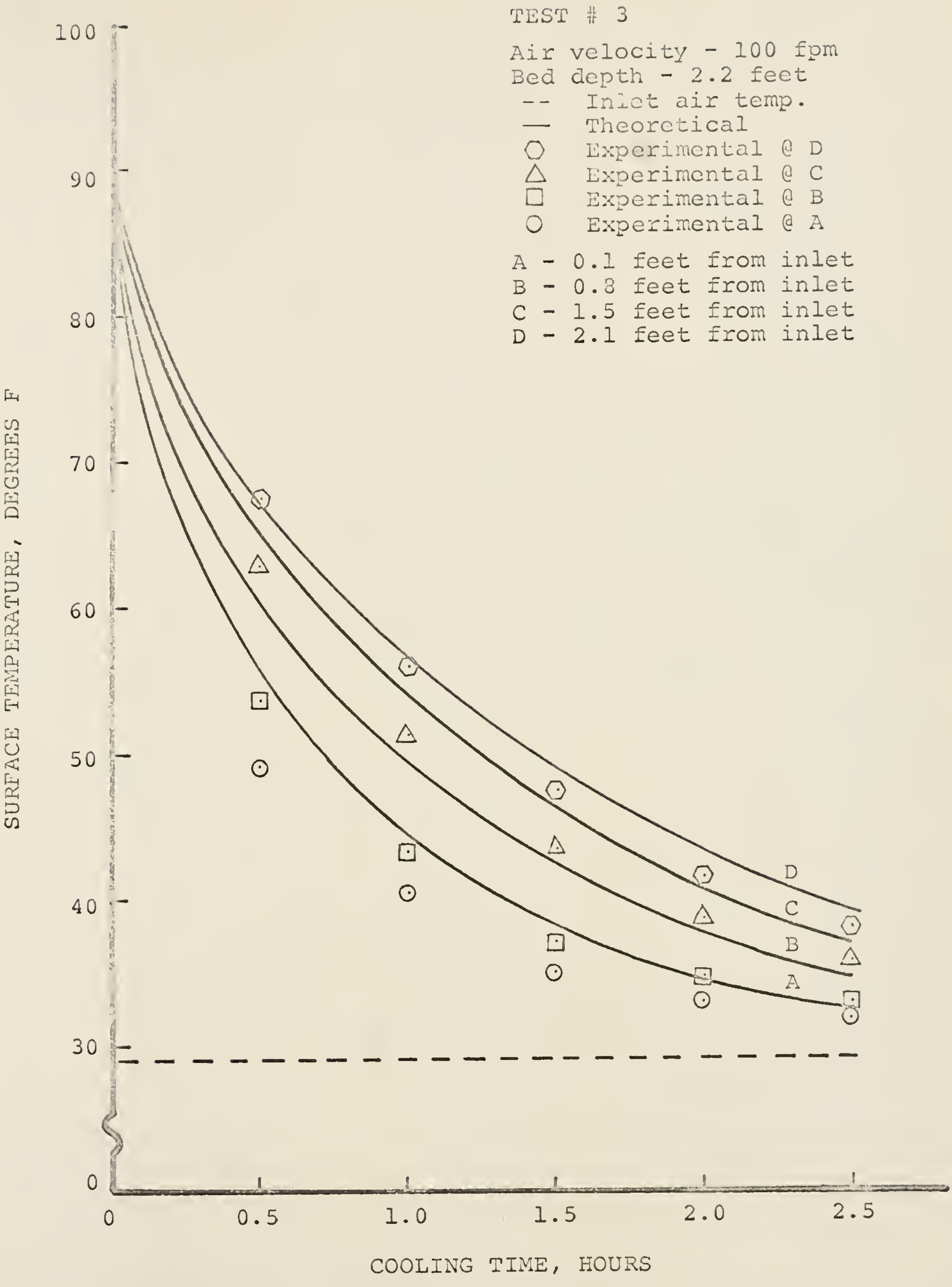

Figure 38. Theoretical and experimental temperature response of oranges to forced-air cooling

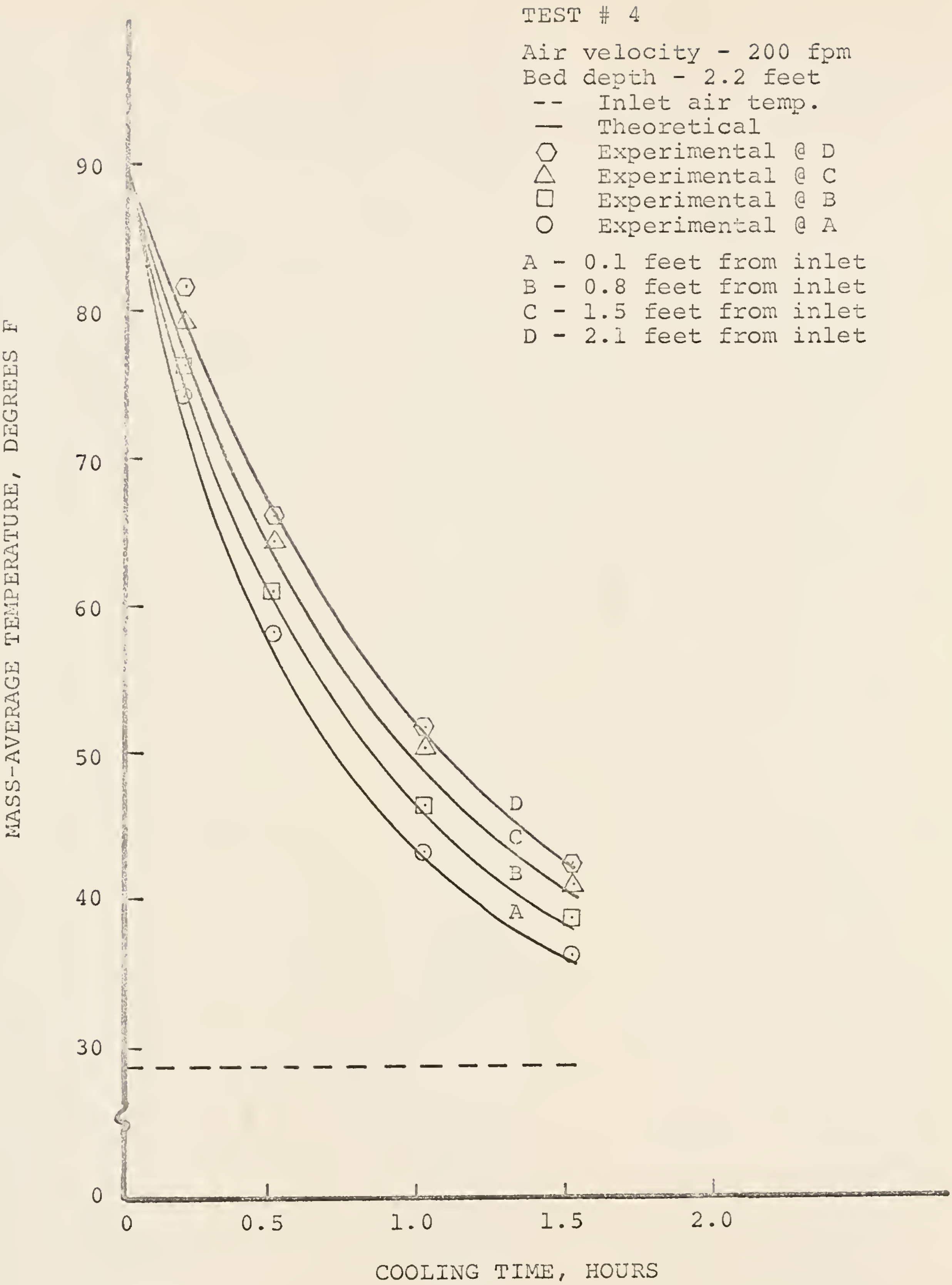

Figure 39. Theoretical and experimental temperature response of oranges to forced-air cooling

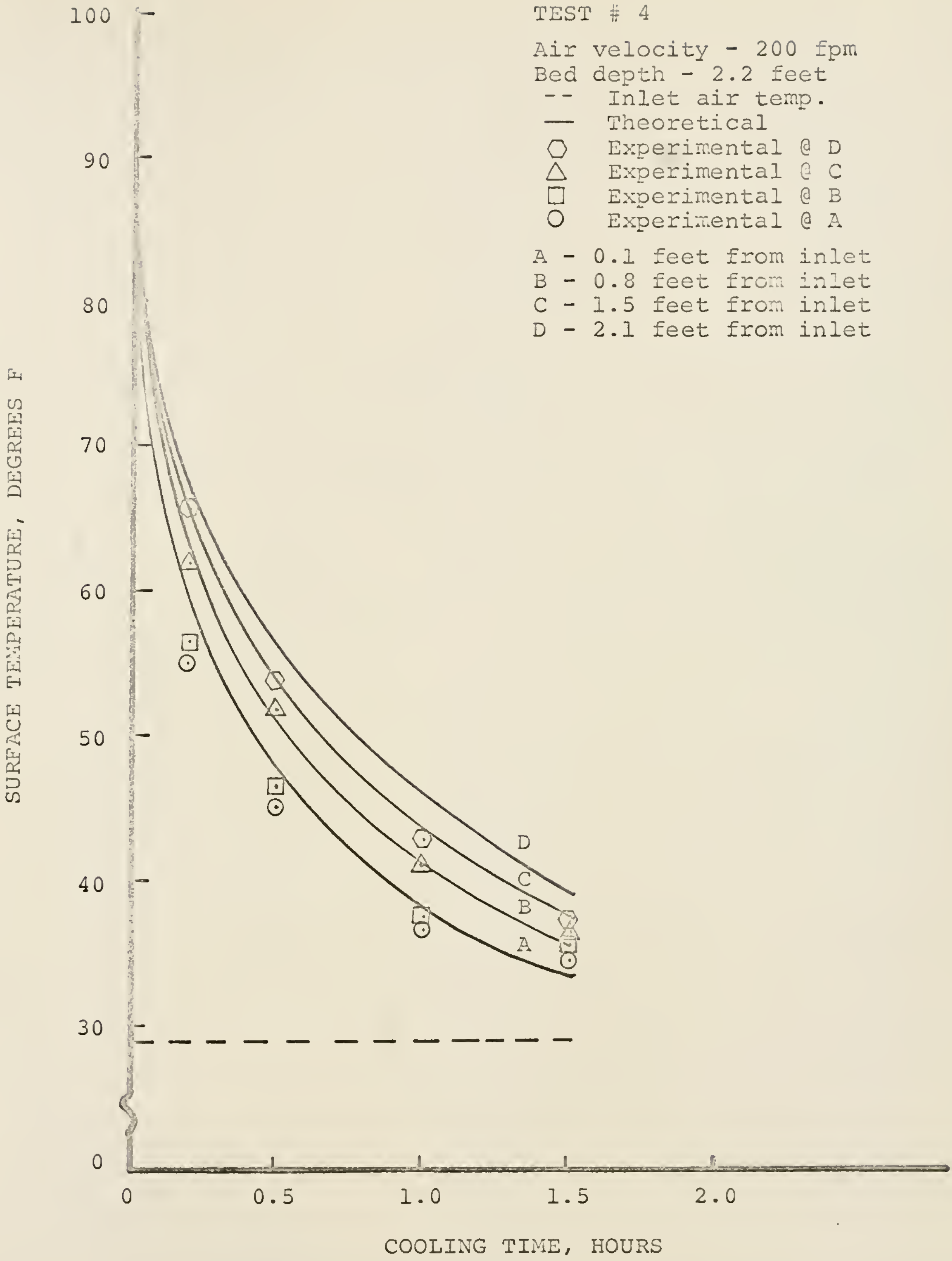

Figure 40. Theoretical and experimental temperature response of oranges to forced-air cooling

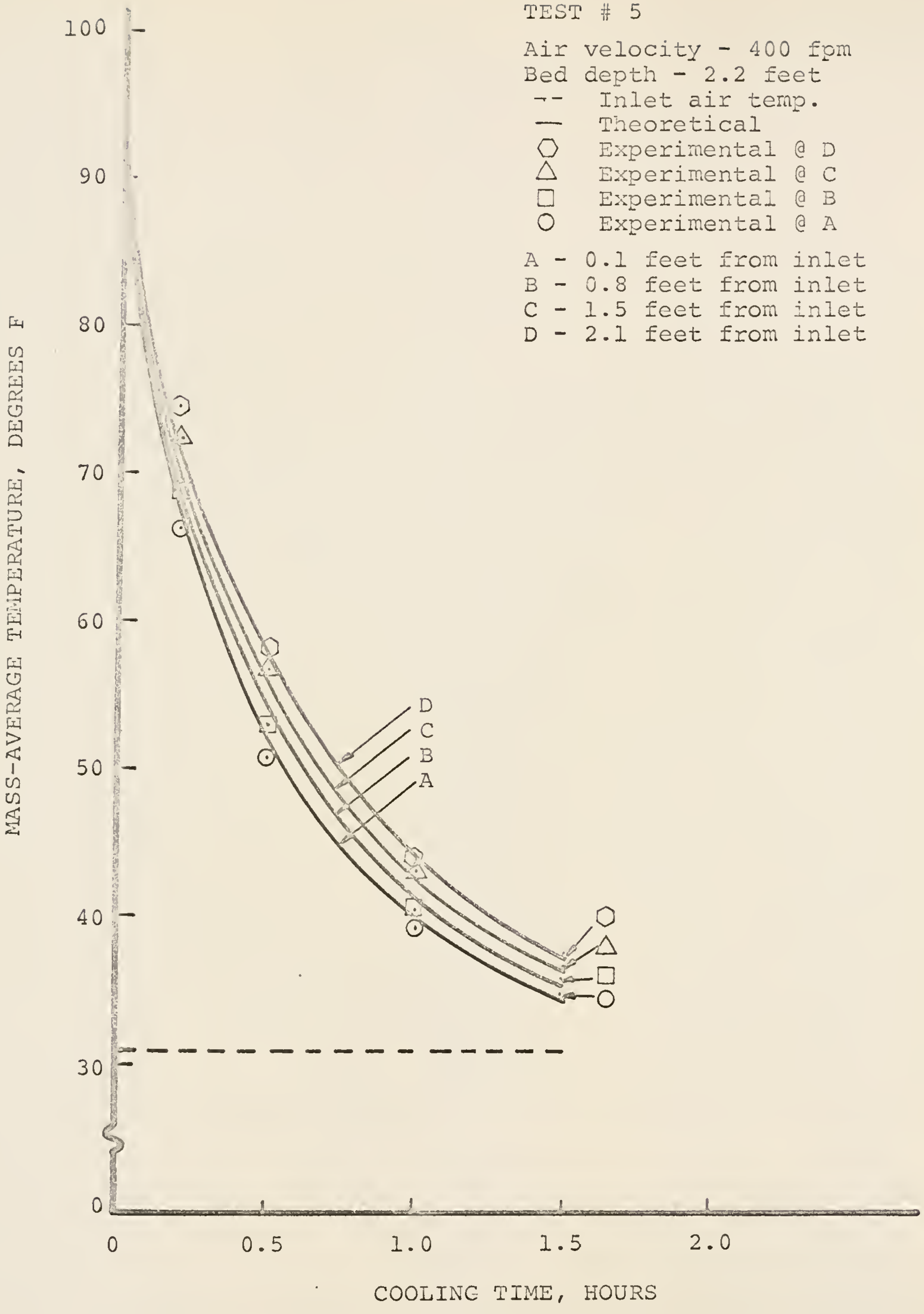

Figure 41. Theoretical and experimental temperature response of oranges to forced-air cooling

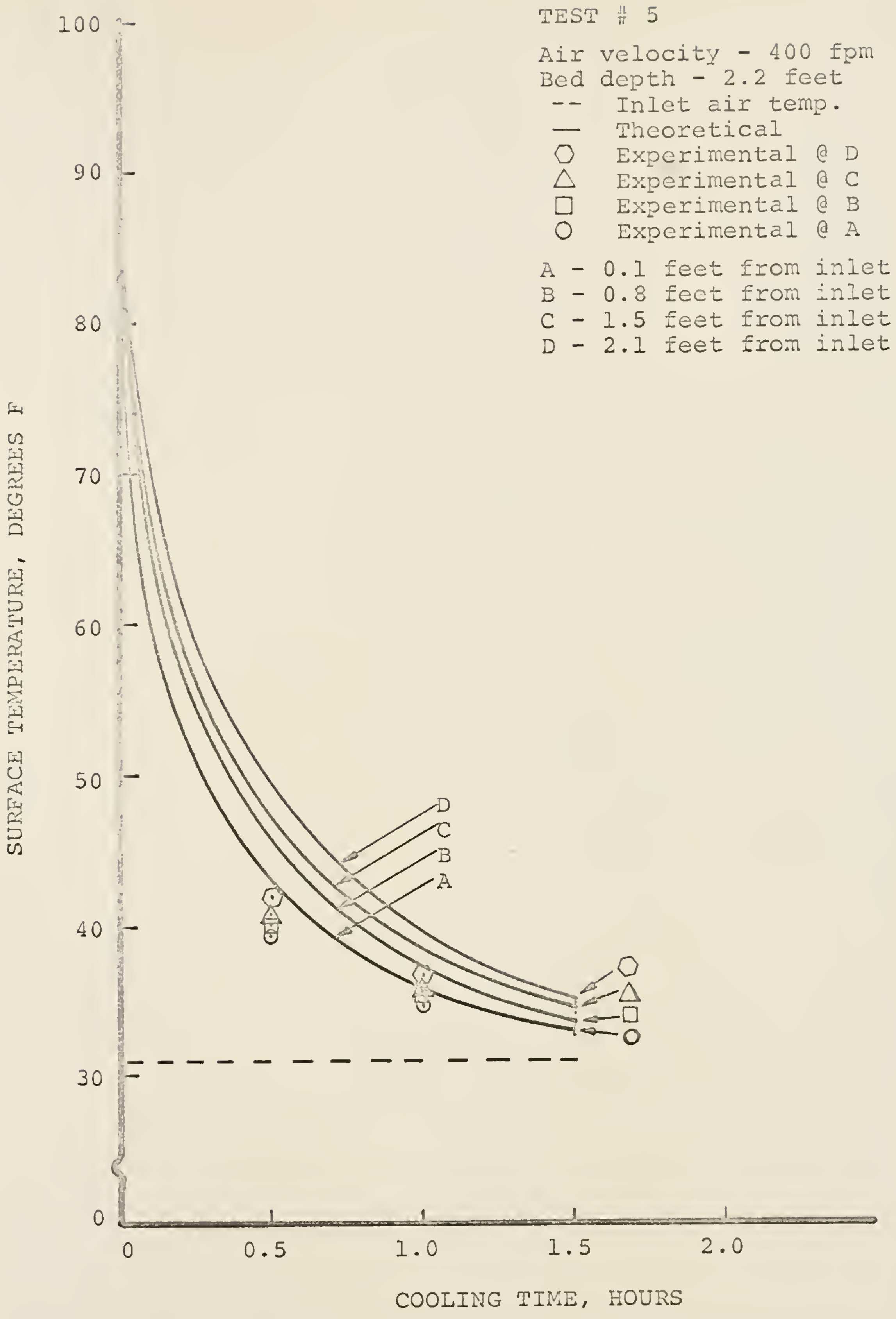

Figure 42. Theoretical and experimental termperature response of oranges to forced-air cooling.

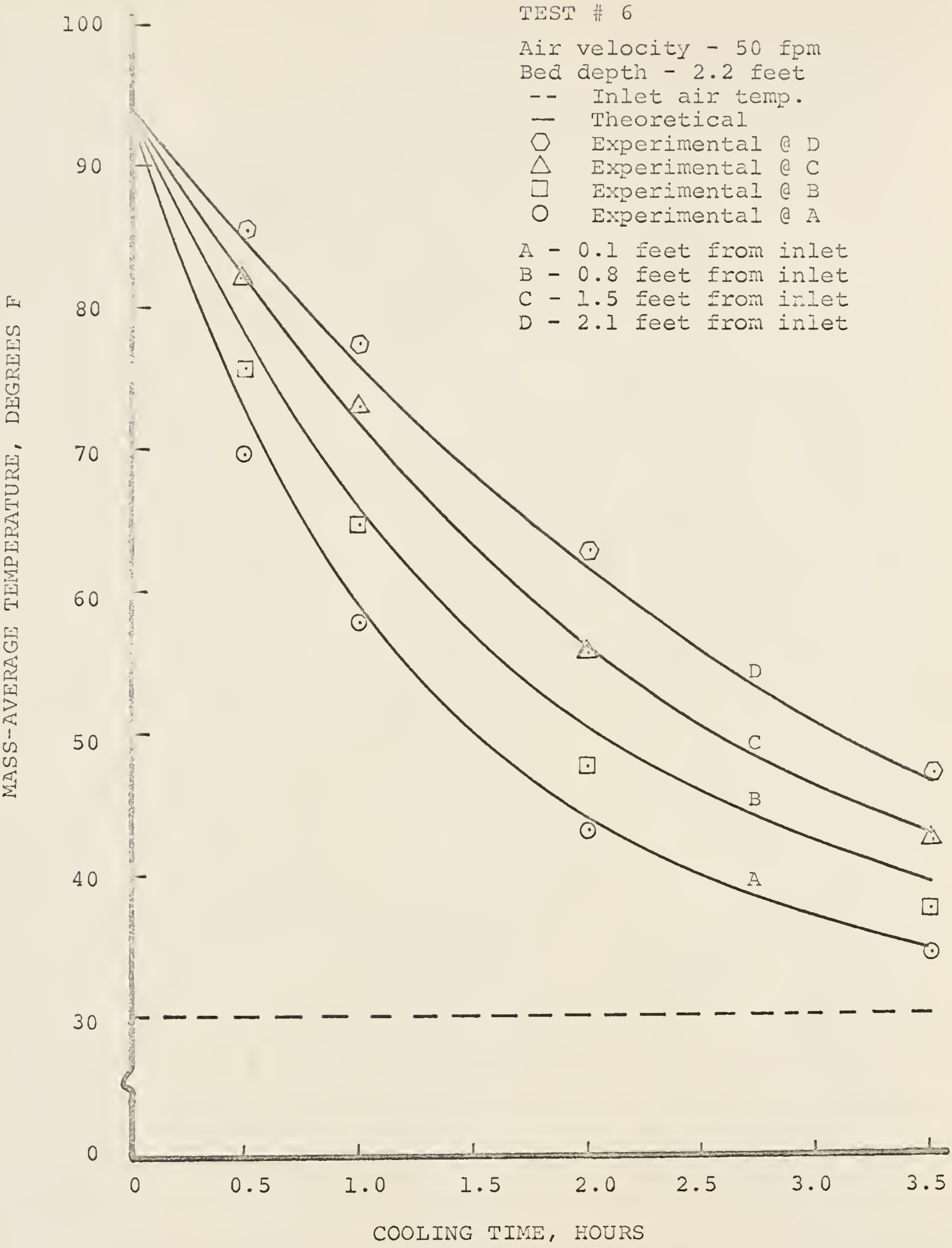

Figure 43. Theoretical and experimental temperature response of oranges to forced-air cooling.

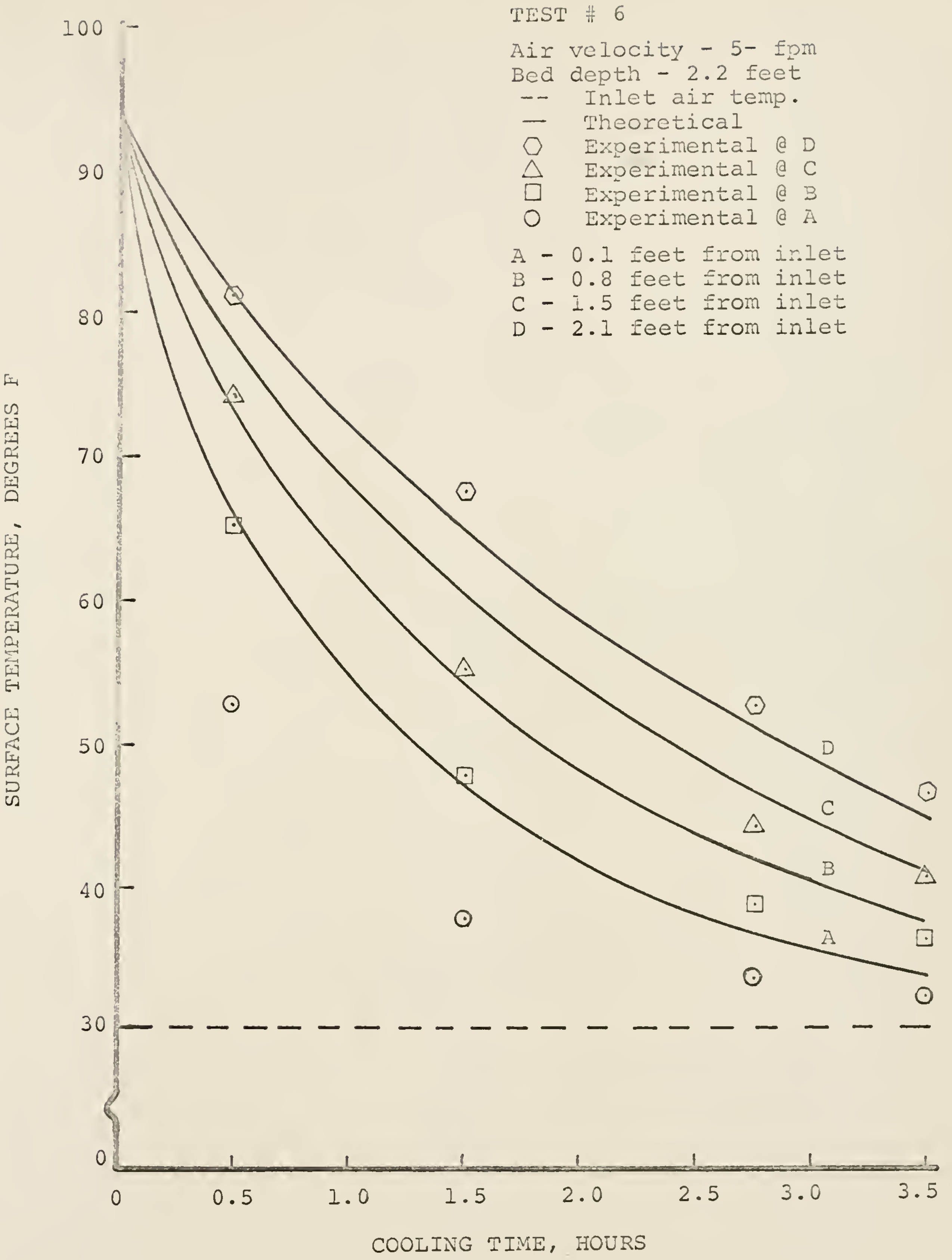

Figure 44. Theoretical and experimental temperature response of oranges to forced-air cooling.

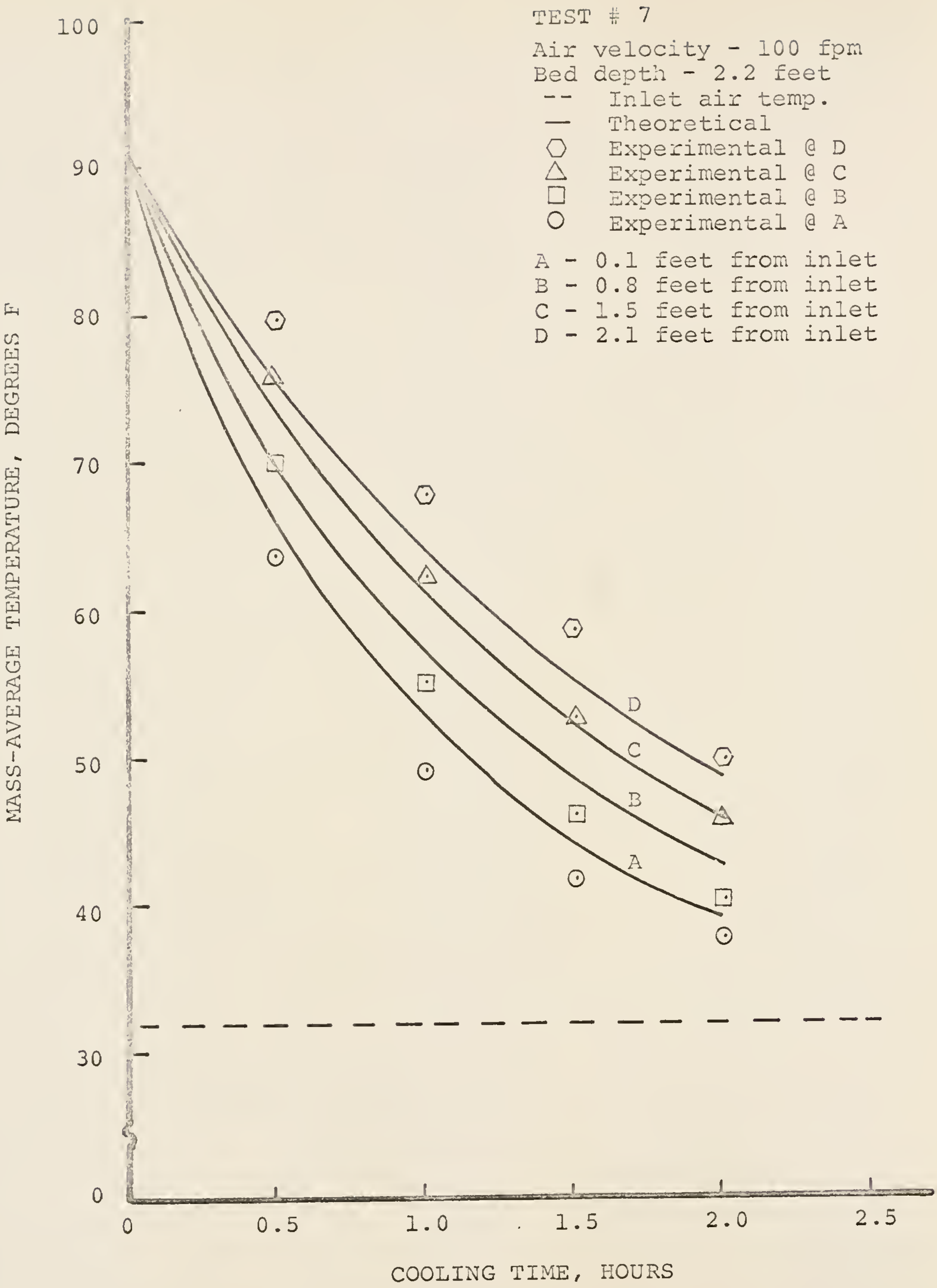

Figure 45. Theoretical and experimental temperature response of oranges to forced-air cooling.

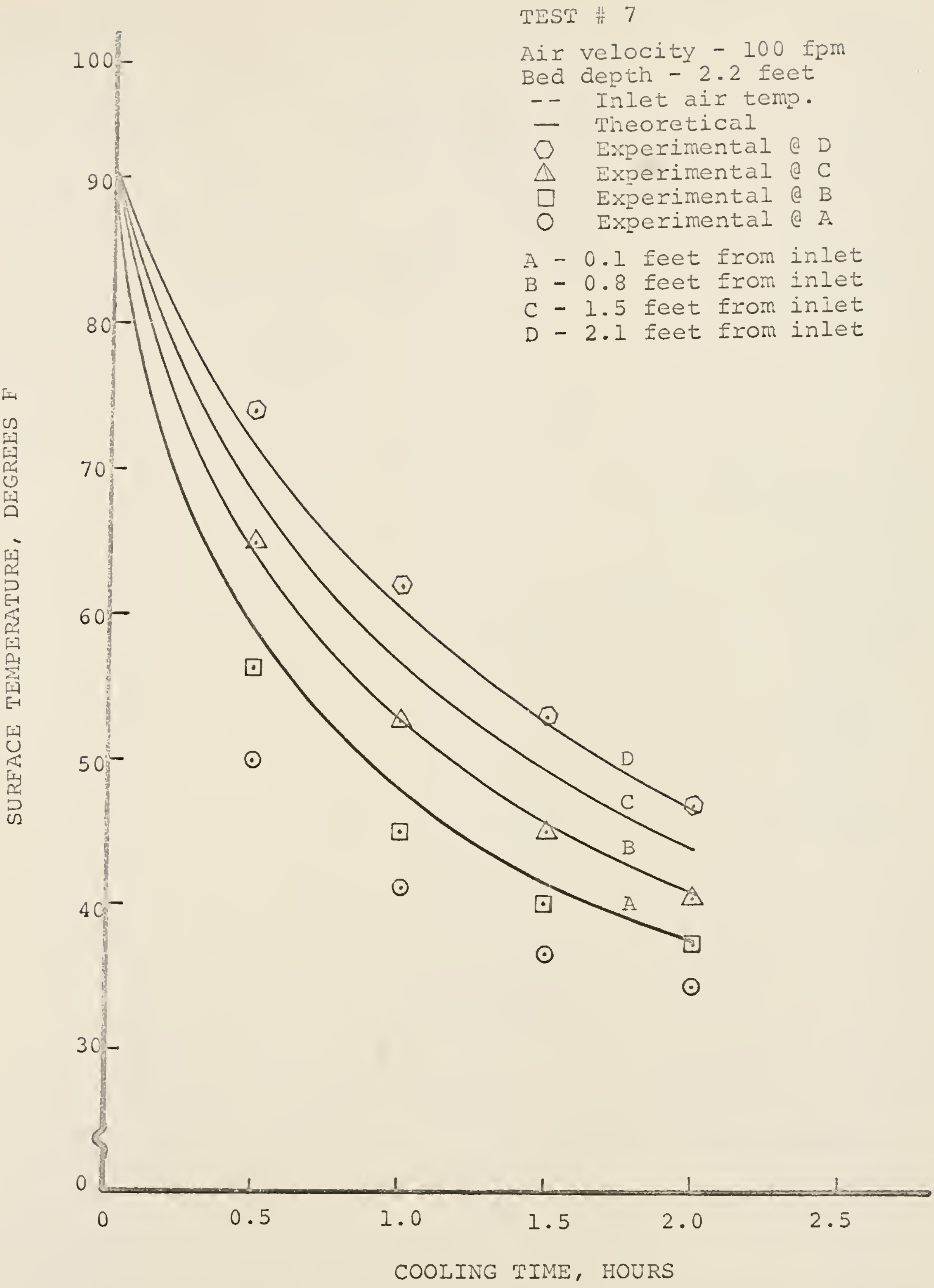

Figure 46. Theoretical and experimental temperature response of oranges to forced-air cooling.

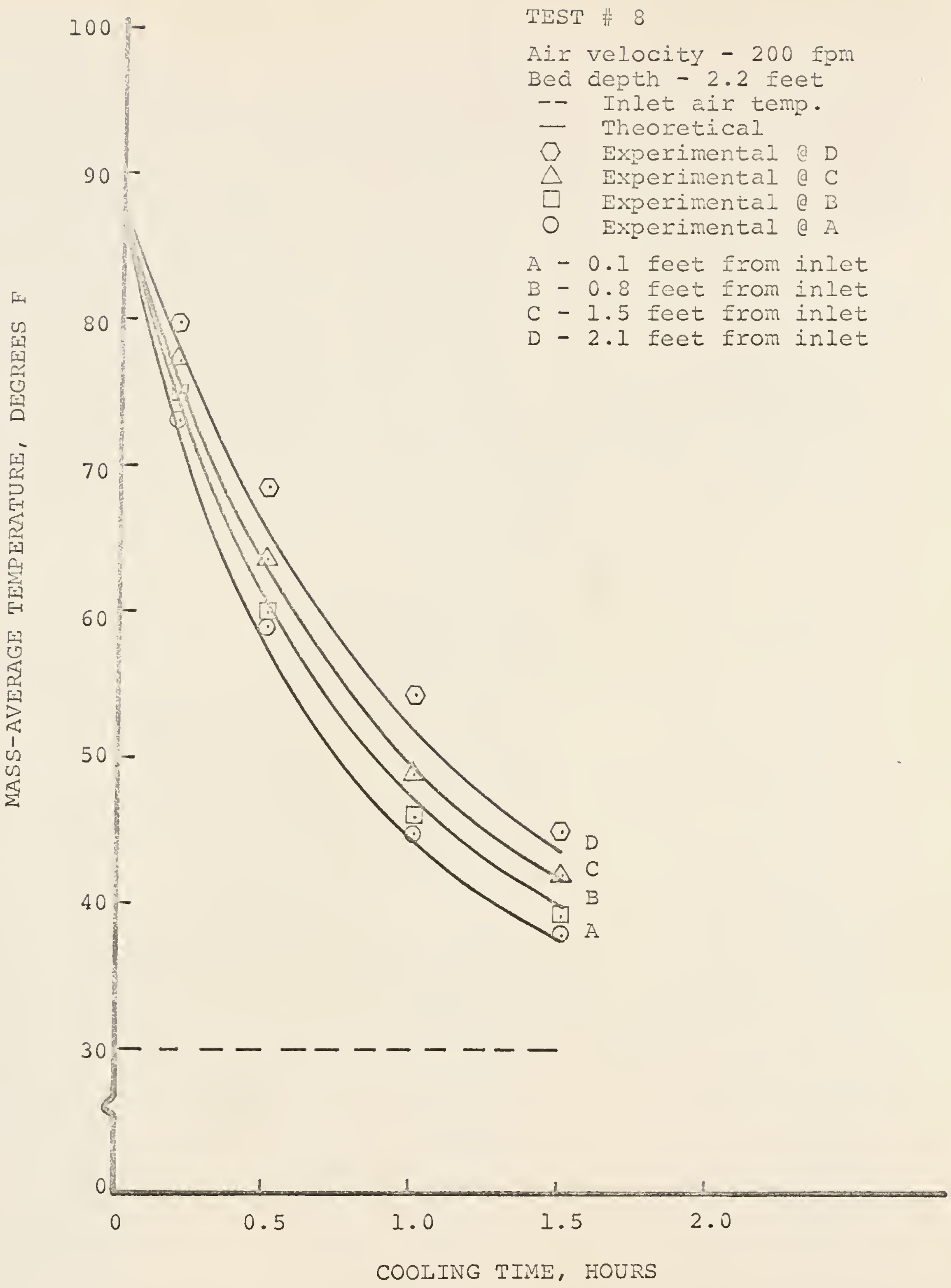

Figure 47. Theoretical and experimental temperature response of oranges to forced-air cooling.

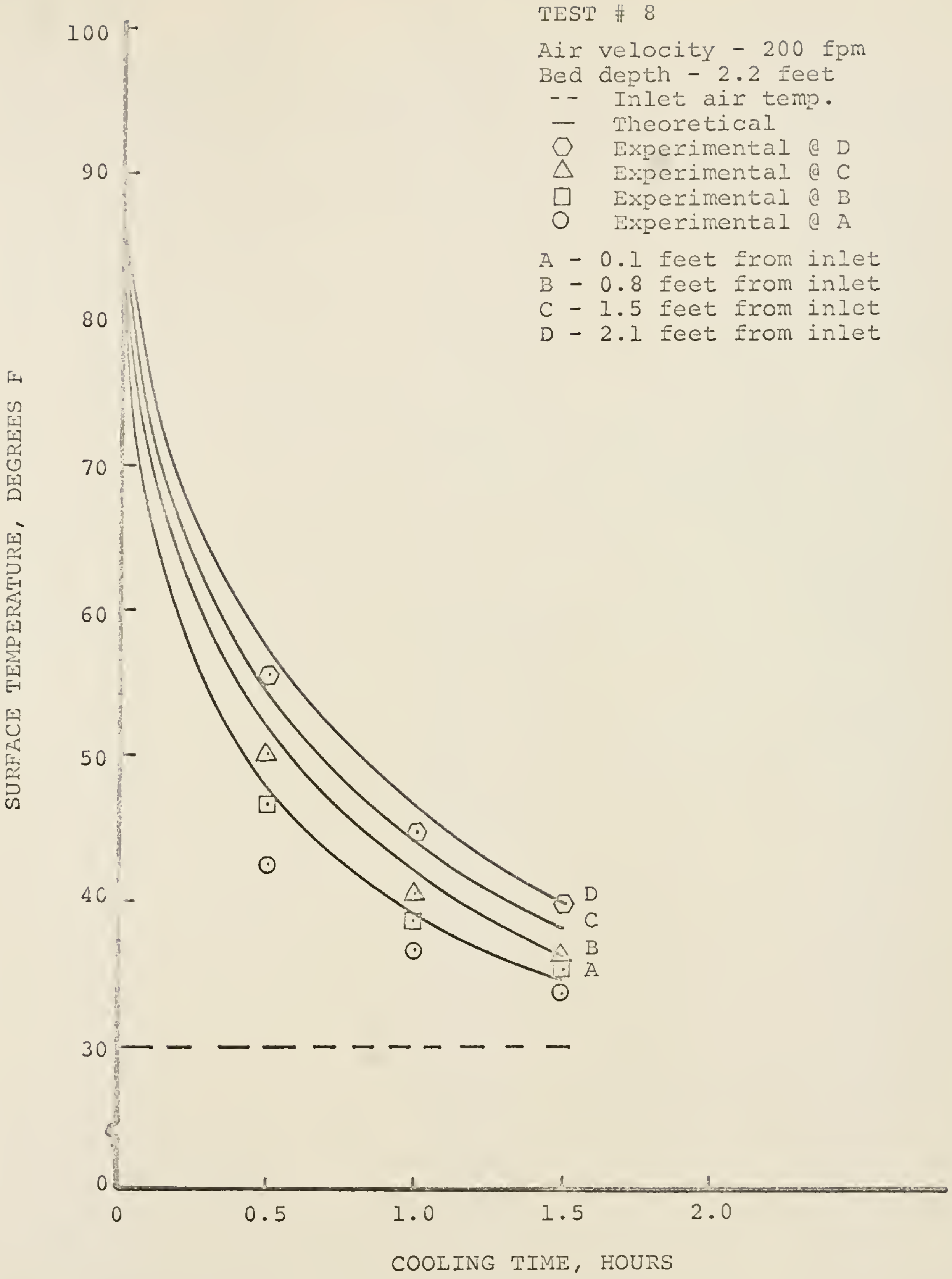

Figure 48. Theoretical and experimental temperature response of oranges to forced-air cooling.

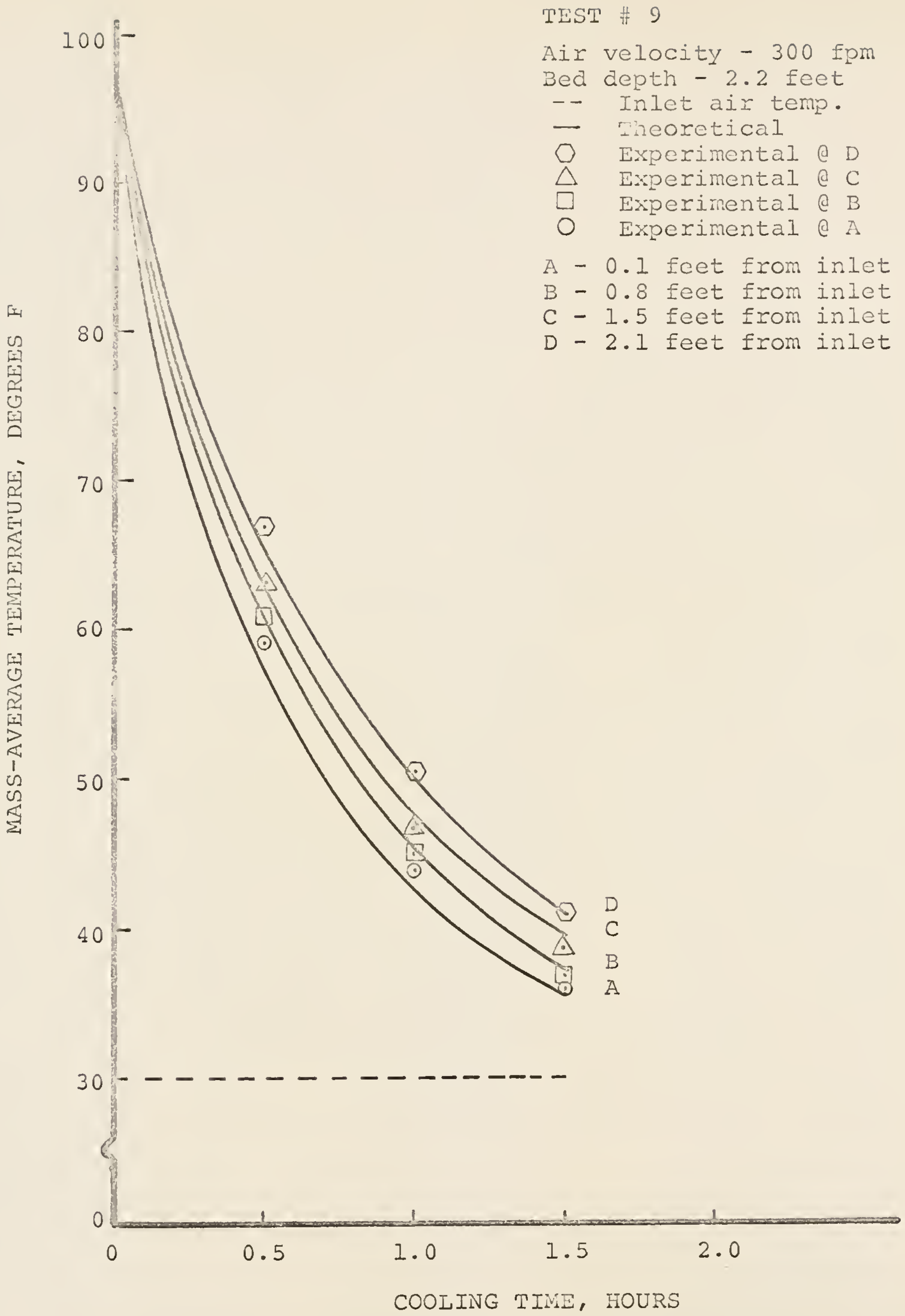

Figure 49. Theoretical and experimental temperature response of oranges to forced-air cooling

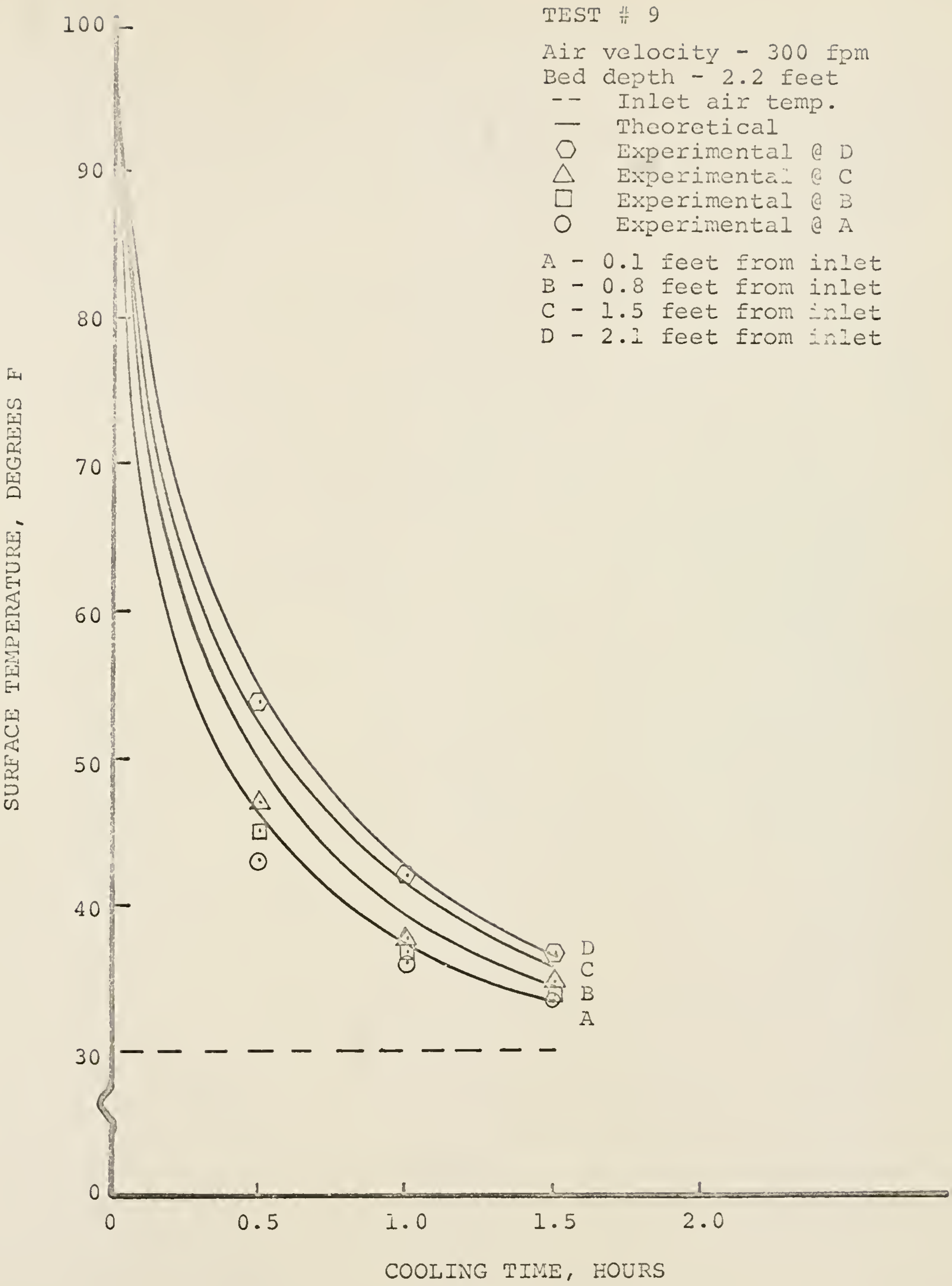

Figure 50. Theoretical and experimental temperature response of oranges to forced-air cooling

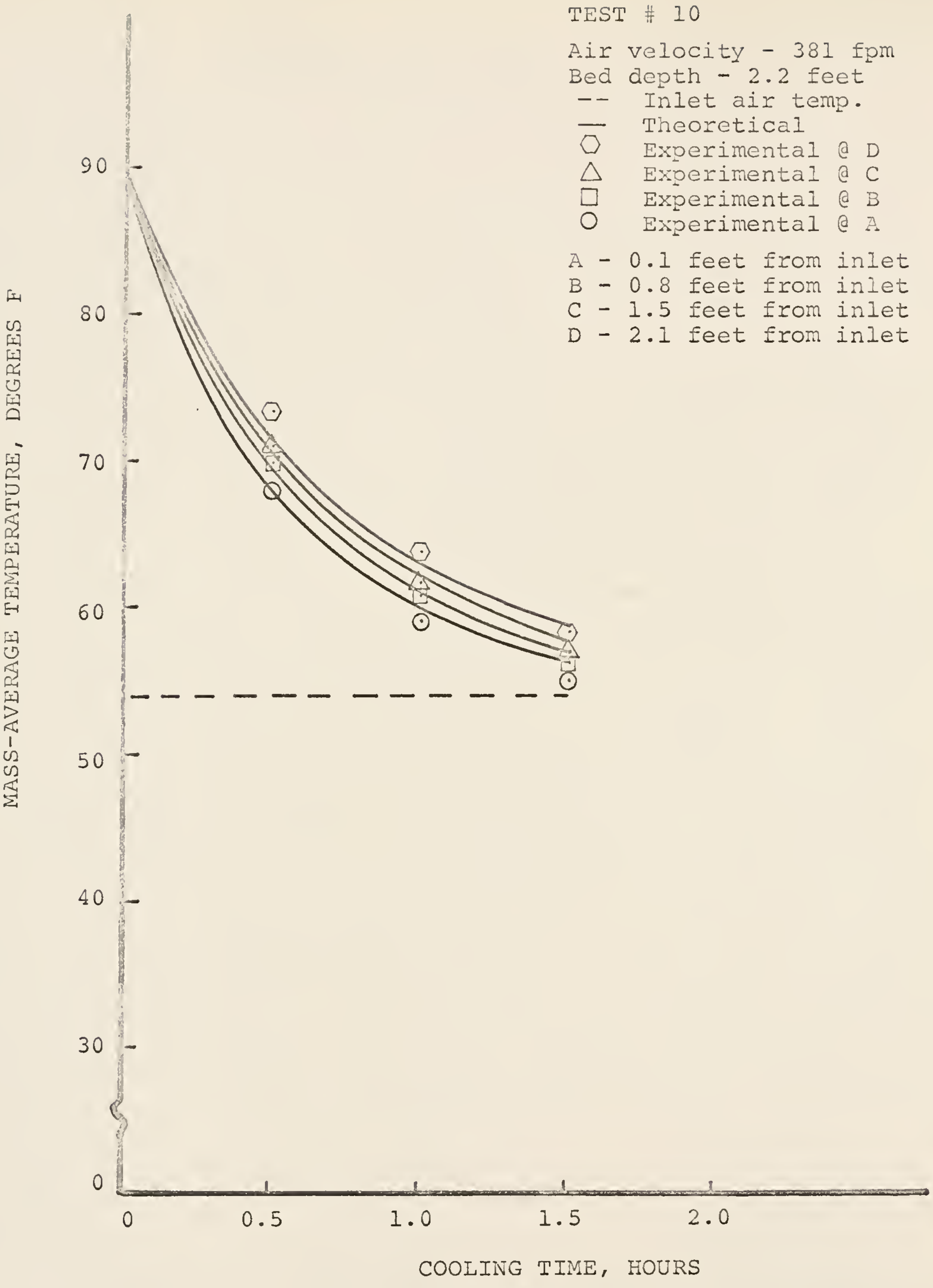

Figure 51. Theoretical and experimental temperature response of oranges to forced-air cooling

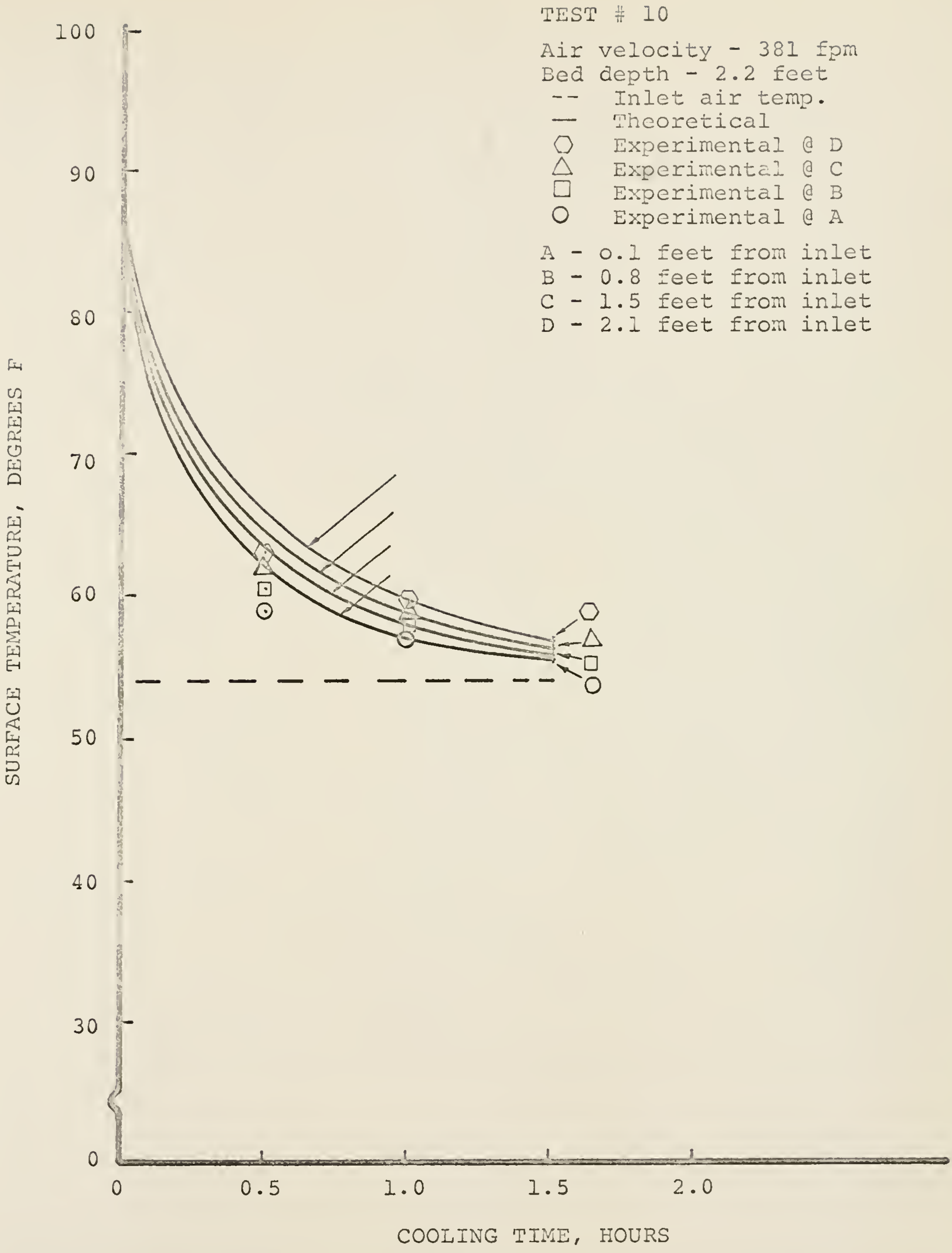

Figure 52. Theoretical and experimental temperature response of oranges to forced-air cooling

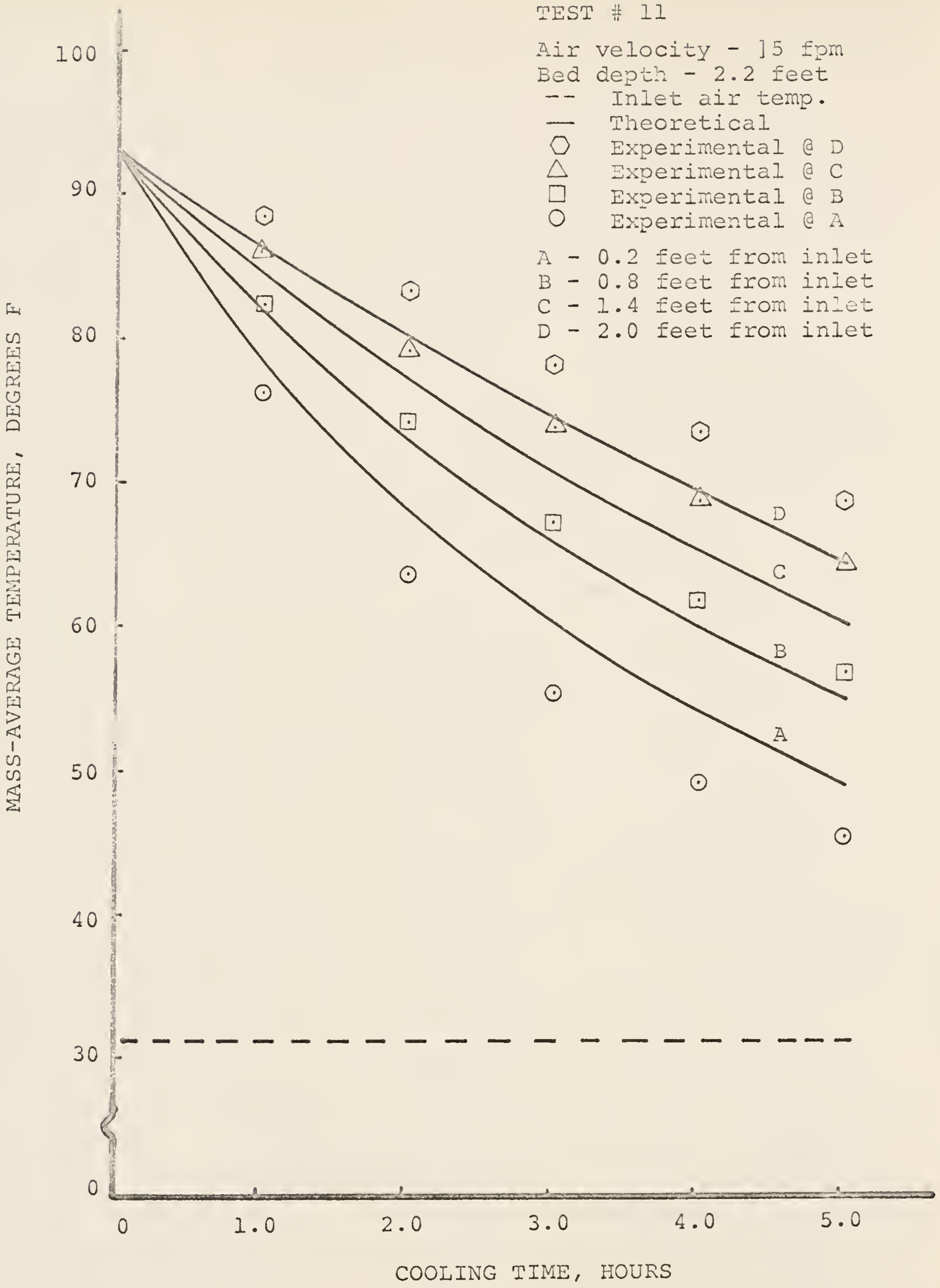

Figure 53. Theoretical and experimental temperature response of grapefruit to forced-air cooling

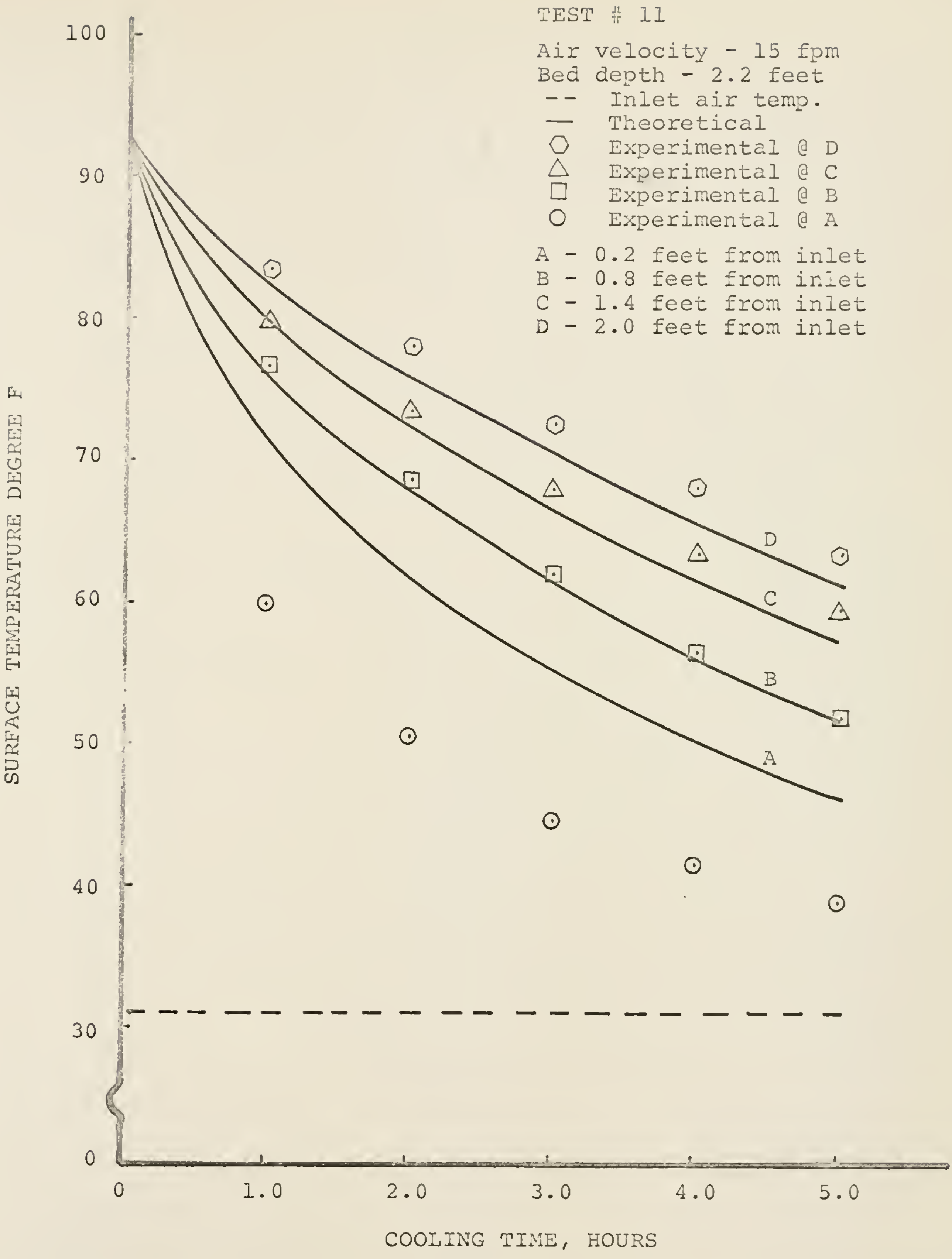

Figure 54. Theoretical and experimental temperature response of grapefruit to forced-air cooling

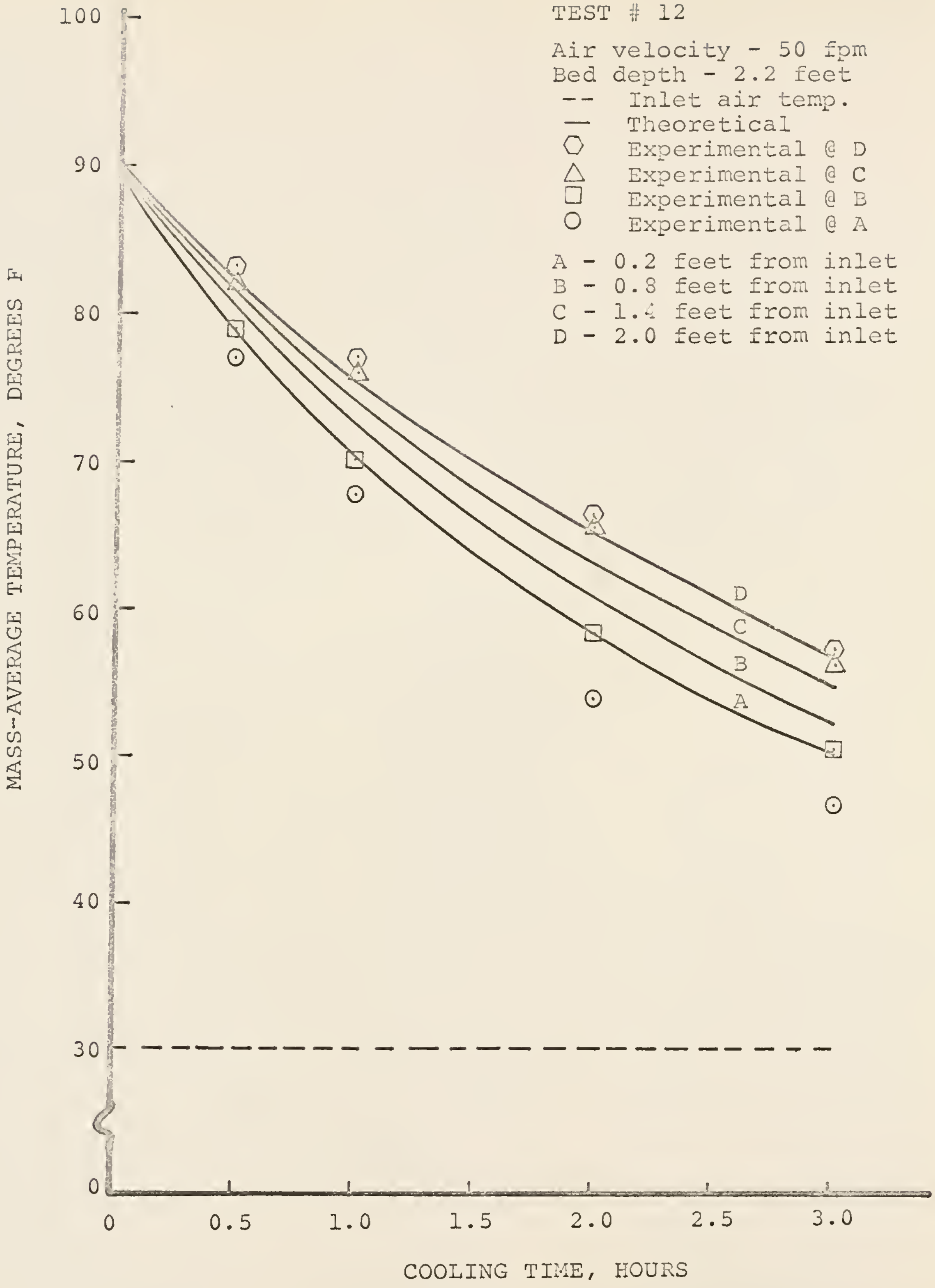

Figure 55. Theoretical and experimental temperature response of grapefruit to forced-air cooling

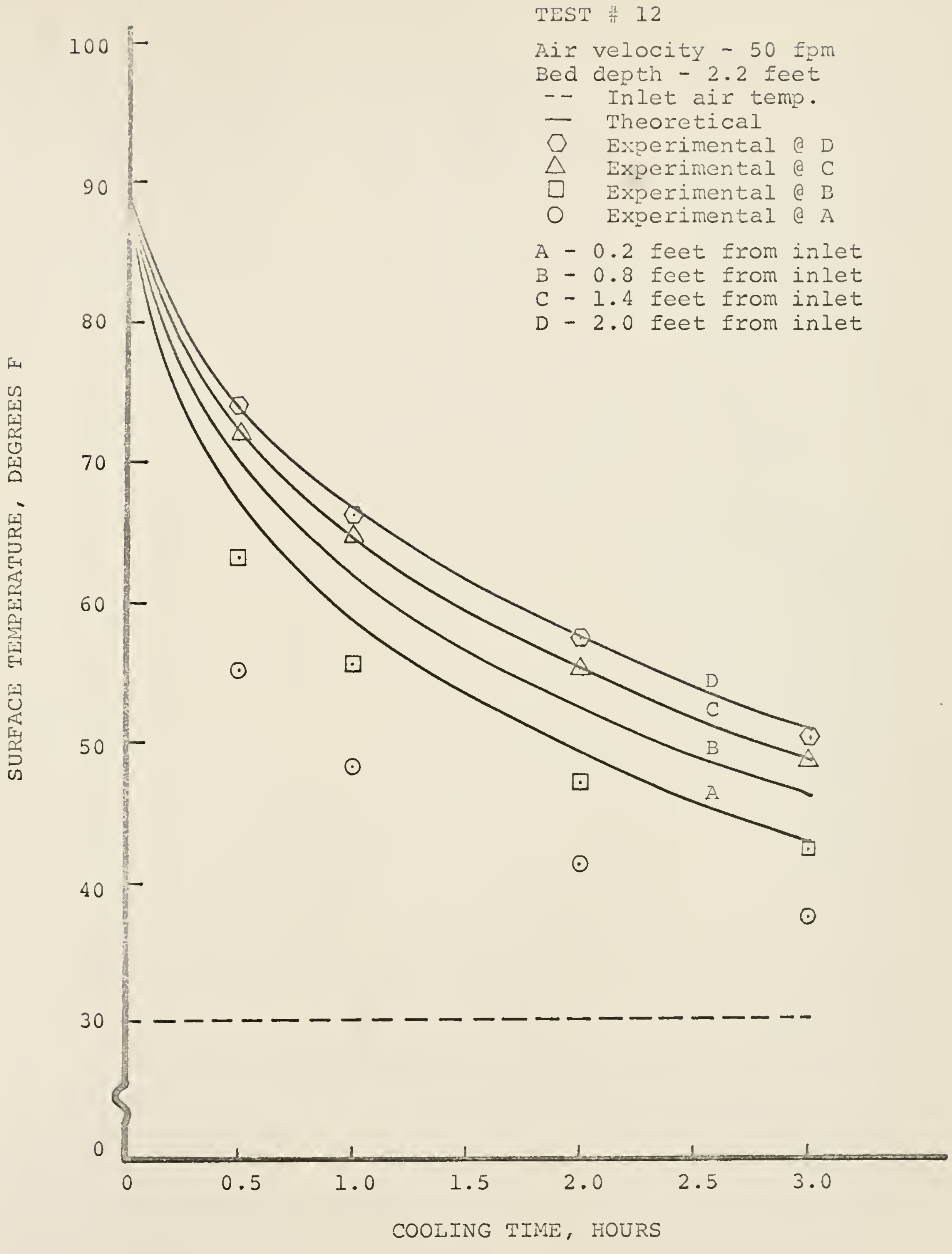

Figure 56. Theoretical and experimental temperature response of grapefruit to forced-air cooling

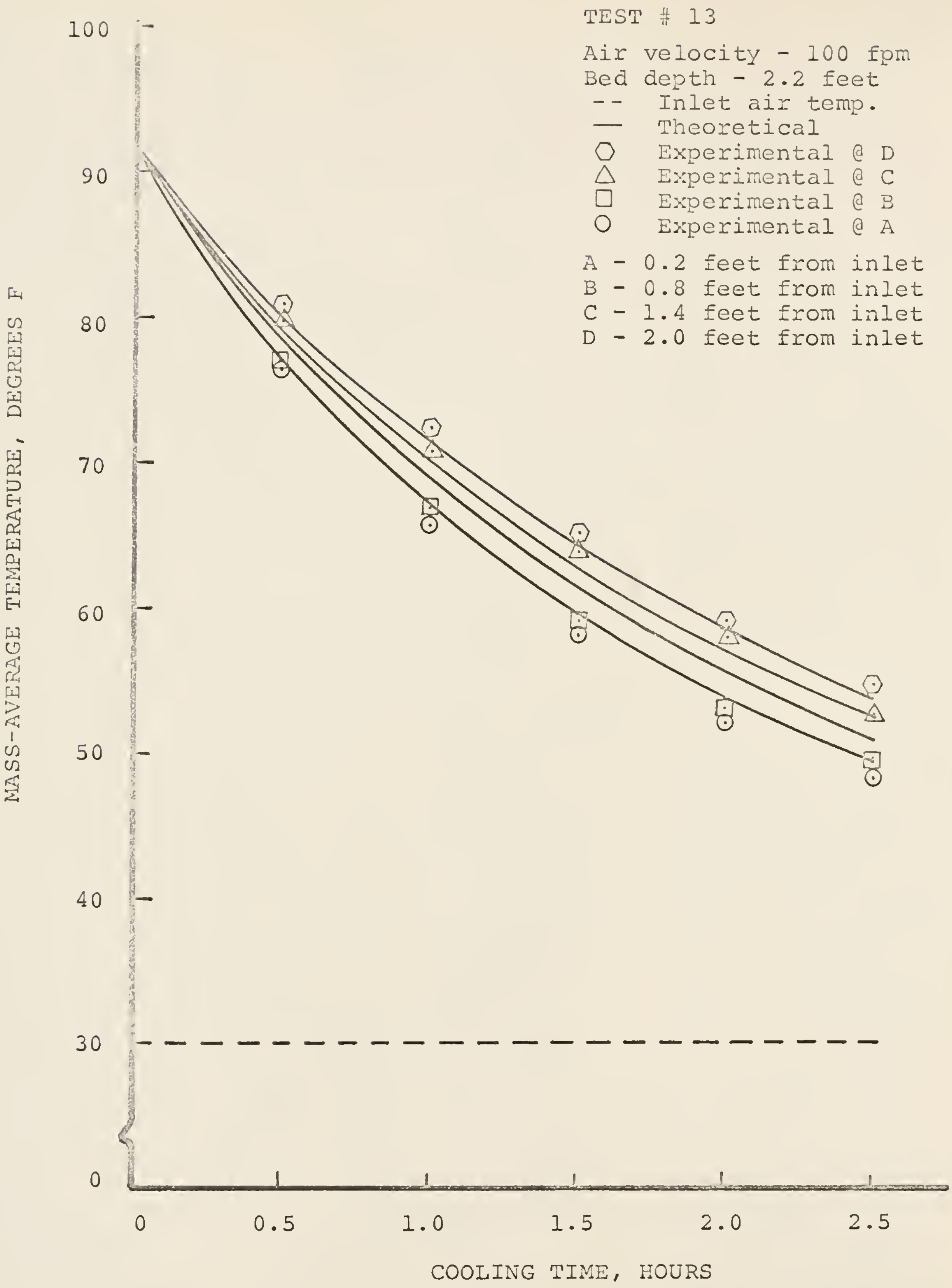

Figure 57. Theoretical and experimental temperature response of grapefruit to forced-air cooling

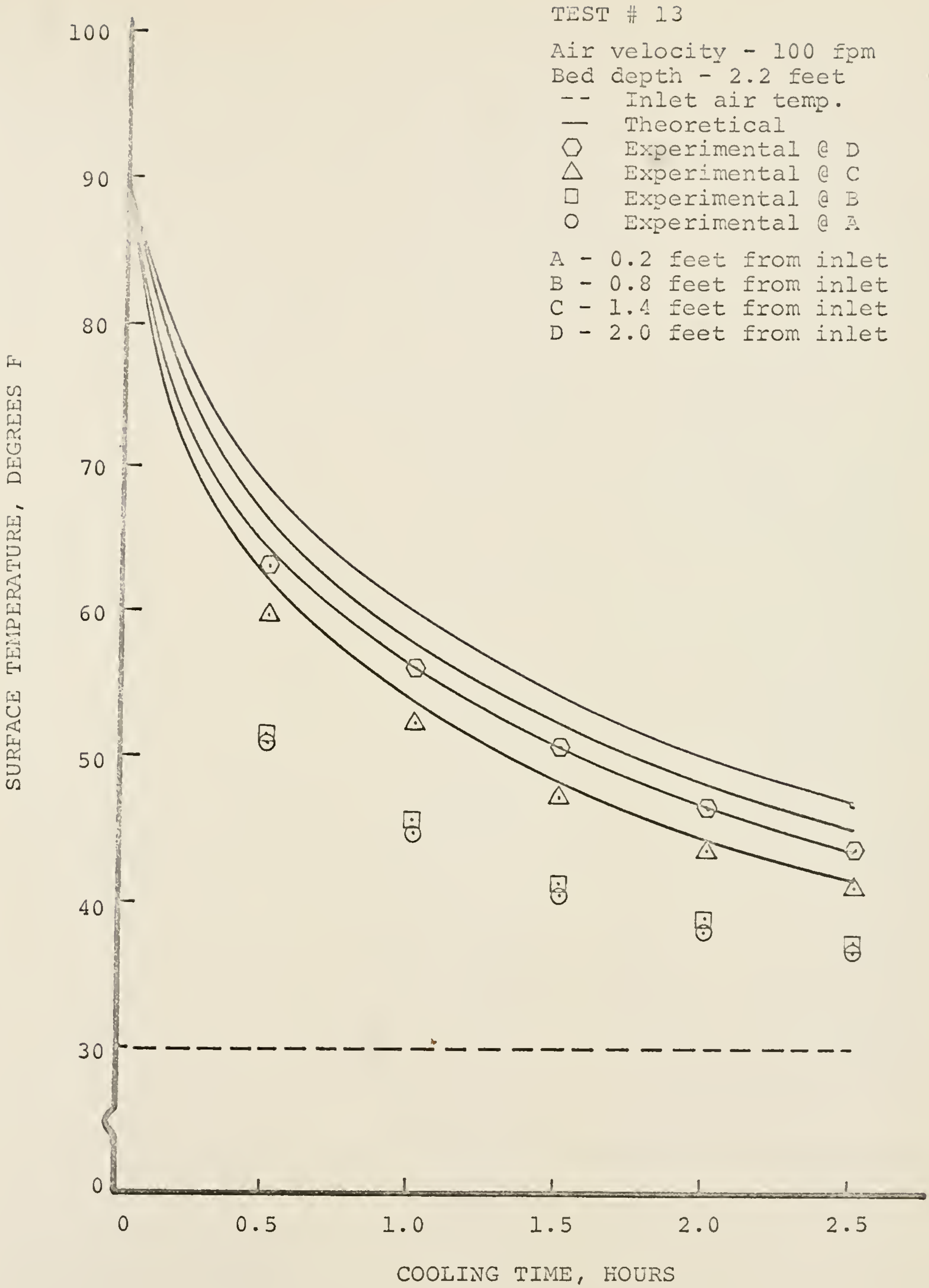

Figure 58. Theoretical and experimental temperature response of grapefruit to forced-air cooling

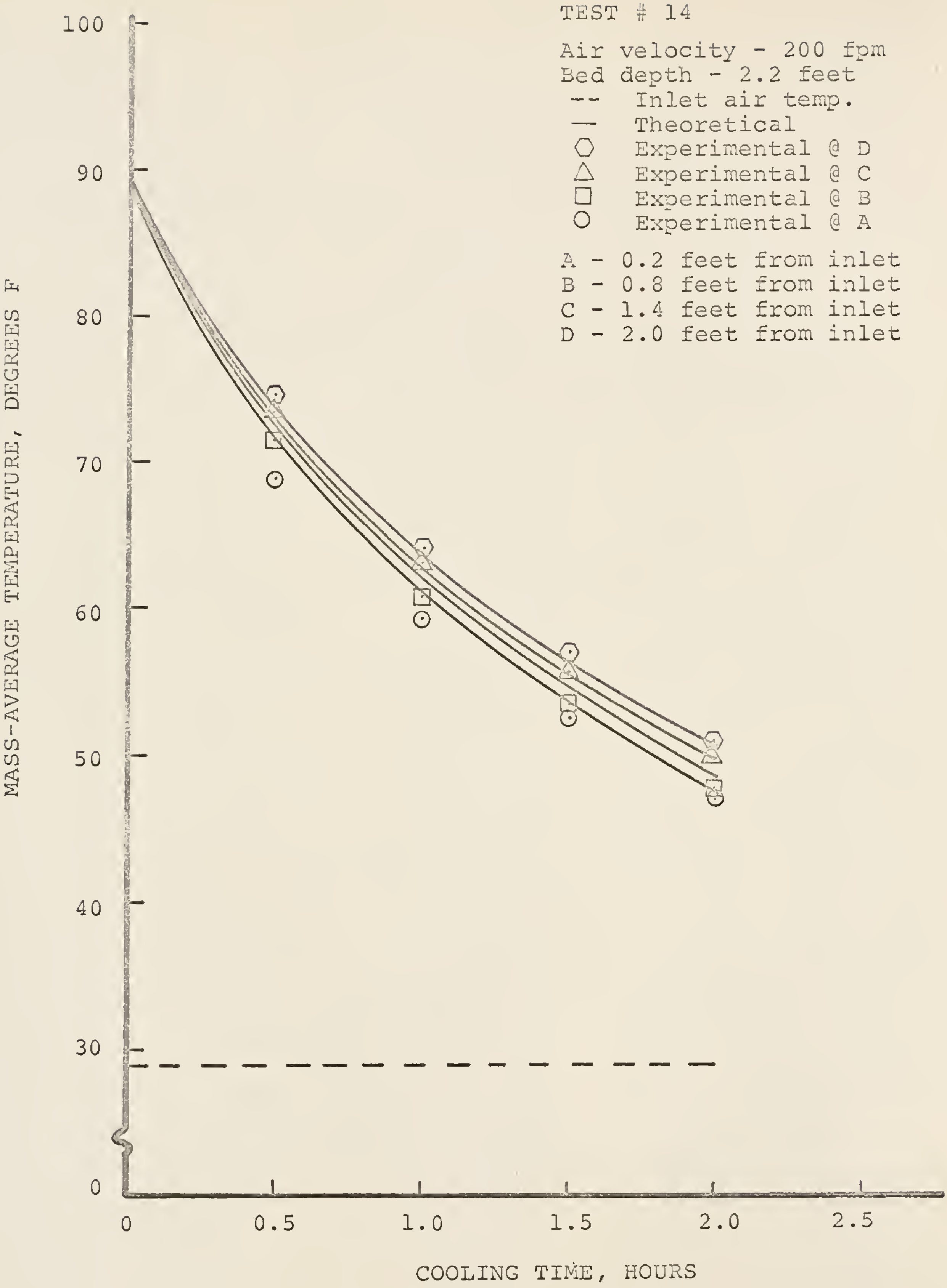

Figure 59. Theoretical and experimental temperature response of grapefruit to forced-air cooling

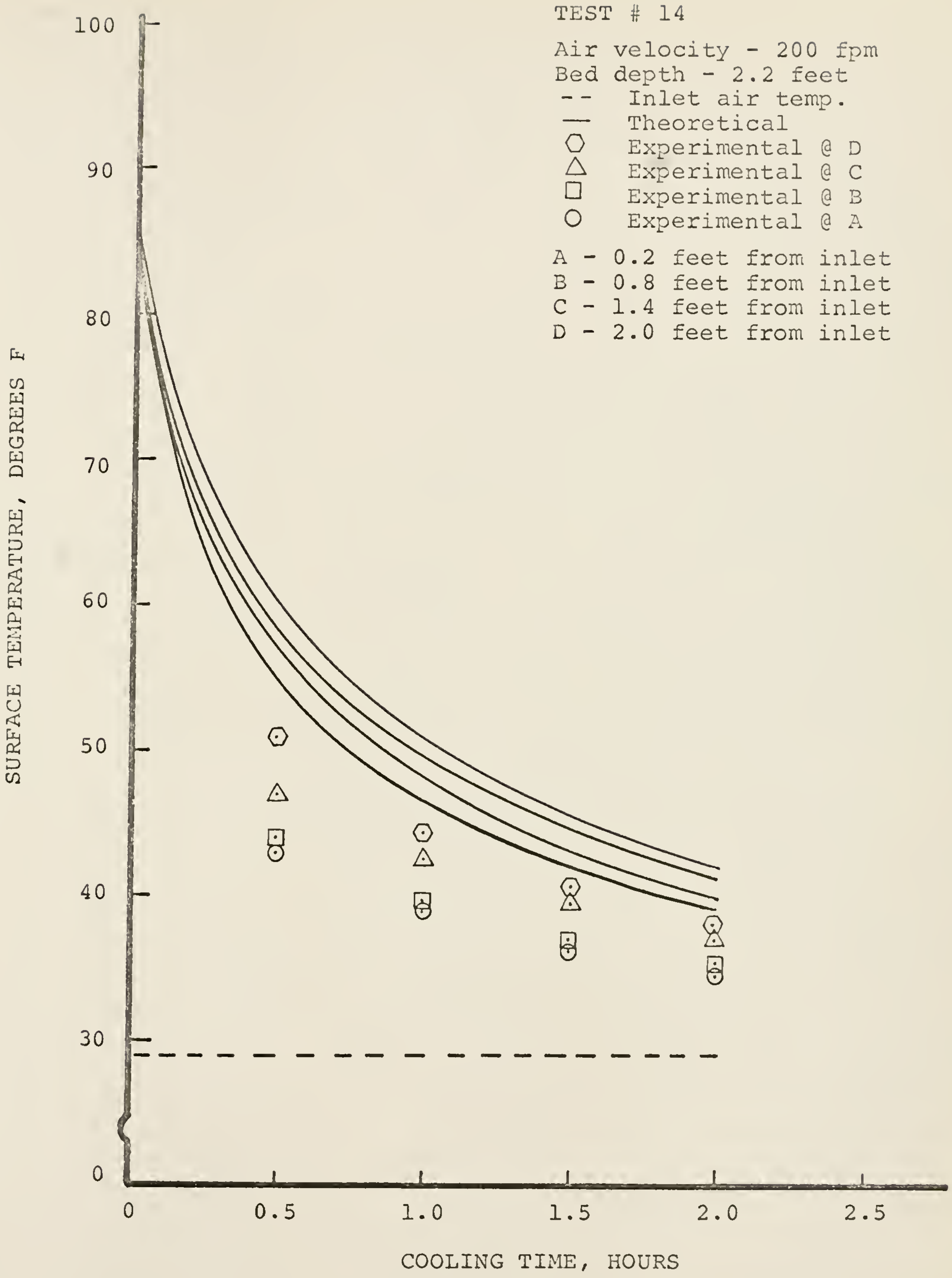

Figure 60. Theoretical and experimental temperature response of grapefruit to forced-air cooling

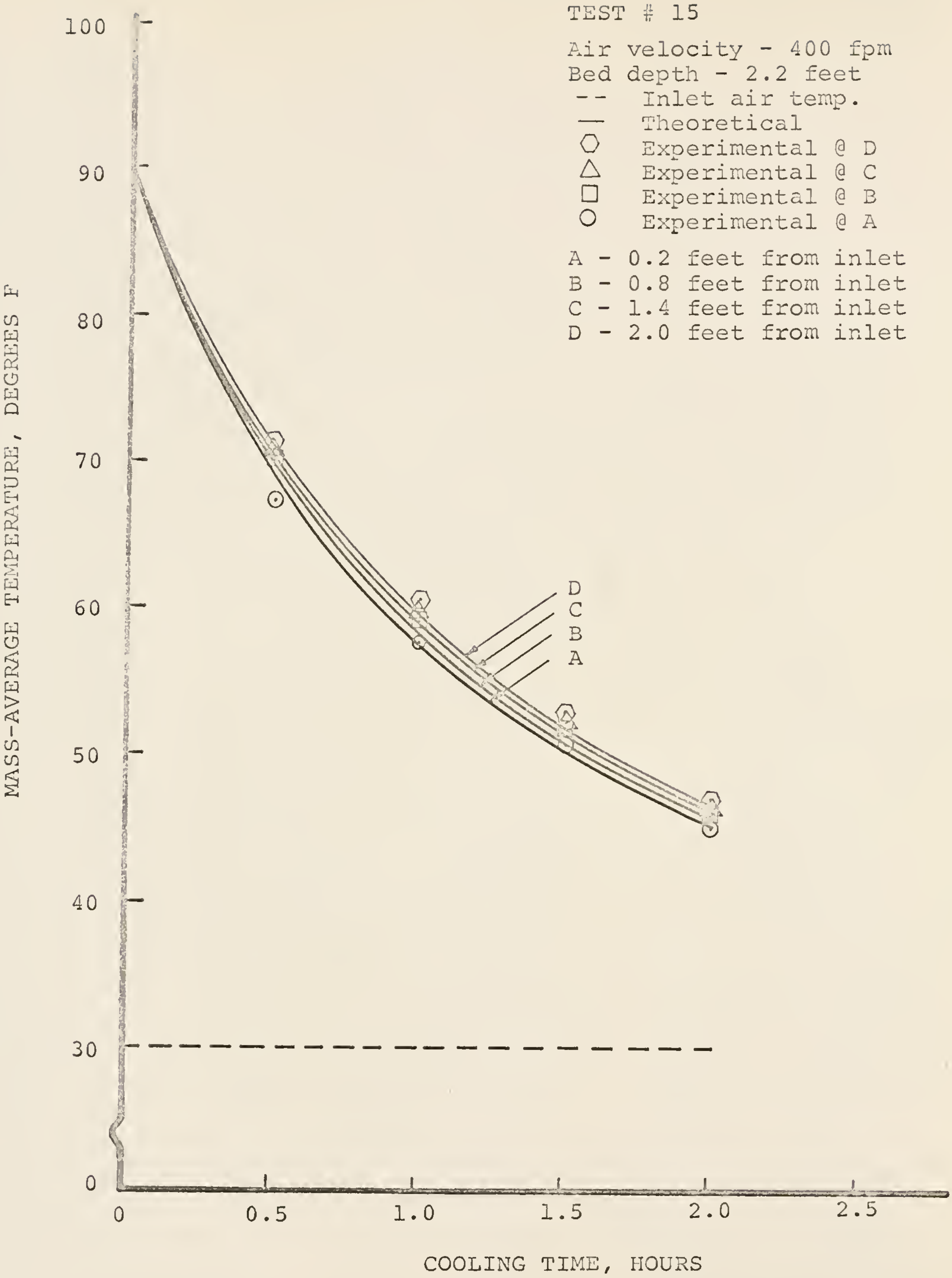

Figure 61. Theoretical and experimental temperature response of grapefruit to forced-air cooling

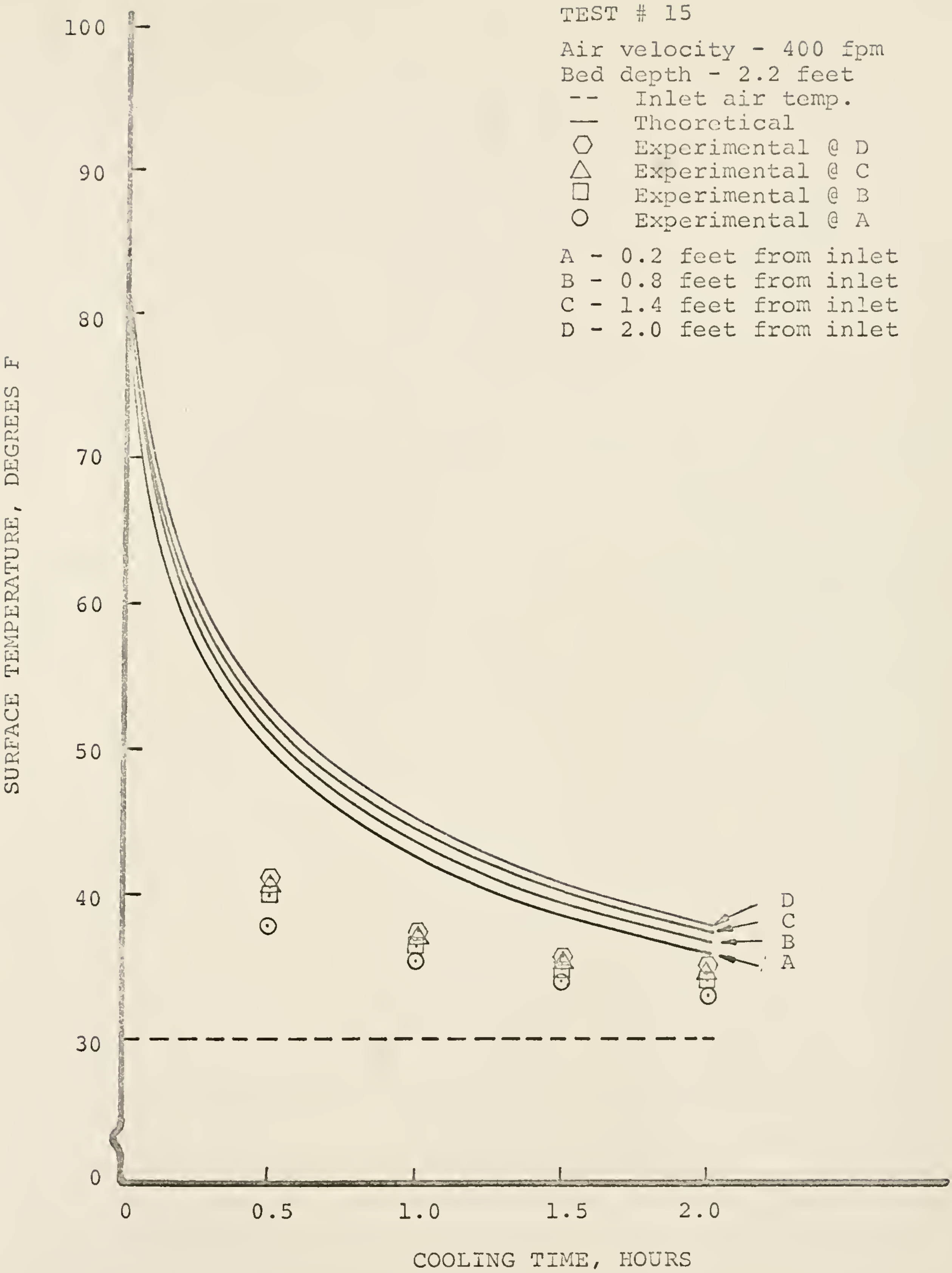

Figure 62. Theoretical and experimental temperature response of grapefruit to forced-air cooling

BIOGRAPHICAL SKETCH

Carl Direlle Baird was born March 10, 1939, in Cookeville, Tennessee. He received his secondary education in Arcadia, Florida. Upon graduation from DeSoto County High School he enrolled in Trevecca College, Nashville, Tennessee and after one year transferred to the University of Florida. He received his Bachelor of Agricultural Engineering degree in December, 1962, and was commissioned as a Second Lieutenant in the United States Army. Upon returning from military service in 1965, he enrolled in the Graduate School at the University of Florida. He received a Master of Science in Engineering in 1967 and accepted a position as Research Associate in the Agricultural Engineering Department, where he is currently employed. He completed all requirements for the degree of Doctor of Philosophy in May 1973.

He belongs to the American Society of Agricultural Engineers, the American Society of Heating Refrigeration and Air-Conditioning Engineers, and is a member of Alpha Zeta, Gamma Sigma Delta, and Tau Beta Pi.

Carl Direlle Baird is married to the former Judy Goodwin and they have two daughters, Sally Ann and Julia.

I certify that I have read this study and that in my opinion it conforms to acceptable standards of scholarly presentation and is fully adequate, in scope and quality, as a dissertation for the degree of Doctor of Philosophy.

E. A. Farber

Erich A. Farber
Professor of Mechanical Engineering

I certify that I have read this study and that in my opinion it conforms to acceptable standards of scholarly presentation and is fully adequate, in scope and quality, as a dissertation for the degree of Doctor of Philosophy.

J. Mostella Myers

J. Mostella Myers
Professor of Agricultural Engineering

I certify that I have read this study and that in my opinion it conforms to acceptable standards of scholarly presentation and is fully adequate, in scope and quality, as a dissertation for the degree of Doctor of Philosophy.

Zoran R. Pop.Stojanovic
Professor of Mathematics

I certify that I have read this study and that in my opinion it conforms to acceptable standards of scholarly presentation and is fully adequate, in scope and quality, as a dissertation for the degree of Doctor of Philosophy.

Frank L. Schwartz

Frank L. Schwartz
Professor of Mechanical Engineering

This dissertation was submitted to the Dean of the College of Engineering and to the Graduate Council, and was accepted as partial fulfillment of the requirements for the degree of Doctor of Philosophy.

June, 1973

Robert E Uhrig

Dean, College of Engineering

Dean, Graduate School

1853

UNIVERSITY OF FLORIDA
3 1262 08553 8014